

W-PM-Sym-1 ^{31}P NUCLEAR MAGNETIC RESONANCE SPECTROSCOPY OF LIVING SYSTEMS. M.J. Dawson, Dept. of Physiology & Biophysics, University of Illinois, Urbana, Illinois 61801.

^{31}P NMR spectroscopy has been used for over a decade in studies of isolated tissues, anesthetized animals and human subjects. Using this technique the concentrations of energetically important metabolites containing phosphorus can be measured noninvasively and intracellular pH and free Mg^{2+} can be determined: Changes in these quantities as a result of experimental intervention can be observed. In addition to measuring net reaction rates, in some instances unidirectional flux rates for equilibrium reactions can be determined. Applications of this technique to the study of the relation between function and metabolism will be described. Examples and conclusions will be drawn from work in our own and other laboratories, including studies of brain, striated and smooth muscle, red cells and reproductive tissues.

W-PM-Sym-2 NMR Investigations of the Control of Mitochondrial Respiration in vivo. Robert S. Balaban. NIH, NHLBI Bethesda MD 20892.

NMR has provided new insights into the regulation of cellular metabolism by directly monitoring these processes in vivo. Previous studies relied on extraction residues which suffered from artifacts of the extraction as well as the statistical handicap of paired data. We have been investigating the control of mitochondrial respiration (QO_2) in the canine heart in vivo as well as the perfused rat heart and mitochondria in vitro using optical spectroscopy and ^{31}P NMR at 4.7 and 8.5 T. These studies investigated the role of ATP and its hydrolysis products, ADP and Pi, in the feedback control between QO_2 and myocardial work by directly measuring [ATP], [CrP], [Pi], free [Mg], NADH, intracellular pH, coronary blood flow and QO_2 . The free [ADP] was calculated from the creatine kinase (CK) equilibrium and from magnetization transfer measurements of CK exchange rates. These studies demonstrated that over physiological work loads (ie 3 fold changes in QO_2) there is little or no change in [ATP] or its hydrolysis products. This suggests that the previous models of respiratory control involving ATP, ADP and Pi alone are either incorrect or must be quantitatively adjusted. An alternative model has been suggested by our data which demonstrate that NADH is an extremely important regulator of QO_2 . This alternative model suggests that the myocardial QO_2 is regulated by the control of substrate oxidation rather than a direct effect of the cytosolic concentrations of ATP or its hydrolysis products.

W-PM-Sym-3 ^1H AND ^{13}C SPECTROSCOPY in vivo. Robert G. Shulman, Dept. of Molecular Biophysics and Biochemistry, Yale Univ., New Haven, CT 06511

W-PM-Sym-4 MICROSCOPIC NMR IMAGING AND PARTICULATE CONTRAST AGENTS. Paul C. Lauterbur, Department of Medical Information Science, College of Medicine, and Department of Chemistry, University of Illinois at Urbana-Champaign, 1307 W. Park St., Urbana, IL 61801.

The three-dimensional resolution of proton magnetic resonance imaging is approaching the dimensions of common animal and plant cells, when special receiver coils and gradient coils are used. New possibilities for the study of subtle changes in the biophysical properties of intact, living, optically-opaque objects are suggested by this development. The labelling of cells with magnetic substances, called "contrast agents" in clinical applications, is analogous to the use of stains, fluorescent beads, and the like in optical microscopy. Examples of experiments and calculations will be given. Various portions of this work have been supported by the NSF, the NCI, the NHLBI, the Exxon Corporation, and the Servants United Foundation.

W-PM-Sym-5 NMR MICROSCOPY OF SINGLE CELLS & TISSUES.
James Aguayo, The Johns Hopkins University School of Medicine, Baltimore, MD 21210

W-PM-MinI-1 A THEORY OF TWO STABLE STATES OF THE NERVE MEMBRANE
 I. Tasaki, National Institute of Mental Health, National Institutes of Health,
 Bethesda, MD 20850

W-PM-MinI-2 THE HYPOTHESIS OF A FERROELECTRIC CHANNEL UNIT FOR ION GATING IN EXCITABLE MEMBRANES.
 H. Richard Leuchtag, Department of Biology, Texas Southern University, Houston, TX 77004.

Because the Hodgkin-Huxley approach and derived approaches are phenomenological, a physical theory of excitability is needed. The hypothesis proposed here views excitability as inherent in the dielectric and ion-conducting properties of a transmembrane unit within the channel (HRL, 1987, *J. Theor. Biol.* 127:321,341). The membrane phenomena of hysteresis, heat block and cold block impose the requirements that the unit be ferroelectric, with upper and lower transition temperatures (Curie points). A mathematical model that differs from classical electrodiffusion only by the addition of two new terms in the dielectric equation of state, ferroelectric electrodiffusion, predicts transverse phase-transition waves accompanied by ion transfer. Using the property of ferroelectrics that a constant biasing field extends the range of polarization, the hypothesis assumes that the majority of ferroelectric channel units in a membrane patch are ferroelectric under the electric field of the resting potential. While a hyperpolarizing field merely increases the polarization, a threshold depolarization lowers the Curie point below the temperature of the unit, which must then undergo a phase transition to a paraelectric state. The transition nucleates at the external surface of the channel unit and carries positive ions (typically Na⁺) inward as it propagates, shielding the negative bound charge at the tails of the polarization vectors. In the absence of mobile cations, the unshielded inward movement of the negative bound charge constitutes the gating current. Individual phase transitions are observed as single-channel currents, known in the physics literature as ferroelectric Barkhausen pulses.

W-PM-MinI-3 The relationship between sodium current, voltage and concentration

David Landowne • Department of Physiology and Biophysics • University of Miami • Miami, FL 33101

A collective model with two parameters for ionic current through nerve membrane in the excited state

| | |
|--|--|
| Current is a function of voltage and two conc. | $I = I(V, c_o, c_i)$ |
| Taylor expansion in Voltage | $I = I_{V=0} + \frac{\partial I}{\partial V} V + \frac{\partial^2 I}{\partial V^2} V^2 + \dots + \frac{\partial^n I}{\partial V^n} V^n + R_n$ |
| Rename 1st two terms, discard rest | $I = I_o(c_o, c_i) + g(c_o, c_i) V$ |
| Taylor expansion in both concentrations discarding I_{oo} and g_{oo} and higher terms | $I = \frac{\partial I_o}{\partial c_o} c_o + \frac{\partial I_o}{\partial c_i} c_i + \left\{ \frac{\partial g}{\partial c_o} c_o + \frac{\partial g}{\partial c_i} c_i \right\} V$ |
| When $V=0$ Fick's Law applies | $\frac{\partial I_o}{\partial c_o} = - \frac{\partial I_o}{\partial c_i} = - P\mathcal{F}$ \mathcal{F} is Faraday's constant |
| Rename terms | $\frac{\partial g}{\partial c_o} = a\mathcal{F}$ $\frac{\partial g}{\partial c_i} = b\mathcal{F}$ |
| a & b are the two parameters | |
| Collected results | $I = -P\mathcal{F}(c_o - c_i) + (a c_o + b c_i)\mathcal{F} V$ |
| Einstein's observation | $P = (a + b) RT/\mathcal{F}$ |

W-PM-Mini-4 EFFECT OF INTERACTION BETWEEN Ca^{2+} AND CONFORMATIONAL GATING ON MEMBRANE EXCITABILITY. Franklin F. Offner, Northwestern University, Evanston, IL 60201.

A statistical mechanical analysis of channel gating reveals that its sensitivity can be much higher than predicted by classical theory (Offner, *Biophys. J.* 46:447 (1984)). The opening and closing of channel gates results in a cyclic decrease and increase in the local electric field acting on the gates. This cycling of the field will result in the field migrating towards a steady state, where its mean increase equals its decrease. If the cycling is rapid compared with the field's relaxation time, a stimulus producing a small change in the voltage across the membrane may produce a change in the potential acting on the gate many times greater than the size of the stimulus. The rapid cycling on and off of adsorbed Ca^{2+} (or Mg^{2+}) at the channels' mouths provides such gating, which may thus be highly voltage-sensitive. The increased interfacial field produced by the adsorbed Ca^{2+} will in turn interact with the charge of the conformational gates, increasing the probability of their closure; such coupling has been observed experimentally. The high voltage sensitivity of Ca^{2+} is thus coupled to the slower, and thus inherently less sensitive, conformational gates, increasing their voltage sensitivity; the converse occurs on depolarization. The theory predicts that the channels may be distributed between a high and a low conductance steady state; a small change in membrane voltage will then shift the channel population distribution between these states. Calculations based on this analysis show that the experimentally observed sensitivities can be explained without invoking molecules of large dipole moments, or other hypothetical structures.

W-PM-Mini-5 THE APPLICABILITY OF THERMODYNAMIC CONTINUUM THEORY TO TRANSMEMBRANE DIFFUSION. T.L. Schwartz, Dept. of Mol. & Cell Biology, Univ. of Connecticut, Storrs, CT 06268.

It has become stylish to ascribe certain contradictions between some of the classical expressions used in the investigation of transmembrane ionic diffusion and experiment to an alleged inapplicability of the thermodynamics of diffusion. It is, for example, held that since transmembrane diffusion phenomena clearly involve discrete channels as well as discrete intrachannel sites, and thermodynamics makes no direct reference to discrete entities, it follows that a thermodynamic approach cannot possibly be applicable. If correct, this trend would have some serious consequences. It would force the abandonment of a major tool for the investigation of transmembrane diffusion in the absence of any other equally flexible and general tool. One should therefore be careful of any inadequately investigated conclusions. The problem is further aggravated by the fact that, in the final analysis, all diffusion of whatever sort involves discrete events. Thermodynamic theory has, nonetheless served us well in investigations of diffusion, whether through liquids, gases, or solids, clays, artificial membranes, glasses, etc. The tendency to consider it invalid for biological membranes would therefore imply that passive diffusion through them is in some special category. The unlikelihood of this has led us to investigate the failures of the theory in depth. We have found, in case after case, that they were produced by the insertion of doubtful physical assumptions in the process of deriving popular expressions from the parent general thermodynamic theory. This reexamination also demonstrated the ability of thermodynamic theory to reveal previously unavailable information. This includes the dependence of permeability on membrane potential, concentration of the permeable species, and intrachannel charge density.

W-PM-Mini-6 A CRITICAL APPRAISAL OF THEORIES OF MEMBRANE EXCITABILITY. V.S.Vaidhyathan, Biophysics department, School of Medicine, State University of New York at Buffalo, Buffalo, New York, 14214.

A brief review of various theories of excitability of membranes will be presented. The inherent assumptions involved, and the limitations of different approaches will be emphasized. The role of physico-chemical constraints, such as mass conservation and tendency towards electro-neutrality on the electric potential profile and ion transports, during excitation will be included.

W-PM-MinII-1 STRUCTURAL STUDIES OF INTERDIGITATED PHOSPHOLIPID PHASES. G.G. Shipley. Biophysics Institute, Departments of Medicine and Biochemistry, Housman Medical Research Center, Boston University School of Medicine, Boston, MA 02118

While most hydrated phospholipids form non-interdigitated bilayer gel phases, several examples of fully or partially chain-interdigitated lamellar phases have now been observed. Modifications at the polar, interfacial and chain regions of phospholipids can result in complete chain interdigitated, examples to be discussed from our own studies being β -DPPC, DHPC and lysoPC. On the other hand, alterations in the chain region can lead to partially interdigitated gel phases and examples will be illustrated with our studies of a series of mixed-chain PCs. The structural evidence for the presence of chain-interdigitated phases will be reviewed and the possible mechanism underlying the conversion between non-interdigitated and interdigitated phases will be discussed.

W-PM-MinII-2 MIXED INTERDIGITATED BILAYER SYSTEMS. Ching-hsien Huang, Department of Biochemistry, Univ. of Virginia, Sch. of Med., Charlottesville, VA 22908.

Based on structural studies of C(18):C(10)PC lamellae (McIntosh et al. (1984) *Biochemistry* 23, 4038; Hui et al. (1984) *Biochemistry* 23, 5570), it is established that pure C(18):C(10)PC molecules form mixed interdigitated bilayers at $T < T_m$. In this bilayer, two lipid molecules from opposing bilayer leaflets are coupled noncovalently to form a packing unit. In the packing model, the long acyl chain adopts a nearly fully extended conformation, and it is interdigitated fully across the entire hydrocarbon width of the bilayer. The short chain, however, packs end-to-end with a short chain of another lipid molecule from the opposing bilayer leaflet. This conformation permits close van der Waals contacts between lipid species. We have employed high-resolution differential scanning calorimetry (DSC) to investigate the thermotropic behavior of liposomes prepared from 10 different asymmetric PCs: C(16):C(9)PC, C(16):C(10)PC, C(18):C(10)PC, C(18):C(11)PC, C(20):C(11)PC, C(20):C(12)PC, C(22):C(12)PC, C(22):C(13)PC, C(8):C(18)PC, and C(10):C(22)PC. These asymmetric PCs have a common characteristic; i.e., the longer acyl chain in the fully extended conformation is about twice as long as that of the shorter chain. Our experimental results support the conclusion that all these pure asymmetric PCs self-assemble, at $T < T_m$, into a mixed interdigitated bilayer in excess water. Furthermore, mixtures of C(10):C(22)PC/C(22):C(12)PC of various molar ratios are miscible in all proportions in both gel and liquid-crystalline states as shown by DSC and ^{31}P -NMR, further suggesting that these lipids form mixed interdigitated bilayers. Based on these results, one can conclude that asymmetric PCs with one acyl chain twice as long as the other can pack into mixed interdigitated bilayer at $T < T_m$. Supported by NIH Grant GM-17452.

W-PM-MinII-3 VIBRATIONAL RAMAN AND INFRARED SPECTROSCOPIC STUDIES OF INTERDIGITATED BILAYER ASSEMBLIES. Ira W. Levin, Laboratory of Chemical Physics, NIDDK, National Institutes of Health, Bethesda, MD 20892.

Raman and infrared spectroscopic techniques provide discriminating, non-invasive methods for investigating the behavior of lipid bilayer dispersions on the vibrational time scale. In particular, the spectroscopic characteristics of the acyl chain methylene carbon-hydrogen (C-H) stretching modes reflect sensitively the structural and dynamical properties of the hydrophobic internal regions of the bilayers. Using these vibrational "probes," we shall first survey spectroscopically the thermotropic behavior of bilayer assemblies representing several examples of interdigitated gel phase systems of differing chain packing geometries. Systems including both symmetric and asymmetric chain phospholipids, as for example, aqueous dispersions of DHPC and sphingomyelin bilayers, will be compared and contrasted. The effect of ethanol on inducing interdigitated acyl chains in aqueous DPPC assemblies will be visualized in terms of Raman spectra recorded from spatially resolved multilamellar domains within an alcohol concentration gradient. Infrared spectra of intact liver plasma membranes subjected to both *in vivo* and *in vitro* ethanol exposure will be discussed in the context of domains of interdigitated chains.

W-PM-MinII-4 USE OF A FATTY ACID SPIN LABEL TO DETECT INTERDIGITATED LIPID AND LIPID-PROTEIN BILAYERS.

Joan M. Boggs, Research Institute, Hospital for Sick Children, Toronto M5G 1X8, and Department of Clinical Biochemistry, University of Toronto, Toronto, Ontario, CANADA.

ESR spectroscopy is proving to be a useful technique to detect interdigitated gel phase bilayers. A nitroxide group located on a fatty acid near its terminal methyl, as in 16-doxyl-stearate, normally has more motion and/or less order in a non-interdigitated gel phase bilayer than when it is located closer to the carboxyl, as in 5-doxyl-stearate. However, in fully interdigitated bilayers of symmetric forms of phospholipids in the presence of amphipathic substances such as glycerol and polymyxin B, the motion of 16-doxyl-stearate is restricted (or the order is increased) to a degree similar to that experienced by 5-doxyl-stearate (1). Addition of myelin basic protein to saturated forms of phosphatidylglycerol causes similar motional restriction of 16-doxyl-stearate, suggesting that the gel phase of this lipid-protein complex is also fully interdigitated (2). This protein is envisioned to interact with the lipid in a similar way as the amphipathic polymyxin, with its basic residues bound electrostatically to the lipid head groups and its hydrophobic amino acid side chains dipping partway into the bilayer. Motional restriction of 16-doxyl-stearate also occurs in the mixed interdigitated bilayers formed by highly asymmetric 18:10, 18:12, and 10:18 species of phosphatidylcholine (3), and in the gel phase of highly asymmetric C26:0 and C24:0 species of the sphingolipid, cerebroside sulfate, suggesting that they also form a mixed interdigitated bilayer. Spectral subtraction techniques can be used to detect a population of interdigitated lipid in the presence of non-interdigitated lipid.

(1) Boggs and Rangaraj, *Biochim. Biophys. Acta* 816 (1985) 221; (2) Boggs et al, *Biochemistry* 20 (1981) 6066; (3) Boggs and Mason, *Biochim. Biophys. Acta* 863 (1986) 231.

W-PM-MinII-5 THE INTERDIGITATED PHASE AS A PROBE FOR DETERMINING THE DEPENDENCE OF HYDRATION REPULSION ON HEAD GROUP DENSITY. T. J. McIntosh, S. A. Simon, and A. D. Magid, Departments of Anatomy and Physiology, Duke University Medical Center, Durham, N. C. 27710.

The interdigitated phase can be induced in dipalmitoylphosphatidylcholine (DPPC) by the addition of several different surface active molecules, including ethanol, glycerol, chlorpromazine, tetracaine, and heptanetriol (HTO). In this unusual phase hydrocarbon chains from apposing monolayers fully interpenetrate or interdigitate, so that the terminal methyl groups of the acyl chains abut the interfacial region on the opposite sides of the bilayer. Thus, the interdigitated phase has nearly twice the area per lipid molecule, A_1 , as a normal gel phase and makes an ideal system to test the dependence of the repulsive hydration pressure, P_h , on the density of bilayer zwitterionic head groups. We have applied osmotic stress to interdigitated bilayers by incubating multilamellar suspensions of DPPC:HTO in aqueous solutions of polyvinylpyrrolidone (PVP). X-ray diffraction analysis was used to obtain the thickness of the fluid space between adjacent bilayers, d_f , as a function of applied osmotic pressure, i.e. PVP concentration. It is found that P_h for the interdigitated phase obeys the same relationship as for other lipid phases, $P_h = P_o \exp(-d_f/\lambda)$. Comparisons of results from normal gel, interdigitated gel, and liquid-crystalline phases show that λ increases only slightly with increasing A_1 , whereas P_o is inversely proportional to the square of A_1 . Monolayer measurements show that the dipole potential (V) is inversely proportional to A_1 , indicating that P_o is proportional to V^2 . Since P_h acts to prevent adjacent bilayers from coming into contact, this observation may help to explain why several molecules which reduce V also promote membrane fusion.

W-PM-MinII-6 INDUCTION OF THE INTERDIGITATED GEL STATE IN SYMMETRICAL PHOSPHATIDYLCHOLINES BY ALCOHOLS. Elizabeth S. Rowe, Department of Biochemistry, University of Kansas Medical School, and Veterans Administration Medical Center, Kansas City, MO 64128.

Alcohols and other small amphipathic molecules induce a fully interdigitated gel state in saturated symmetrical chain phosphatidylcholines. The interdigitated gel state ($L_{\beta I}$) can be differentiated from the usual bilayer gels ($L_{\beta'}$ or $P_{\beta'}$) indirectly by changes in the characteristics of their apparent pretransition and main melting transitions. Since many of the methods generally used to study phase transitions cannot distinguish between the interdigitated and non-interdigitated gel phases, we have developed a fluorescence method to directly monitor the transition from the bilayer gel to the interdigitated gel. We have focused on the induction of the interdigitated state in PC's as a function of alcohol chain length, lipid chain length, alcohol concentration, and temperature. We have also studied the $L_{\beta I}$ to $P_{\beta'}$ and $L_{\beta I}$ to L_{α} phase transitions of the ether linked DPPC analogue, dihexadecylphosphatidylcholine (DHPC) as a function of alcohol concentration. Our results suggest that the differences in stability between the interdigitated gel and the non-interdigitated gel states are small, and depend on a complex combination of factors. (Supported by the Veterans Administration and by the National Institutes of Alcohol Abuse and Alcoholism).

W-PM-A1 MECHANISM OF BINDING OF COOMASSIE BLUE G-250 TO BOVINE SERUM ALBUMIN AND THE ASSOCIATED COLOR CHANGE. Michelle A. Markus and Charles P. Bean, Physics Department, Rensselaer Polytechnic Institute, Troy, NY 12180-3590.

The triphenyl methyl dye Coomassie Brilliant Blue G-250 (CBB G-250) is commonly used to quantify the amount of protein in solutions. In the assay, a stock solution of the dye in acid is brown. In the presence of protein, the solution turns blue. The optical absorbance of a solution containing protein and dye is measured at 595 nm and compared against a standard curve to determine the amount of protein present. We have studied the mechanism of the interaction of CBB G-250 and bovine serum albumin using dialysis techniques. Over 200 dye molecules have been found to bind to each protein molecule. Preliminary results suggest that the mechanism of interaction involves a phase transition in the protein molecule, similar to the transition observed when detergents, such as SDS, bind to protein. The color change of the dye has been shown to be a function of pH. We hypothesize that the color change in the presence of protein is caused by a higher pH at the surface of the protein as compared to that of the CBB stock solution. A color change has been observed at the surface of silicone oil droplets, supporting this proposed mechanism. Supported by an NSF Grant, "Research Experiences for Undergraduates".

W-PM-A2 CONFORMATIONAL STABILITY OF γ -CRYSTALLINS: THERMODYNAMICS OF THERMAL AND ATHERMAL DENATURATION. M. Kono and B. Chakrabarti. Eye Research Institute, Boston, MA 02114.

The three major γ -crystallins of the eye lens, γ -II, γ -III, and γ -IV, have closely related amino acid sequences and similar three-dimensional folding (secondary structure) of the polypeptide backbone, but differ in critical temperatures for cryoprecipitation (cold cataract) and in photoinduced aggregation behavior. To account for these differences, we measured the thermal (this study) and chemical (Mandal et al, *J Biol Chem* 262:8096, 1987) denaturation of these proteins and determined the thermodynamic parameters of their order-disorder transition. The denaturation was studied by circular dichroism to monitor the peptide band at 217 nm (beta conformation minimum). The transition curves are sigmoidal for both thermal and athermal denaturation, and the data were treated in terms of a two-state transition to obtain the thermodynamic parameters. The midpoint temperatures of transition are 70.5°C, 75.2°C, and 75.4°C for γ -II, γ -III, and γ -IV, respectively. The ΔH values at these temperatures ($\Delta G = 0$) are 137, 80, and 67 kcal/mol, respectively; corresponding ΔS values are 399, 229, and 191 cal mol⁻¹K⁻¹. $\Delta G_0^{\text{H}_2\text{O}}$ at 25°C was calculated by extrapolation of the ΔG vs [GuHCl] denaturation plot to 0 M GuHCl; the values are 5.21, 4.03, and 8.28 kcal/mol for γ -II, γ -III, and γ -IV, respectively. The results indicate that the conformational stability of γ -crystallins differ significantly from each other, presumably because their tertiary structures are not similar.

W-PM-A3 POLYELECTROLYTE PROPERTIES MEASURED BY GEL PERMEATION CHROMATOGRAPHY (GPC) Martin Potschka, Porzellangasse 19/2/9, A-1090 Vienna, Austria

Proteins, being polyelectrolytes, largely perturb their surrounding solvent by electrostatic forces. This double layer of surrounding counter ions is described by

$$\Psi = \Psi_s \frac{a}{x+a} e^{-\kappa x}$$

where Ψ_s is the potential at the outer edge of the Stern layer, i.e. the net charge minus the tightly bound counter ions, a is the radius of the macromolecule, κ^{-1} the Debye length and x the distance from the surface. This equation predicts that (1) the thickness of the double layer depends on net charge up to a level of saturation beyond which the diffuse double layer remains constant, that (2) it increases with the radius of the macromolecule becoming largest for a flat plane and that (3) it increases with decreasing ionic strength in an $I^{-1/2}$ law. All three predictions have been verified experimentally using GPC, which was thus demonstrated to elute macromolecules according to their unperturbed dimension, i.e. the radius proper plus the surrounding double layer. The equilibrium distance between macromolecule and matrix walls, neutral or bearing charges of equal sign, measures Ψ in relation to kT and thus provides an operational means to define the thickness of the constituent double layers in absolute terms. First measurements indicate that the maximal thickness of the diffuse double layer is 1-2 times Debye length for a sphere of 3nm radius and some 3 times Debye length for spheres of 14nm radius. Future experiments will determine the corresponding saturating net charge as a function of macromolecular size and thus the number of tightly bound counter ions.

W-PM-A4 SOLUTION ELECTROSTATICS OF ION-ION INTERACTIONS.

Alexander A. Rashin, Department of Physiology and Biophysics, Mount Sinai School of Medicine, One Gustave L. Levy Place, New York, New York 10029.

A new method for calculation of solvation energies of polar molecules, based on a continuum description of the solvent, is applied to the study of interactions of spherical ions in solution. Only the electrostatic contribution to the free energy of solvation is taken into account. Repulsion at short distances is represented by a potential derived from vacuum quantum mechanical calculations. The charge distribution of each ion is represented by a point charge on its nucleus. It is found that: 1) Theory, based on a continuum description of the solvent, leads to an adequate representation of the essential features of interionic Potentials of Mean Force (PMF), including a solvent separated minimum, a contact minimum, and a barrier between them; 2) Calculated PMF's for $\text{Li}+\text{Cl}^-$, $\text{Na}+\text{Cl}^-$ and $\text{K}+\text{Cl}^-$ are in good quantitative agreement with PMF's from molecular theories, showing increase in depth of the contact minimum and decrease of the barrier between the minima with increasing size of the cation; the effects are due to the difference between Coulomb attraction and a loss of solvation energy upon association; 3) This agreement suggests that the nonelectrostatic contribution to PMF's is small, and that saturation effects and a specific structure of the solvent around ions do not dominate PMF's; 4) Ionic association constants in a nonassociated solvent can be higher than in an associated solvent, when both have the same dielectric constant, due to a larger cavity size in the nonassociated solvent; 5) Details of PMF's for like charged ions (e.g., presence or depth of minima) are likely to be unreliable because of errors involved in large hydration energies of small double charged systems. Supported by NSF grant DMB-8519273.

W-PM-A5 CD MEASUREMENTS OF GLIAL FIBRILLARY ACIDIC PROTEIN. M. Farooq*, W.T. Norton*, W.T. Winter#, and N.M. Tooney#. *Department of Neurology, Albert Einstein College of Medicine, Bronx, N Y, 10461 and #Polytechnic University, Brooklyn, N Y, 11201.

Glial Fibrillary Acidic Protein, GFAP, forms intermediate filaments in the cytoplasm of astroglial cells in the central nervous system. GFAP has been classified with desmin and vimentin as type III based on amino acid sequence and is presumed to contain alpha helical domains. Recent X-ray diffraction studies (Farooq et al, submitted for publication) have demonstrated that fibers prepared from GFAP show characteristic features of alpha helical proteins. We have been able to solubilize GFAP and obtain CD spectra under both denaturing and nondenaturing conditions.

Cytoskeletal pellets containing GFAP were isolated from bovine brain by the method of Chiu and Norton (1). GFAP was purified from the pellets by a modification of the method of Tokutake et al (2). SDS Gel electrophoresis methods indicated a virtually homogeneous sample of molecular weight 50,000 daltons. Immunological techniques confirmed the identity of GFAP. The CD spectrum of GFAP in Tris buffer (10 mM Tris, pH 8, 20 mM NaCl, 1 mM DTT) shows that the protein is 40% - 50% alpha helical, about 20% beta structure and about 30% random coil (method of Saxena and Wet-Laufer). The GFAP spectrum is relatively unaffected by urea at concentrations of up to 3-4 M. At concentrations of 6 M urea or greater, the protein is largely random coil. These CD studies, taken together with X-ray data, provide experimental evidence for the alpha helical nature of GFAP both in solution and as fibers.

(1) Chiu, F.C. and Norton, W.T., (1982) J. Neurochem 39, 1262-1258

(2) Tokutake, S. et al (1983) Anal. Biochem. 135, 102-105

W-PM-A6 THERMODYNAMIC AND KINETIC LINKAGES BETWEEN LIGAND BINDING, FOLDING AND ASSEMBLY OF THE CATALYTIC SUBUNIT OF E. COLI ASPARTATE TRANSCARBAMOYLASE. S. Bromberg and N. Allewell, Wesleyan University, Middletown, CT 06457.

Analytical gel chromatography (AGC) coupled with post-column derivatization with o-phthalaldehyde and fluorescence detection has been used to study the mechanism of denaturation of the trimeric catalytic subunit (c_3) in urea. This method allows dissociation and unfolding to be distinguished and can be used in the presence of ultraviolet absorbing materials. In the absence of urea, the contraction of the protein produced by binding of PALA, a bisubstrate analog, and the expansion which occurs at high ionic strength (0.25 M NaCl or 50 mM ATP) can be readily detected. The Stokes radius of the protein in 7M urea indicates that it exists as monomeric random coils in both the absence and presence of 56 μM PALA, 5 mM carbamoyl phosphate, 50 mM ATP, and 0.25 M NaCl. In the absence of ligands or in the presence of ATP c_3 dissociates at 1.5 M urea before cooperatively unfolding. Active site ligands which bind between c chains stabilize the trimer against both dissociation and unfolding; in their presence, relatively compact trimeric intermediate species exist at urea concentrations at which the unliganded protein is dissociated and partially unfolded. The urea concentration required to dissociate and cooperatively unfold these intermediates increases with the strength of ligand binding. The data are fit to models which assume a linear dependence of free energy upon urea concentration. Higher resolution AGC studies are being carried out to investigate the protein concentration dependence, linkage to ligand binding and pathway of trimer dissociation. Kinetic experiments are also underway. Supported by NIH grant AM-17335.

W-PM-A7 VOLUME CHANGES WITH Ca^{2+} -SEQUESTRANT MODELS FOR THE CALCIUM-BINDING PROTEINS.

D. W. Kupke and Beverly S. Shank, Dept. of Biochemistry, Sch. of Med., The University of Virginia, Charlottesville, VA 22908.

The distinctive volume increases, ΔV , observed upon sequential addition of Ca^{2+} to calmodulin, skeletal troponin-C and parvalbumin suggest that this bulk property reflects principally on the coordination event to specific binding loops in these proteins. In order to interpret more properly the ΔV upon uptake of Ca^{2+} , we have selected various Ca^{2+} sequestrants which bear similarities to the microenvironments of these binding loops (EF hands). We find that the common tetracarboxylate sequestrants exhibit distinctive volume increases upon complexation with Ca^{2+} ; EGTA and its derivatives (BAPTA and QUIN-2) showing the largest increases. These ΔV were comparable to those found for some of the Ca^{2+} equivalents to the above proteins. They were smaller, however, than the ΔV determined for the putative binding loops in troponin-C which contain 2 pairs of convergent carboxylates. According to current stereoelectronic theory, this convergence should increase the affinity for Ca^{2+} and further decompress the electrostricted water dipoles, leading to a larger ΔV . Sequestrant models of this type are not available for use in aqueous media to make such comparisons. Also, peptide sequences (13 residues) simulating some binding loops in calmodulins have generated no appreciable volume changes, indicating that the full domain structure must be present. The results of this study, however, are consistent with the hypothesis that the ΔV of Ca^{2+} complexation to these proteins reflects largely the coordination event to specific binding loops and may, therefore, be used to indicate whether a protein binds multiple ions in an ordered manner.

Supported by NIH grant, GM-34938.

W-PM-A8 INTERFACE-INDUCED CONFORMATIONAL CHANGES IN THE FILAMENTOUS PHAGE fd: SPECTRAL CHANGES ASSOCIATED WITH THE CONVERSION OF PHAGE TO I-FORM OR TO SPHEROIDS. A. K. Dunker and L. Roberts, Chemistry Department and Biochemistry/Biophysics Program, Washington State University, Pullman, WA 99163-4660.

Previously it has been shown that exposure of the filamentous phage fd to a CHCl_3 /water interface at 0° to 15°C leads to the contraction of the phage into a shortened rod known as the I-form. Exposure of phage or I-form to a CHCl_3 /water interface at room temperature and above leads to the formation of spheroidal particles, which we call S-form. The earlier work relied primarily on electron microscopy to characterize these conformational changes. Further study of these conformational changes may provide additional insight about the mechanism by which the filamentous phage penetrates the cell membrane. We have characterized the I- and S-forms by fluorescence, 90° light scatter, uv absorbance, Raman spectroscopy and circular dichroism. We have also characterized a mixing device to define conditions such that diffusion of phage or I-form to the solvent/water interface is not rate limiting for their respective conversions. Below 15° the conversion from phage to I-form is rapid and complete. Above this temperature, the conversion from phage to S-form is slow and incomplete, whereas the conversion from I-form to S-form is rapid and complete. A decrease in the conversion rate of the phage with increasing temperature could suggest a change in the reaction pathway, an increase in phage stability due to the increasing importance of hydrophobic interactions, or a decrease in the ability of the water/solvent interface to catalyze the conformational change.

W-PM-A9 TESTS OF THE RELIABILITY OF PROTEIN INTERATOMIC POTENTIALS BY COMPARISON OF CALCULATED AND OBSERVED STRUCTURES, VIBRATIONAL FREQUENCIES AND INTERNAL DYNAMICS OF MOLECULAR CRYSTALS. Q.-Y. Shang, D.L. Harris, and B. Hudson, Department of Chemistry and Institute of Molecular Biology, University of Oregon, Eugene, OR 97403.

The non-bonding, torsional and hydrogen bonding interactions that are the main determinants of atomic motion in proteins also determine the conformational and unit cell structure, lattice vibrational modes and reorientational dynamics of molecular crystals. The polarized single crystal vibrational spectroscopy of molecular crystals provides a rich and reliable source of data for the evaluation of intermolecular potentials. The crystalline nature of the samples eliminates ambiguities in vibrational assignment and molecular conformation. For flexible molecules a full lattice dynamics calculation is necessary. The success of this approach for the hydrocarbon species tetraphenylmethane has been demonstrated (1). Urea and the complexes formed between urea and long chain n-alkanes provide examples where many of the hydrogen bonding interactions of proteins are present. Experimental and theoretical studies of these systems will be presented. The simple cyclic peptides diketopiperazine (2) and d,l-alanine provide additional examples where this method provides a useful test of potential functions. The case of crystalline 1-methionine is of particular interest. In this case the two molecules in the asymmetric unit have different conformations and there is evidence of significant torsional motion about both the α - β and β - γ bonds in the lattice. Molecular dynamics simulation calculations of this system will be presented. (1) N. Schlotter and B. Hudson, *J. Phys. Chem.* 90, 719 (1986). (2) T.C. Cheam and S. Krimm, *Spectro. Chim. Acta* 6, 481 (1984); 6, 503 (1984).

W-PM-A10 PREPARATION AND CHARACTERIZATION OF A DANSYLAZIRIDINE DERIVATIVE OF WHEAT GERM CALMODULIN. Henry G. Zot and David Puett, Department of Biochemistry and the Reproductive Sciences and Endocrinology Laboratories, Univ. of Miami, Miami, Florida 33101.

A dansylaziridine (1,5-dimethylaminonaphthalenesulfonylaziridine) derivative of wheat germ calmodulin was prepared which retains the native sulfhydryl reactivity of the single cysteine after modification. A labeling ratio of 0.85-0.95, determined from the extinction coefficient of the dansyl moiety, was achieved by incubation with a 2-fold molar excess of dansylaziridine (in suspension), provided that Ca^{2+} was present. Ca^{2+} , but not Mg^{2+} , induced a 10-15 nm blue shift in the emission maximum, a 2.5-fold intensity increase at the $-\text{Ca}^{2+}$ emission maximum, and a 3.5-fold intensity increase at the $+\text{Ca}^{2+}$ emission maximum. The binding of Ca^{2+} to labeled and unlabeled wheat germ calmodulin was measured by equilibrium dialysis, and, compared with unlabeled wheat germ calmodulin, the dansylated derivative exhibited a slightly greater affinity. The fluorescence change of dansylated wheat germ calmodulin was found to have about a 3-fold greater sensitivity to Ca^{2+} than the binding of Ca^{2+} to this derivative. These relationships between binding curves and between binding and fluorescence changes were determined from the midpoints of apparently parallel curves. The results suggest that dansylated plant calmodulin is a useful fluorescence indicator that responds to subsaturating Ca^{2+} binding. Work is underway to determine the site(s) of dansylaziridine binding. Supported by NIH GM35415 and AHA Florida Affiliate.

W-PM-A11 SETSCHENOW COEFFICIENTS OF AMINO ACID SOLUTIONS. R.P. Kennan and G.L. Pollack, Physics and Astronomy Dept., Michigan State Univ., East Lansing, MI 48824 and J.F. Himm, Dept. of Physics, North Dakota State Univ., Fargo, ND 58105.

The Setschenow coefficient, $k_s = (1/M) \log_{10}(L/L_0)$, has been measured at 25°C in aqueous solutions for 15 amino acids, NaCl, and sucrose. In the defining equation M is the molar concentration of solute and L and L_0 are, respectively, the Ostwald solubility of gas in water and in solution. Xenon-133, a γ emitting isotope with $t_{1/2} = 5\frac{1}{2}$ days was used as the solute gas; the corresponding value of L_0 is 0.1057. Values for k_s ranged from 0.058 ± 0.011 for arginine and 0.059 ± 0.008 for proline to 0.17 ± 0.03 for asparagine. For arginine, glycine, and proline, temperature dependence of L was measured in the range 5-40°C and the corresponding values of $k_s(T)$ have been obtained. Some connections between Setschenow coefficients and solvent-solute interactions, for example amino acid hydration, have been investigated. The relation of Setschenow coefficients to scaled-particle theory and to thermodynamic functions of solution will also be discussed.

W-PM-A12 MECHANOCHEMICAL COUPLING IN SYNTHETIC ELASTOMERIC POLYPEPTIDES BY CHARGE MODULATION OF AN INVERSE TEMPERATURE TRANSITION

Dan W. Urry, Bryant Haynes, Hong Zhang, R. Dean Harris and Kari U. Prasad
Laboratory of Molecular Biophysics, School of Medicine, The University of Alabama at Birmingham
P. O. Box 311/University Station, Birmingham, Alabama 35294

A reversible elastic contraction is achieved by a change in pH in a synthetic polypeptide matrix, $(\text{Val}^1\text{-Pro}^2\text{-Gly}^3\text{-}\phi^4\text{-Gly}^5)_n$ where ϕ is Val or Glu randomly at a ratio of 4:1, i.e., 4 Glu residues per 100 residues of polypentapeptide; n is greater than 120 and the matrix is formed by γ -irradiation cross-linking. This pH modulated contraction and relaxation demonstrates the principle that a reversible change in the hydrophobicity (alternatively hydrophilicity or polarity) of an elastic polypeptide chain, which is capable of undergoing an inverse temperature transition, can result in mechanochemical coupling. The contracted state is demonstrably a dominantly entropic elastomer; it occurs on the high temperature side of an inverse temperature transition; it is a more ordered state than the relaxed state as directly shown by a number of physical methods, and it denatures at temperatures above 60°C with loss of elastic force. The entropic elastic force is considered to arise from damping of internal chain dynamics on extension. Therefore, the structural transition and the development or relaxation of the entropic elastic forces could occur in a non-random fibrous protein or in a chain segment of a globular protein. Since phosphorylation/dephosphorylation would provide a biochemical means for reversibly changing the hydrophobicity of a polypeptide domain, it is proposed that modulation of an inverse temperature transition be a means whereby phosphorylation and dephosphorylation modulate structure and forces in protein mechanisms, such as in cytoplasmic components of channels and pumps and in contraction. The structural change that is contraction and that attends many other protein mechanisms is proposed to be a reversible change of polarity of the polypeptide chain which alters the temperature of an inverse temperature transition.

W-PM-B1 INTERACTION OF HOECHST 33342 AND HOECHST 33258 WITH THE SARCOPLASMIC RETICULUM Ca^{2+} CHANNEL OF RAT SKELETAL MUSCLE Troy Beeler, Department of Biochemistry, Uniformed Services University of the Health Sciences, Bethesda, Maryland 20814-4799

Hoechst (H) 33342 (MW 534.6) and H 33258 (MW 497.6) are cationic bisbenzimidazol dyes that differ in structure only in that H 33342 contains an ethoxy group on a phenyl ring where H 33258 has an hydroxy group. This difference in structure is enough to completely alter the interaction of these dyes on the sarcoplasmic reticulum (SR) Ca^{2+} channel since H 33342 is a strong antagonist whereas H 33258 is an agonist. The interaction of these dyes with the SR Ca^{2+} channel was investigated by measuring the effect of the dyes on Ca^{2+} uptake and release from SR terminal cisternae vesicles of triads isolated from rat skeletal muscle. H 33342 blocked Ca-induced Ca^{2+} release (Ca activation of SR Ca channel) release whereas H 33258 enhanced it. H 33342 inhibits the SR Ca^{2+} channel in a way that is different from that observed with other organic inhibitors (safranin O, 1,1'-diheptyl-4,4'-bipyridinium, neomycin) or inorganic inhibitors (Mg, ruthenium red). Unlike these other inhibitors, H 33342 inhibits the SR Ca^{2+} channel even after the channel is activated by ryanodine. H 33342 and H 33258 compete with each other to alter the activity of the SR Ca^{2+} channel. H 33258 decreases the apparent affinity of channel inhibitors and increases the apparent affinity for Ca^{2+} binding to the regulatory site of the SR Ca^{2+} channel. These data suggest the H 33342 and H 33258 bind to a common site on the SR Ca^{2+} channel. Since H 33342 contains a more bulky, hydrophobic ethoxy group on its phenol ring (as compared to the smaller, hydrophilic hydroxy group of H 33258) we propose that this ethoxy group physically blocks the movement of Ca^{2+} through the channel. (Supported by NIH)

W-PM-B2 HALOTHANE DECREASES CARDIAC MUSCLE CONTRACTILITY BY INCREASING CALCIUM PERMEABILITY OF THE SARCOPLASMIC RETICULUM. Masayuki Katsuoka and S. Tsuyoshi Ohnishi. Membrane Research Institute, University City Science Center. Philadelphia, PA 19104.

It has been known that general anesthetics reduce myocardial contractility (1). We studied the mechanism of this negative inotropic effect using the isolated perfused heart (Langendorff model) and isolated cardiac cells (myocytes) prepared from rats. Since both caffeine and halothane are known to release Ca from the sarcoplasmic reticulum (SR) of skeletal muscle by increasing the Ca permeability (2), we compared the modes of action of halothane and caffeine on the heart. We found that caffeine decreased contractility of the perfused heart similar to halothane. It was also observed that both caffeine and halothane decreased the Ca-transient in Fura-2 loaded myocytes. The Ca-content of the SR as estimated by caffeine-induced contraction was also decreased by halothane. Halothane decreased the amount of caffeine-induced Ca release in myocytes. These results suggest that modes of action of caffeine and halothane may be the same. Upon addition, halothane caused an immediate Ca release; the release was suppressed by procaine but not influenced by nitrendipine. This suggests that halothane-induced Ca release may be the same as the Ca-induced Ca release. Supported by GM35681 and 33025. Reference: (1) Price and Ohnishi. *Fed. Proc.* 39:1575-1579 (1980). (2) Ohnishi. *B.B.A.* 897:261-268 (1987).

W-PM-B3 THE 3'-ARYLAZIDO-ATP BINDING SITES ON THE Ca-ATPASE OF SARCOPLASMIC RETICULUM. Anne A. Kearns and F. Norman Briggs, Virginia Commonwealth University, Richmond, VA 23298.

The suitability of 3'-arylazido-ATP (aATP) as a photoaffinity analog of ATP for labeling the nucleotide binding domain of the Ca-ATPase of sarcoplasmic reticulum (SR) has been investigated. Molecular sieve HPLC of photoincorporated aATP showed that 4 peaks are labeled. Peak 1 is a dimer and peak 2 a monomer of the Ca-ATPase. The other labeled peaks were of low molecular weight. Although the labeling of SR increased regularly as aATP concentration was increased from 3 to 450 μM the labeling of the Ca-ATPase monomer saturated at 75 μM , the concentration at which inhibition of ATPase activity saturated. Ten millimolar ATP inhibited photoincorporation at 30 μM aATP into SR by 31 percent. The inhibition of incorporation into the Ca-ATPase monomer was 61 per cent. Incorporation into the other three peaks, including the Ca-ATPase dimer, were virtually unaffected by ATP. Limited digestion of the Ca-ATPase by trypsin showed that ATP strongly blocked the labeling of fragment B and produced only slight inhibition of the labeling of fragment A_1 . Inhibition of labeling of fragment A_2 was intermediate.

There was good stoichiometry between inhibition of ATPase activity and photoincorporation of aATP into the Ca-ATPase monomer when photoincorporation was carried out between 3 and 30 μM concentrations. When photoincorporation was carried out at 30 μM , where stoichiometry was good, all three of the major domains, A_1 , A_2 and B were labeled. Occupancy of each of these domains by aATP was thus able to impede the hydrolytic activity of the Ca-ATPase and each domain must be part of the ATP binding domain.

W-PM-B4 ACTIVATION AND INACTIVATION OF THE SKELETAL SR Ca^{2+} RELEASE CHANNEL BY TRYPSIN. ERIC ROUSSEAU, F. ANTHONY LAI, JULIA S. HENDERSON, AND GERHARD MEISSNER. Department of Biochemistry, University of North Carolina, Chapel Hill, NC 27599.

The effect of trypsin proteolysis on skeletal sarcoplasmic reticulum (SR) Ca^{2+} release has been examined using (i) rapid ion flux measurements, (ii) ryanodine binding, (iii) sedimentation analysis of the ryanodine receptor, (iv) SDS polyacrylamide gel electrophoresis and (v) single channels incorporated into planar lipid bilayers. Trypsin digestion of SR Ca^{2+} release vesicles in the presence of 1 mM Ca^{2+} results in a rapid disappearance of the Ca^{2+} release channel band (M_r 360,000) on SDS gels without an appreciable effect on [^3H]ryanodine binding or sedimentation behaviour of the channel complex. Continued exposure to trypsin results in a decrease in ryanodine receptor size from 30S to \sim 10S and loss of high-affinity [^3H]ryanodine binding (assayed after trypsinization). [^3H]Ryanodine binding performed prior to digestion required prolonged incubation times before the bound ryanodine was affected by trypsin. Parallel experiments show that a reduction of ryanodine receptor complex size results in an increase of Ca^{2+} release rate followed by reduction in Ca^{2+} release activity. In planar lipid bilayers, addition of trypsin to the cytoplasmic side of the channel also initially increases the fraction of open time of the Ca^{2+} -activated channel, which is followed by a complete and irreversible loss of channel activity. Trypsin added to the luminal side of the channel has no effect on single channel activity. These results demonstrate that the T-SR junction-spanning portion of the SR Ca^{2+} release channel is sensitive to proteolysis.

Supported by Fellowships from MDA(FAL) and CHF(ER), and NIH grant AR 18687.

W-PM-B5 IMMUNOLocalIZATION OF THE \sim 450 kDa Ca^{2+} -RELEASE CHANNEL/RYANODINE RECEPTOR IN ADULT SKELETAL AND CARDIAC MUSCLE. A.O. Jorgensen*, W. Arnold*, A. McLeod*, T. Imagawa+, S. Kahl+, and K.P. Campbell+ *Dept. of Anatomy, University of Toronto, Toronto, Canada M5S 1A8 and +Dept. of Physiology & Biophysics, University of Iowa, Iowa City, IA 52242

The subcellular distribution of the \sim 450 kDa Ca^{2+} -release channel/ryanodine receptor in skeletal and cardiac muscle was determined using 5-8 μm cryosections of rabbit skeletal and cardiac muscle and indirect immunofluorescence (IF) labeling with monoclonal and polyclonal antibodies specific for the \sim 450 kDa Ca^{2+} -release channel/ryanodine receptor. In transverse sections, specific labeling showed a hexagonal staining pattern within each myofiber. The relative intensity of labeling of the Type II (fast) fibers was judged to be 2 to 3-fold higher than that of the Type I (slow) fibers. In longitudinal sections rows of discrete foci were observed in the interface between the A- and the I-band regions of the sarcomere. These results support the idea that the \sim 450 kDa Ca^{2+} -release channel/ryanodine receptor is densely distributed in the junctional sarcoplasmic reticulum of both the Type I and Type II skeletal muscle fibers. Results of similar IF studies comparing the distribution of the \sim 450 kDa Ca^{2+} -release channel/ryanodine receptor with that of calsequestrin in rat ventricular muscle tissue showed that the distribution of the \sim 450 kDa Ca^{2+} -release channel/ryanodine receptor and calsequestrin were indistinguishable. These results are consistent with the idea that the \sim 450 kDa Ca^{2+} -release channel/ryanodine receptor in cardiac muscle is also localized in the junctional sarcoplasmic reticulum. (Supported by MRC and NIH.)

W-PM-B6 SARCOBALLS: DIRECT ACCESS TO SARCOPLASMIC RETICULUM Ca^{2+} CHANNELS IN SKINNED FROG SKELETAL MUSCLE FIBERS. P. G. Stein and P. T. Palade, Department of Physiology and Biophysics, University of Texas Medical Branch, Galveston, Texas 77550.

Our findings grow from an original observation that frog skeletal muscle fibers mechanically skinned in Ca^{2+} -containing physiological saline solution exhibit vesicles of membrane at their surfaces within seconds of skinning. These vesicles coalesce to form large hemispherical to spherical membranes which we have termed "sarcoballs". Conventional patch-clamping techniques (10-15 M Ω pipettes) are used to study excised patches which contain 0-4 (avg.=2) relatively large conductance Ca^{2+} channels. This channel exhibits two predominant conductance levels, the most common being 90-100 pS (53 mM Ca^{2+}) and the other appearing as bursts above this level to 140-150 pS. Several other discrete conductance levels are seen less frequently. Additional characteristics include a limited selectivity for Ca^{2+} over K^+ ($P_{\text{Ca}^{2+}}/P_{\text{K}^+}=6.5$) and a marked sensitivity to potential (E_m). The relationship between open probability (P_o) and E_m is altered by the [Ca^{2+}] in the pipette (presumptive cytoplasmic face of the membrane). With 25 μM Ca (and 103 mM K pipette, 53 mM Ca bath), steady-state P_o is near 0 at and below 0 mV and it increases sharply with E_m , approaching 1.0 between +30 and +40 mV. Lowering pipette [Ca^{2+}] to 0.3 μM causes a reduction in P_o over this range of E_m ; raising pipette [Ca^{2+}] to 53 mM increases P_o at 0 and negative E_m . Additionally, this channel is blocked by 1 μM ruthenium red on the cytoplasmic face and may be opened at potentials where P_o is low by the addition of caffeine (5 mM). The fundamental similarities between these channels and those reported from isolated rabbit SR (Smith et al. Nature 316:446, 1985) indicate that we are studying the frog SR Ca^{2+} -release channel rendered accessible by a very simple method. Supported by PHS 1 P01 HL37044.

W-PM-B7 STABILITY OF SARCOPLASMIC RETICULUM ATPase AGAINST PRESSURE INACTIVATION. R. L. Mendonça and S. Verjovski-Almeida. Dept. of Biochemistry, Federal University of Rio de Janeiro, 21910 Rio de Janeiro, BRAZIL.

Sarcoplasmic reticulum ATPase was studied under hydrostatic pressures up to 2.3 kilobar. Tryptophan fluorescence emission spectra were obtained under pressure. After pressure release the hydrolytic activity of the ATPase was measured under optimal conditions. The stability of the different intermediate enzymatic species which accumulate during the catalytic cycle of the enzyme was investigated. The ATPase was most unstable towards pressure inactivation when calcium was bound to either the high or the low affinity calcium sites, with half-time for irreversible inactivation of 15 min under 1 kilobar. The nucleotide analog AMPPCP (that binds to the ATPase but is not hydrolyzed) promotes a dramatic stabilization of the ATPase which is not inactivated under 1 kilobar even after one hour. In the presence of ATP and micromolar calcium the ATPase becomes sensitive to pressure inactivation and millimolar calcium restores the stability. The spectroscopic data show that in all conditions a significant change in the microenvironment of tryptophan occurs when pressure is applied with a decrease in the center of mass of the spectra. Taken together, the spectroscopic and activity data indicate that a significant change in the conformation of the enzyme occurs at the nucleotide binding step in the presence of calcium. (Supported by CNPq and FINEP).

W-PM-B8 TRYPsin-INDUCED EFFLUX FROM SARCOPLASMIC RETICULUM: EVIDENCE FOR THE INVOLVEMENT OF THE (Ca²⁺ + Mg²⁺)-DEPENDENT ATPase. A. K. Dunker, J. L. Huang, T. B. Topping, Z. He and B. Folsom, Chemistry Department and Biochemistry/Biophysics Program, Washington State University, Pullman, WA 99163-4660.

Trypsin digestion of the sarcoplasmic reticulum membrane (SR) has been shown to lead to increased calcium permeability, the temperature dependence of which suggests the exposure of a channel rather than the tryptic release of a mobile carrier (Toogood et al., *Membrane Biochemistry* 5, 49-75; 1983). Here we will present data showing that: 1. an increased rate of efflux is not observed for membranes digested and kept at 15°C, but a temperature shift following arrested digestion leads to the development of increased calcium permeability; 2. two inhibitors of the ATPase, adenylyl-5'-yl imidodiphosphate and dicyclohexyl-carbodiimide (DCCD), both measurably retard the development of increased permeability at the higher temperature following arrested digestion - since previous results show that radioactive DCCD labels only the ATPase, this is strong evidence for the involvement of the ATPase in the trypsin-sensitive release process; 3. the permeability increase following digestion at 15°C and incubation at 35°C correlates ($r > 0.98$) with the second tryptic cleavage step of the calcium ATPase; 4. the rate of efflux depends on the concentration of the doubly cleaved ATPase molecules to the first power; possible second or higher power dependencies were subjected to the F test and could be rejected (confidence > 0.90 to 0.98). These data are most consistent with a model in which the second tryptic digestion step facilitates a separation of a single calcium ATPase molecule into functional ATPase and channel domains.

W-PM-B9 COVALENT LINKAGE OF BIOTIN TO CA²⁺ RELEASE PROTEIN OF SARCOPLASMIC RETICULUM (SR) ISOLATED FROM SKELETAL MUSCLE. N.F. Zaidi, J.J. Abramson*, C. Lagenaur†, and G. Salama. Intr. by J.H. Collins. University of Pittsburgh, Departments of Physiology and Neurobiology†, Pittsburgh, PA 15261 and *Portland State University, Department of Physics, Portland, OR 97207.

Reactive disulfide compounds like N-succinimidyl 3(2-pyridyl) dithiopropionate (SPDP) induces Ca²⁺ release from actively loaded SR vesicles. Their mode of action is via the oxidation of a free SH group on the SR Ca²⁺ release protein (RP) and the formation of disulfide bonds with the exogenously added reagents. SPDP has 2 reactive groups: its reactive S-S moiety covalently links with SH groups on the RP, and its succinimidyl group can be substituted with a probe, like biotin, useful for its high affinity to avidin. Two biotinylated disulfides were synthesized: SPDP-biotin and SPDP-biotin hydrazide triggered Ca²⁺ release from SR vesicles with the concomitant production of thiopyridone and the covalent linkage of biotin to SR proteins. The specificity of reactive disulfides to the RP was enhanced by iodoacetamide (0.5mM) or iodoacetic acid (1mM) which bound to SH groups without causing rapid Ca²⁺ release. SPDP-biotin and SPDP-biotin hydrazide (10 nmoles/mg SR) induced Ca²⁺ release was blocked by caffeine (2mM), ATP (1mM), or AMP-PCP (5mM) and reversed by dithiothreitol (1mM). SPDP biotin hydrazide labelled at most 10 out of 186 nmoles of accessible SH sites in SR (186 nmoles SH/mg SR) and the labelled proteins were identified by gel electrophoresis, followed by avidin-peroxidase reaction. DTT reduced the disulfide bond linking biotin to SR proteins and dissociated biotin from high molecular weight SR proteins. SPDP conjugated with appropriate probes can be used to elucidate the gating mechanism of the Ca²⁺ RP. Supported by AHA grants 87915 to J.J.A., 871065 to G.S., the Western Pennsylvania, and Oregon affiliates of the AHA, an RCDA to G.S. J.J.A. is an Established Investigator of the AHA.

W-PM-B10 VARIATION IN ACTIVITY OF SCALLOP SARCOPLASMIC RETICULUM WITH TEMPERATURE AND pH.

Vassilios Kalabokis and Peter Hardwicke, Department of Chemistry, Southern Illinois University, Carbondale, Illinois 62901.

The Arrhenius plot of Ca^{2+} -ATPase activity against $1/T$ of SR from *Placopecten magellanicus* could be resolved into two linear segments intersecting at 12°C . Above 12°C the activation energy was $8.5 \text{ kcal mole}^{-1}$ and below $22.6 \text{ kcal mole}^{-1}$. These are substantially below the values for rabbit skeletal muscle SR, but very similar to those found for lobster SR¹, indicating a similar adaptation of these two invertebrates to low ambient temperatures. The dependence of specific activity on pH was examined at two temperatures above the Arrhenius discontinuity and two temperatures below. The pH optimum was 7.3 above the discontinuity and 7.8 below the discontinuity; however the change in slope of the Arrhenius plot cannot be accounted for simply by the change in the optimum.

1. Madeira, V.M.C., Antunes-Madeira, M.C. and Carvalho, A.P. (1974) Biochem. Biophys. Res. Comm., 58, 897-904.

W-PM-B11 ANTHRAQUINONE INDUCED CALCIUM RELEASE FROM SR VESICLES IS INHIBITED BY CAFFEINE

Jonathan J. Abramson, Edmond Buck, Guy Salama¹, Issac N. Pessah². Portland State University, Dept. of Physics, P.O. Box 751, Portland, OR 97207, ¹Dept. of Physiology, University of Pittsburg, Pitts., PA 15261, ²Pesticide Chemistry and Toxicology Lab., Dept. of Entomological Sciences, University of California, Berkeley, CA 94720.

The interaction of various anthraquinones and the Ca^{2+} release protein from skeletal muscle sarcoplasmic reticulum (SR) has been examined. We have observed that micromolar concentrations of the anthracycline antibiotic adriamycin increases the Ca^{2+} sensitivity of ^3H -ryanodine binding to the SR Ca^{2+} release protein. The sensitizing effect elicited by adriamycin on Ca^{2+} activation of ryanodine binding is similar to that previously seen with caffeine. Adriamycin, daunorubicin, and mitoxantrone are all shown to stimulate Ca^{2+} release from actively loaded SR vesicles, and to induce transient contractions in chemically skinned muscle fibers. Upon the addition of millimolar concentrations of caffeine, anthracycline induced Ca^{2+} release from SR vesicles is inhibited. A caffeine concentration of 1 mM causes a 50% inhibition of the daunorubicin induced Ca^{2+} release rate, while 2 mM caffeine inhibits the rate to 20% of the zero caffeine control. Caffeine inhibition of anthracycline induced Ca^{2+} release is not competitive. The effective binding affinity of daunorubicin remains unchanged by caffeine, but the maximal Ca^{2+} efflux rate is decreased. The Hill coefficient, a measure of the degree of cooperativity for daunorubicin stimulated release of Ca^{2+} , also increases in the presence of millimolar concentrations of caffeine. Supported by AHA, Oregon and Western PA Affiliates of AHA. J.A. is an Established Investigator of AHA. G.S. supported RCDANS00909

W-PM-C1 IDENTIFICATION OF K⁺ CHANNEL TYPES MEDIATING SPIKE EVENTS IN CEREBELLAR PURKINJE NEURONS.

D.L. Gruol and A.J. Yool, Div. Preclin. Neurosci., Res. Inst. Scripps Clinic, La Jolla, CA 92037.

Using the single channel recording technique we have identified 6 K⁺ channel types that are present in the somatic and dendritic membrane of cerebellar Purkinje neurons (PNs), our experimental model. These K⁺ channel types are preferentially active over different voltage ranges, suggesting that differences in the population of active K⁺ channels may contribute to the voltage-sensitive nature of the intracellularly recorded electrical activity. For example, PNs exhibit fast spikes at depolarized membrane potentials and prolonged multiphasic spike events referred to as complex spikes (CS) at hyperpolarized potentials. In the present study, we correlated K⁺ channel activity with CS events that occur spontaneously and can be observed in cell-attached single channel recordings. Two K⁺ channel types, with single channel conductances of 27 pS and 40 pS, were commonly associated with the late phase of the CS, suggesting a functional role in the repolarizing phase of the CS. Consistent with this possibility is the fact that the late phase of the CS is relatively resistant to low concentrations of TEA (1-5 mM), as are the 27 and 40 pS K⁺ channel types. The K⁺ channel types highly sensitive to TEA, having conductances of 100 pS and 70 pS, if observed, were usually associated with the early fast phase of the CS which exhibits the most sensitivity to TEA. These data indicate that multiple K⁺ channels are active at membrane potentials that support complex spike activity and contribute to the CS event. Supported by NIH grant NS21777.

W-PM-C2 ARE THERE MULTIPLE TYPES OF DEPOLARIZATION-ACTIVATED K⁺ CHANNELS IN ADULT VENTRICULAR MYOCYTES? M. Apkon and J.M. Nerbonne (Intr. by Albert Roos). Washington Univ. Sch. of Med., St. Louis, MO.

In voltage-clamped adult rat ventricular myocytes, depolarizations evoke outward K⁺ currents which rise rapidly to a transient peak and decay to a plateau. Previously, as a result of differences in the pharmacological and voltage-dependent properties of the peak and plateau currents, we suggested that outward current waveforms reflect contributions from at least two distinct K⁺ current/channel types (Apkon and Nerbonne, 1986, *Biophys. J.* 49:55a). Here, we report preliminary studies aimed at characterizing the properties of depolarization-activated single K⁺ channels underlying the macroscopic currents. During depolarizations (-30 to +50mV) from holding potentials of -90 to -50mV, currents through single (K⁺) channels were measured in excised, outside-out membrane patches from isolated myocytes; the bath contained 5 mM Co²⁺ and 20 μM TTX (to block Ca²⁺ and Na⁺ currents) and recording pipettes contained (in mM): 135 KCl; 10 EGTA; 10 HEPES; 5 Glucose; 3 Mg-ATP; 0.5 Tris-GTP. Voltage-dependent channel activity was observed in ~10% of the patches (1-4 channels/patch). Leakage and capacity compensation were used and current signals were filtered (0.5-2kHz), digitized (2-20kHz) and stored; prior to analyzing records containing channel activity, idealized null records were subtracted in order to correct for uncompensated transients. Ensemble averaging of data obtained during 50-150 depolarizations revealed three types of activity: (1) channels with an opening probability which peaks in ~10 ms and decays to baseline within ~100 ms; (2) channels with an opening probability which rises rapidly and is sustained; and, (3) channels with a rapidly rising and slowly decaying opening probability. These results are consistent with the above-mentioned whole-cell data. Single channel conductances, estimated from all points (amplitude) histograms assuming a reversal potential of -80 mV, varied over the range 15-25 pS and were not clearly correlated with the ensemble averages. Present efforts are devoted to defining other characteristics (e.g., pharmacology, kinetics) which might allow the different K⁺ channel types to be more readily distinguished. Support: NIH: T-32 #GM07200, and #HL34161; and, AHA: Est. Inv. Award.

W-PM-C3 RELATION BETWEEN K⁺ CHANNEL EXPRESSION AND SCHWANN CELL PROLIFERATION IN WALLERIAN DEGENERATION S.Y. Chiu & G. Wilson (Intr. by David Brems). Dept. of Neurophysiology, Univ. of Wisconsin, Madison, WI 53706

When a peripheral nerve is transected, the myelin and axons distal to the transection site degenerate, and Schwann cells undergo a well-documented proliferation commonly referred to as Wallerian degeneration. Recent patch-clamp studies have shown that this occurrence of proliferation *in vivo* is accompanied by changes in excitable membrane properties of Schwann cells (Chiu, 1988, *J. Physiol.*, vol. 396, in press). In particular, voltage-gated Na and K channels, which are normally undetectable in Schwann cells of myelinated fibres, are expressed as degeneration ensues. In this report we examine whether the expression of excitable membrane properties plays a role in Schwann cell proliferation. Sciatic nerves from adult rabbits were excised, desheathed, cut into 2-4 mm segments and placed in tissue culture medium to allow Wallerian degeneration to occur *in vitro*. At 0-10 days, the explant segments were either treated with collagenase to dissociate Schwann cells for patch-clamp whole-cell recordings, or pulsed with ³H-thymidine to assay proliferation. The ³H-thymidine incorporation in the explant nerve segments increased progressively from 0 to 10 days as Schwann cell proliferation occurred. Concomitantly, an increase was observed in both the K and Na current density (pA/pF) in Schwann cells of myelinated fibres as measured in whole-cell patch clamp recordings. This expression of K current following nerve cut is similar to that observed in *in vivo* studies, and appears to be functionally important for Schwann cell proliferation to occur. Thus, specific blockers of K channels (quinine, TEA and 4-AP), when present in the culture medium, are found to also block Schwann cell proliferation. Indeed, the dose-response curves for inhibition of proliferation and blockage of K currents are quite similar, with the K_D for quinine, TEA and 4-AP being 0.04 mM, 1.5 mM and 0.2 mM for inhibition of proliferation, and 0.03 mM, 0.2 mM and 0.4 mM for blockage of K currents. It is unlikely that the inhibition of proliferation results from a block of mitogen release; cross-sectional EM examinations of nerves show that TEA did not retard the axonal and myelin degeneration which presumably is responsible for stimulating Schwann cell division after nerve cut. Rather a simpler explanation is that in Schwann cells the transduction of mitogenic signals at the plasma membrane might involve a voltage-gated K channel, as has been suggested in T-lymphocytes. Supported by NS-23375 (NIH), RG-1839 (National Multiple Sclerosis Society) and a Pew Scholar Award in the Biomedical Sciences to S.Y. Chiu

W-PM-C4 BLOCK OF MAMMALIAN BRAIN K CHANNELS BY THREE SCORPION VENOMS. Mary J. Schneider, Bruce K. Krueger, and Mordecai P. Blaustein. Department of Physiology, University of Maryland School of Medicine, Baltimore, Maryland 21201.

Scorpion venoms contain a variety of polypeptide neurotoxins that affect voltage-gated channels. Known scorpion toxins include an inhibitor of inactivation of voltage-dependent Na channels and blockers of non-inactivating K channels in squid axon and of the "maxi" Ca-activated K channel found in many excitable tissues. We have examined the effects of three scorpion venoms (Leiurus quinquestriatus, Tityus serrulatus, and Centruroides sculpturatus) on voltage-gated K channels in rat brain synaptosomes. By measuring depolarization-induced efflux of ^{86}Rb to assay for K channel function, we previously identified 1) a non-inactivating K channel, which is blocked by phencyclidine (PCP) and 4-aminopyridine (4-AP), 2) an inactivating K channel, which is also blocked by 4-AP and may be associated with the "A-current", and 3) a Ca^{2+} -activated K channel which is blocked by tetraethylammonium but is insensitive to 4-AP (Bartschat and Blaustein, *J. Physiol.* 361: 419, 1985). All three scorpion venoms (5 $\mu\text{g}/\text{ml}$) inhibited the non-inactivating K channel but none of the three venoms affected the inactivating K channel. In contrast, only L. quinquestriatus venom inhibited ^{86}Rb efflux through Ca-activated K channels. This activity may be due to charybdotoxin, a specific blocker of the "maxi" Ca-activated K channel present in L. quinquestriatus venom (Miller et al., *Nature* 313: 316, 1985). Thus, while all three scorpion venoms tested blocked the non-inactivating voltage-dependent K channels in rat brain synaptosomes only L. quinquestriatus venom also contained a blocker of the Ca-activated K channel. Supported by NIH.

W-PM-C5 VOLTAGE GATED K CHANNELS IN BROWN FAT. M.T. Lucero and P.A. Pappone, Department of Animal Physiology, University of California, Davis, CA 95616.

Brown adipose tissue (BAT) maintains body temperature and weight in newborn and hibernating mammals. Membrane permeability changes associated with adrenergic stimulation of BAT are postulated to regulate the metabolic response. To test this theory, we examined membrane electrical properties of isolated brown fat cells using the patch clamp technique in the whole cell mode. Interscapular BAT from 1 day old Osborne-Mendel rats was dissociated by collagenase treatment and plated in DMEM + 5% fetal calf serum. Our standard pipette solution was 155mM KF, 2mM MgCl_2 , 10mM HEPES, 0.5mM CaCl_2 , 5.5mM BAPTA, pH7.2. Our standard bath solution was 150mM NaCl, 5mM KCl, 2mM CaCl_2 , 10mM HEPES, pH 7.4. Under these conditions the only channel type present was a voltage dependent K channel with a peak current @ +50mV of $2000 \pm 700\text{pA}$ ($n=31$). Peak conductance in 155mM KCl bath solution @ +50mV ranged from 8 to 37 nS and a Boltzman equation fitted to the data gave $V_{1/2} = -29 \pm 3\text{mV}$, K (slope) = 4.7 ± 0.9 , ($n=6$). The K current also inactivated with depolarization; $V_{1/2} = -60\text{mV}$. We examined the selectivity of this channel and found relative permeabilities from the change in reversal potential of $\text{K}(1) > \text{Rb}(.81) > \text{NH}_4(.18) > \text{Na}(.03) = \text{Cs}(.02)$. Channel closing rates were affected by the current-carrying ion; Rb slowed and NH_4 speeded deactivation of the currents. The K_d for block by either TEA or 4AP was $\sim 2\text{mM}$. We did not observe K current block by 500nM apamin or 150nM charybdotoxin. Adding 3 μM norepinephrine (NE) had no effect on the K currents. Previous microelectrode recordings of NE application to BAT reveal a triphasic membrane response: a transient depolarization, a hyperpolarization, and a second sustained depolarization. We conclude that the voltage gated K channel in brown fat may be involved in the hyperpolarizing phase of the triphasic response. Supported by NIH grant AR34766.

W-PM-C6 COMPARISON OF MONOVALENT IONIC PERMEATION THROUGH THE INWARDLY RECTIFYING K CHANNEL IN GUINEA PIG VENTRICULAR MYOCYTES. R. Mitra and M. Morad, University of Pennsylvania, Dept. of Physiology, Philadelphia, PA 19104.

We have previously shown that Cs^+ carries significant current through the inwardly rectifying K^+ channel; that the activation of these currents is slower than K^+ currents through this channel; and that the Cs^+ currents are blocked by Mg^{2+} , Ca^{2+} , Cd^{2+} , Sr^{2+} , and Ba^{2+} in a voltage and time dependent manner (Mitra, R. and Morad, M. (1987) *J. Physiol.* (Lond.) 382: 128P). We now compare the inward currents through the channel carried by Li^+ , Na^+ , NH_4^+ , K^+ , Rb^+ , and Cs^+ . The results indicate that neither Li^+ nor Na^+ is significantly permeable through this channel while the order of permeability and rate of activation of the other ions is $\text{Cs}^+ < \text{NH}_4^+ < \text{Rb}^+ < \text{K}^+$. Furthermore, the degree to which divalent cations block these monovalent currents and thereby cause inactivation is exactly opposite to this permeability sequence. This order of permeation suggests that the selectivity of this channel is not based upon size alone since NH_4^+ (1.43A) is less permeable than the larger Rb^+ ion (1.49A); while neither Na^+ (0.98A) nor Li^+ (0.78A) carry appreciable current. The sequence of permeability and divalent block is similar to the binding sequence of those crown ethers and cryptands which selectively complex K^+ among monovalent ions (Pedersen, C.J. (1967) *J. Am. Chem. Soc.* 89: 7017; Lehn, J.M. & Sauvage, J.P. (1975) *J. Am. Chem. Soc.* 97: 6700). These observations suggest the importance of selective binding of the permeant ion in membrane channels as a step in permeation.

W-PM-C7 GLUCOSE MODULATION OF TWO K CHANNELS IN AN INSULIN-SECRETING CELL LINE.
 B. Ribalet, G.T. Eddlestone and S. Ciani. Dept. of Physiology; BRI; JLNRC. Univ. of Calif., Los Angeles, Ca 90024.

Using the Patch Clamp technique in studies of RINm5F cells two potassium channels were seen in the absence of glucose. In cell-attached patches we observed a voltage-independent, inward rectifying 55 pS channel and a voltage-dependent 140 pS channel with a linear I-V between -60 mV and +60 mV, the latter only following depolarization with 30 mM K^+ . In inside-out patches in symmetrical 140 mM K^+ solutions, two channels were observed, one with the same 55 pS conductance and inward rectification as the smaller channel in cell-attached patches, the other with a 205 pS linear conductance and calcium- and voltage-dependent kinetics. Adding physiological concentrations of Mg^{2+} reduced the conductance of this latter channel to a level close to that of the larger K channel seen in intact cells. The former channel we identify with the ATP-sensitive K (K(ATP)) channel, the latter with the calcium- and voltage-sensitive K (K(Ca,V)) channel.

The effect of glucose on open channel probability (P_o) was observed in cell-attached patches. (P_o in zero glucose was normalized to 100%). The K(ATP) channel P_o was reduced by 50% by 0.5 mM glucose and by >90% by 5 mM. The K(Ca,V) channel P_o was reduced by 50% by 4 mM glucose and by >90% by 15 mM. While cellular ATP (which is close to maximum at 5 mM glucose) modulates K(ATP) channel activity, the basis for modulation of K(Ca,V) channel activity was not known. The observation that the K(Ca,V) channel was rapidly and reversibly blocked by the phorbol ester TPA suggests that channel modulation may occur via protein phosphorylation.

The channels are affected by glucose in two ranges, one corresponds to the sub-threshold range for insulin release the other to the range in which release displays a sigmoid pattern. Therefore, we hypothesize that K(ATP) channel modulation determines membrane potential in the sub-threshold glucose range while K(Ca,V) channel modulation determines at least in part the periodicity of the electrical burst pattern accompanying insulin release.

W-PM-C8 BETA-ADRENERGIC MODULATION IN THE HEART: EVIDENCE FOR INDEPENDENT REGULATION OF K AND CA CHANNELS. K.B. Walsh, T.B. Begenisich and R.S. Kass. University of Rochester, Department of Physiology, 601 Elmwood Avenue, Rochester, NY 14642.

Beta-adrenergic stimulation of heart cells results in the enhancement of two important ionic currents: the delayed rectifier potassium current (I_K) and the L-type calcium current (I_{Ca}). The temperature-dependence of the actions of external application of isoproterenol or forskolin as well as internal dialysis of cyclic AMP (cAMP) or the catalytic subunit of cAMP-dependent protein kinase (CS) were examined on these two currents in patch-clamped guinea pig ventricular myocytes. Isoproterenol-mediated increases in I_K , but not I_{Ca} were very temperature-dependent over the range of 20 to 32 °C. At room temperature (20-22 °C) isoproterenol produced a large (3-fold) enhancement of I_{Ca} but had no effect on I_K . In contrast, at warmer temperatures (28-32 °C) both currents increased in the presence of this agonist. A similar contrast in the temperature-sensitivity of these currents also existed following exposure to forskolin, cAMP and CS, suggesting that this temperature-sensitivity of I_K does not arise at the level of the beta-receptor, the enzyme adenylate cyclase or the protein kinase holoenzyme. Thus, regulation of I_K channels but not I_{Ca} channels involves a temperature-dependent step either immediately preceding or following the CS-induced phosphorylation reaction of the I_K channel.

W-PM-C9 UP-REGULATION OF VOLTAGE-SENSITIVE K^+ CHANNELS IN MITOGEN-STIMULATED B LYMPHOCYTES.
 Jeffrey B. Sutro, Bharathi S. Vayuvegula*, Sudhir Gupta*, and Michael D. Cahalan, (intro. by R.V. McDaniel), Depts. of Physiology & Biophysics and Medicine (*), Univ. of Cal., Irvine, CA 92717.

Using the whole-cell patch clamp method we have studied ion channels in mouse splenic B lymphocytes before and after stimulation with lipopolysaccharide (LPS). The predominant channel in resting or activated cells is a K^+ -selective channel whose gating properties and single-channel conductance (16 pS) are similar to those of the K^+ channels in human T lymphocytes. No Na^+ currents or inward rectifier K^+ currents were found in these cells. Resting B cells have diameters of 5-7 μ m, and a geometric mean K^+ conductance of 250 pS, representing about 15 channels/cell. Treatment with 50 μ g/ml LPS for \geq 24 hrs can activate resting B cells to proliferate and to secrete antibodies. Activated B cells are enlarged (8-13 μ m diameter) and have greatly increased K^+ conductance (4300 pS/cell, ~270 channels per cell), representing a four-fold increase in conductance per unit surface area. Some B cells do not enlarge in response to LPS treatment, and such cells do not have increased conductance. The K^+ channel is blocked by quinine (25), verapamil (8 μ M), cetiedel (20 μ M), 4-aminopyridine (300 μ M) and tetraethylammonium (10 mM). These drugs inhibit B-lymphocyte activation (as measured by either 3H -thymidine uptake or inhibition of Ab production) with a potency sequence similar to that for channel block, indicating that K^+ channels must be functional for B cells to be activated. We confirm results by Dr. S. Hagiwara and colleagues that antibody-secreting hybridomas express voltage-gated Ca^{++} channels, but we have not found Ca^{++} channels in either resting or LPS-activated B cells. Supported by a postdoctoral fellowship from the American Cancer Society (PF-2789) and NIH grants NS14609 and AI 21808.

W-PM-C10 PINACIDIL, A PUTATIVE K-CHANNEL AGONIST, ENHANCES K-SENSITIVE CURRENT IN ISOLATED GUINEA PIG VENTRICULAR CELLS. J.P. Arena and R.S. Kass. University of Rochester, Department of Physiology, 601 Elmwood Ave, Rochester, NY 14642.

We report a reversible enhancement of an outward K-sensitive current induced by Pinacidil (*N*'-Cyano-*N*-4-pyridyl-*N*'-1,2,2-trimethylpropylguanidine, monohydrate) in enzymatically isolated guinea pig ventricular cells. Membrane currents were recorded at room temperature using a whole cell arrangement of the patch voltage clamp. Physiological internal and external solutions were used with the addition of 3mM ATP and 11 mM EGTA to internal solution. In some experiments external Na was replaced with TRIS. Current was measured in response to brief (40 ms) voltage pulses applied from holding potentials of -40 mV or -80 mV in the absence and presence of Pinacidil. Pinacidil-induced current (p-current) was measured as the difference between the average of currents in control and washout and current in the presence of Pinacidil. Pinacidil (50-100 μ M) induces an outward current at voltages positive to E_K . This response to pinacidil does not require Ca entry via L- or T-type channels because it is neither blocked by nisoldipine (200 nM at -40 mV), nor changes in holding potentials from -80 to -30 mV. The current-voltage relationship for p-current is linear from E_K to approximately 100mV positive to E_K . We were unable to detect inward pinacidil-sensitive current at voltages negative to E_K , but the zero current potential was close to E_K over a K concentration range of 1 to 140 mM, suggesting that this is a K channel current. In support of this, we found this current fully blocked by addition of external Ba^{2+} (10 mM). Our results suggest that this compound does indeed enhance K channel currents in guinea pig ventricular cells, but the voltage- and ion-dependence of this current are markedly different from other K-channel currents previously described in these preparations.

W-PM-C11 REMOVAL OF FAST K CHANNEL INACTIVATION IN GH3 CELLS BY PAPAINE AND N-BROMOACETAMIDE. D.R. Matteson and P. Carmeliet, University of Maryland School of Medicine, Department of Biophysics, Baltimore, MD. We have used the whole-cell variation of the patch clamp technique to study voltage dependent potassium currents in GH3 cells. An inactivating, voltage-dependent K current was isolated from Ca-activated K currents using internal Ca chelators and external tetraethylammonium (TEA) ions. Patch pipettes were filled with a solution containing (in mM) 80 Kglutamate, 30 KCl, 25 KF, 2 $MgCl_2$, 10 EGTA (KOH) and 10 Hepes (pH 7.2). The external solution contained 130 NaCl, 5 KCl, 10 $CaCl_2$, 10 Hepes (pH 7.4), 10 TEA and 200 nM TTX. During a step to +70 mV under these conditions, an outward potassium current activates rapidly to a peak in 4 to 5 ms, and then declines due to inactivation. Inactivation in these control cells is best fit by the sum of two exponentials, with time constants of 25 and 79 ms. This normal, relatively fast inactivation process is removed by treatment with internal proteolytic enzymes (papain at 0.1 to 0.7 mg/ml in the internal solution) or external N-bromoacetamide (NBA; 3 to 100 μ M). For example, five to seven minutes after breaking into a cell with internal solution containing papain, the K current inactivated very slowly with a time constant of 500 to 750 ms, and inactivation was less complete. At earlier times after break-in with papain, inactivation appeared to be partially modified, with one population of channels inactivating normally and another population undergoing only slow inactivation. In contrast to inactivation, activation of the K channels is not significantly affected by papain or NBA. The action of these reagents on K channels is comparable to their action on Na channels, suggesting that inactivation in Na and K channels occurs by a similar mechanism.

W-PM-C12 THE α_K SUBUNIT, NOT THE $\beta\gamma$ DIMER MEDIATES THE EFFECT OF G_k , THE G PROTEIN THAT ACTIVATES MUSCARINIC ATRIAL K^+ CHANNELS. A. M. Brown (1), A. Yatani (1), G. Kirsch (1), J. Codina (2), and L. Birnbaumer (2). Departments of Physiology and Molecular Biophysics (1), and Cell Biology (2), Baylor College of Medicine, One Baylor Plaza, Houston, Texas 77030.

The conclusion of Logothetis et al. (1987) was the opposite to ours (Codina et al., 1987). Our conclusion is reaffirmed in this abstract. They used chick embryo atria and we used adult guinea pig atria, so we examined whether the differences were phylogenetic, ontogenetic or tissue culture-related. We also tested whether the zwitterionic detergent CHAPS used at 184 μ M to prevent their $\beta\gamma$ dimers from reaggregating, had effects. We applied the gigaseal patch clamp method to atrial membranes of single cells from 12-14 d chick embryos, 1-3 d neonatal rats and adult guinea pigs. Solutions were essentially symmetrical (mM): KCl, 140; EGTA, 5; $MgCl_2$, 5; HEPES, 10; pH 7.2. Holding potentials were usually -80 to -100 mV. Single atrial K^+ channel currents were identified by ACh responsiveness, ≈ 40 pS conductances and ≈ 1.0 msec open taus. After excision from cell-attached to inside-out, vesicles formed frequently and changes in bath [GTP] no longer affected currents. Such preparations were discarded. α_K prepared from human rbc's and preactivated with GTP γ S (α_K^*) was added directly to a static bath. α_K^* activated single atrial K^+ channel currents in all three preparations in a concentration-dependent manner. The K_D 's were picomolar. $\beta\gamma$ dimers at pM concentrations were ineffective. CHAPS at 5 μ M stimulated single channel currents that were indistinguishable from single muscarinic atrial K^+ channel currents. We conclude: a) that CHAPS may cause $\beta\gamma$ effects, and b) that regardless of age, species or tissue culture conditions, α_K^* mediates the G_k effects. Just as for transducin and the adenylyl cyclase G protein activator, G_s , the α subunit mediates the effects of the G_k holoprotein.

W-PM-C13 DISCRETE MARKOVIAN MODELS RANKED ABOVE FRACTAL MODELS FOR SINGLE CHANNEL KINETICS OF LARGE CONDUCTANCE CALCIUM-ACTIVATED POTASSIUM CHANNEL, GABA-ACTIVATED CHANNEL, FAST CHLORIDE CHANNEL, AND ACETYLCHOLINE RECEPTOR CHANNEL. K.L. Magleby, O.B. McManus, D.S. Weiss, A.L. Blatz(1), and C.E. Spivak(2). Department of Physiology & Biophysics, University of Miami School of Medicine, Miami Fl 33101; (1)Department of Physiology, University of Texas, Dallas, TX 75235; and (2)NIDA Addiction Research Center, Baltimore, MD, 21224.

Mechanisms usually considered for the gating of ion channels assume that the channels can exist in a number of discrete kinetic states with reversible transitions between the states, and with rate constants which do not vary in time. Such Markovian models predict that distributions of interval durations will be described by sums of exponentials. Recently, Liebovitch et al. (1987; *Biochim et Biophys Acta* 896:173-180) have proposed a fractal model for ion channel kinetics. We have examined single channel data from four different channels to determine whether a discrete Markovian model or a fractal model gave a better description of the distributions of open and shut interval durations. In all ten of the ten different examined distributions of intervals from the four different ion channels, discrete Markovian models gave better visual descriptions of the data than fractal models, and a predictor error statistical test, which compares fits by applying a penalty for additional free parameters, ranked the Markovian models above the fractal models. As the number of analyzed intervals was increased, the superior fits by the Markovian models and the poorer fits by the fractal models became increasingly apparent. These data suggest that the single channel kinetics for at least four different ion channels are best described by Markovian models and inconsistent with fractal models. Supported by grants from the NIH and the Muscular Dystrophy Association.

W-PM-D1 COOPERATIVITY OF GIZZARD ACTO-HMM ATPASE ACTIVITY IN THE PRESENCE OF GIZZARD TROPOMYOSIN. Samuel Chacko and Evan Eisenberg, U. of Pa, Phil., PA and NHLBI, NIH, Bethesda, MD

Although several studies have shown that smooth muscle tropomyosin causes a 3-fold increase in the actin-activated ATPase activity of smooth muscle myosin, the mechanism of this effect is not yet understood. In the present study we reinvestigated the effect of smooth muscle tropomyosin, using smooth muscle actin and phosphorylated smooth muscle HMM to define which steps in the kinetic cycle are affected by tropomyosin and to determine whether, as in the skeletal muscle system, the smooth muscle tropomyosin-actin complex exists in a turned-off and turned-on form. Double reciprocal plots of ATPase activity vs actin concentration showed that smooth muscle actin is very similar to skeletal muscle actin in its ability to activate the smooth muscle HMM ATPase activity. Similar experiments in the presence of smooth muscle tropomyosin, showed that it had no effect on K_{ATPase} but did cause a three-fold increase in V_{max} . This suggests that smooth muscle actin may have to be complexed with tropomyosin, in order for the actin to be in its optimal conformation to activate the HMM ATPase activity. However, even though the tropomyosin-actin complex was more effective than actin alone in activating the HMM ATPase activity, it was not fully turned on. When we added NEM-S-1, which, even in the presence of ATP, forms rigor bonds with actin and is able to fully turn on the skeletal tropomyosin-actin complex, we found a further 3-fold increase in V_{max} and also a 6-fold increase in K_{ATPase} . These results show that, as with skeletal muscle tropomyosin, the smooth muscle tropomyosin-actin complex occurs in a turned-off and a turned-on form, and the presence of rigor bonds between S-1 and actin cooperatively shift it into the turned-on form.

W-PM-D2 PROTEIN PHOSPHORYLATION IN CHEMICALLY-SKINNED AND INTACT VASCULAR SMOOTH MUSCLE: IDENTIFICATION OF MYOSIN HEAVY CHAIN AS A PHOSPHOPROTEIN. L. P. Adam, J.R. Haeberle, D. Lakey, B. A. Trockman and D.R. Hathaway. Depts. of Medicine and Physiology, Indiana University School of Medicine Indianapolis, IN

Intact vascular smooth muscle readily maintains isometric force at low levels of phosphorylation of the 20,000 dalton myosin light chain (LC_{20}) while chemically-skinned muscles do not. Recently, we have compared protein phosphorylation profiles for several proteins including LC_{20} , myosin heavy chain (HC), caldesmon (CD) and a caldesmon immunoreactive protein (CIP) in chemically-skinned (contracted in the presence of 20uM Ca^{++} and 10uM calmodulin) and intact muscles (contracted by K^{+} -depolarization). Caldesmon (Mr-150kDa) was not significantly phosphorylated in either skinned or intact carotid muscle. Interestingly, CIP (Mr-80kDa) was phosphorylated in both skinned and intact muscle. In skinned muscles, phosphorylation of CIP was 0.08 mol/mol at 10 min. and 0.2 mol/mol at 60 min. Myosin HC was also phosphorylated in skinned and intact carotid muscle. In skinned muscles, incorporation of $^{32}PO_4$ into the 200 kDa form of myosin HC occurred slowly and was still rising at 60 min. at which point 0.06 mol/mol was incorporated. Under similar conditions, LC_{20} phosphorylation levels rose to greater than 1 mol/mol in 10 min. and remained elevated. The 204 kDa myosin HC was not phosphorylated under any condition in skinned muscle. Both the 204 kDa and 200 kDa forms of myosin HC were phosphorylated in intact carotid muscle under conditions where "latching" of the muscles occurred; i.e., where LC_{20} phosphorylation levels peaked and then decreased to low levels (<.1 mol/mol). Our data indicate that myosin HC and CIP can be phosphorylated in vascular smooth muscle. These could represent important new mechanisms regulating actin-myosin interaction.

W-PM-D3 PHOSPHORYLATION OF VASCULAR SMOOTH MUSCLE MYOSIN HEAVY CHAIN BY TWO PROTEIN KINASE ACTIVITIES. Robert C. Turner and David R. Hathaway, Department of Medicine and the Krannert Institute of Cardiology, Indiana University School of Medicine, Indianapolis, IN.

Phosphorylation of the heavy chain (HC) has been described for several vertebrate and non-vertebrate myosins. Recently, we have observed phosphorylation of the HC of mammalian vascular smooth muscle myosin. Myofibrils prepared from either porcine carotid artery or bovine aortic smooth muscle contained a protein kinase activity that specifically phosphorylated the 200 kDa form of myosin HC. Phosphorylation required calcium and calmodulin and was inhibited by trifluoperazine (50 uM) or an excess of EGTA. The time course of HC phosphorylation was slow compared to that of the 20kDa light chain. HC phosphorylation continued to rise over 60 min. while light chains were fully phosphorylated in 2-5 min. Maximal phosphate incorporation into the HC was less than 0.2 mol/mol. In an attempt to identify possible candidates for myosin HC kinase activity, protein kinase C was purified to homogeneity from canine brain and incubated with purified bovine aortic myosin. Incorporation of phosphate was measured in both the 204 kDa and 200 kDa forms of vascular myosin HC. At 60 min., phosphate incorporation into the 204 kDa HC was 1.13 ± 0.3 mol/mol, and into the 200 kDa form 0.65 ± 0.2 mol/mol. The two-fold difference was measured after correcting for the small difference in the relative amounts of the HC present (i.e. 204 kDa = 55%; 200 kDa = 45%). Our data indicate that at least 2 protein kinases can phosphorylate the HC of vascular smooth muscle myosin. An endogenous kinase that is calcium and possibly calmodulin-dependent is specific for the 200 kDa form of myosin HC while protein kinase C preferentially phosphorylates the 204 kDa form. HC phosphorylation in mammalian vascular smooth muscle may contribute to the unusual mechanical properties of this muscle.

W-PM-D4 ACTIVE SITE PHOTOLABELING OF THE 6S AND 10S CONFORMATIONS OF GIZZARD MYOSIN WITH 3'(2')-O-(4-BENZOYL)BENZOYL ATP(Bz₂ATP). Douglas G. Cole and Ralph G. Yount. Biochemistry/Biophysics Program and Department of Chemistry, Washington State University, Pullman, WA 99164.

Bz₂ATP was used as a photoprobe of the ATP binding site of unphosphorylated chicken gizzard myosin. Bz₂ADP was stably trapped at the active site of myosin in nearly stoichiometric amounts by complexation with vanadate and Co²⁺. Replacing Mg²⁺ with Co²⁺ was essential to prevent a vanadate dependent photomodification of the enzyme and release of Bz₂ADP (see Cremonesi, Grammer and Yount, these abstracts). Irradiation of myosin containing trapped [³H]Bz₂ADP gave 30% covalent incorporation into the enzyme. Analysis by SDS gel electrophoresis showed that all of the [³H]Bz₂ADP was attached to the 200 kDa heavy chain. No label was found on LC17 as has been observed using other photoreactive ADP analogs to label gizzard myosin (Okamoto *et al.*, *Nature*, 324, 78, 1986). Subfragment one, obtained from papain digested photolabeled myosin, was treated briefly with trypsin to produce characteristic peptides. Only the central 50 kDa peptide and its 68 kDa precursor were found to be labeled by [³H]Bz₂ADP. [³H]Bz₂ADP·Pi was also trapped on gizzard myosin by forming the 10S folded conformation. Again, only the heavy chain was found to be photolabeled. Experiments are in progress to determine the specific sites of labeling. Supported by NIH (DK 05195).

W-PM-D5 THE REGULATORY LIGHT CHAIN IS REQUIRED FOR FOLDING OF SMOOTH MUSCLE MYOSIN. Kathleen M. Trybus and Susan Lowey. Rosenstiel Basic Medical Sciences Research Center, Brandeis University, Waltham, MA 02254.

Light chain phosphorylation causes the folded monomeric form of myosin to extend and assemble into filaments. This observation established the involvement of the regulatory light chain (RLC) in conformational transitions of smooth muscle myosin. In order to assess the role of this subunit in the intramolecular folding of myosin, the RLC of turkey gizzard myosin was completely removed at elevated temperature (41°C) in the presence of EDTA through the use of an antibody affinity column. Metal-shadowed images in 0.5 M ammonium acetate showed that RLC-deficient myosin had a tendency to aggregate through the neck region, as had been previously observed with denuded skeletal muscle myosin. HPLC gel filtration of this material in 0.4 M KCl confirmed that it was a mixture of monomeric myosin, small aggregates that eluted with the void volume, and larger aggregates that pelleted upon centrifugation. When MgATP was added to filaments formed from RLC-deficient myosin, less than 10% of the myosin was solubilized, indicating that myosin could not fold in the absence of light chain. Readdition of regulatory light chain restored the myosin to its original solubility properties, thus establishing reversibility. Addition of foreign light chains from skeletal or scallop muscle myosin, or a chymotryptic-cleaved gizzard light chain, produced a monomeric myosin in high salt that was similar to that obtained by recombination with the homologous light chain. However, the ability of the smooth muscle myosin to assume the 10S conformation was impaired by the heterologous or truncated light chain. These results are consistent with the hypothesis that the regulatory light chain contributes to a binding site for the tail region of myosin. (Supported by NIH grants R29 HL38113 and R37 AR17350.)

W-PM-D6 PHOSPHOPEPTIDE MAPS OF THE 20,000 DA MYOSIN LIGHT CHAIN ISOFORMS PHOSPHORYLATED IN VIVO AND IN VITRO. F. Erdődi, M. Bárány and K. Bárány. College of Medicine, University of Illinois at Chicago, Chicago, IL 60612.

The 20,000 Da myosin light chain (LC) exists as two isoforms in arterial smooth muscle. Phosphorylation of LC isoforms was induced *in vivo* by contracting arteries with K⁺, and *in vitro* by incubating aorta homogenate or crude actomyosin with Mg²⁺, Ca²⁺ and [³²P]ATP. The extent of LC phosphorylation was 0.7, 0.8 and 2 mol phosphate/mol LC in intact artery, aorta homogenate and actomyosin, respectively. Seven phosphorylation sites, labelled A through G, were identified in LC by 2D phosphopeptide mapping. Phosphoamino acid analysis revealed Ser-P in peptides A, B and E, Thr-P in peptides F and G, and both Ser-P and Thr-P in peptides C and D. In contracting artery both isoforms were mono-, and diphosphorylated. The monophosphorylated isoforms exhibited peptides A, B and E, while the diphosphorylated isoforms contained these peptides and in addition peptides C and D. Phosphorylation in homogenate resembled that of intact muscle. In actomyosin mono-, di-, and triphosphorylated isoforms were found. Peptides C, D, E and F were the major phosphorylated sites while peptides A, B and G were phosphorylated to a lesser extent. ML-9, an inhibitor of MLCK, strongly inhibited phosphorylation in homogenate, whereas H-7, an inhibitor of protein kinase C, was less effective. ML-9 and H-7 inhibited LC phosphorylation in actomyosin to the same extent. It appears that in intact muscle and in homogenate, phosphorylation is induced predominantly by MLCK whereas in actomyosin both MLCK and protein kinase C are involved. (Supported by NIH, AM 34602).

W-PM-D7 REGULATION OF THE ACTIN-ACTIVATED ATPase ACTIVITY OF THYMUS MYOSIN BY FILAMENT ASSEMBLY.
Paul D. Wagner and Ngoc-Diep Vu, Laboratory of Biochemistry, National Cancer Institute, Bethesda, MD 20892.

Both the actin-activated ATPase activities of vertebrate nonmuscle myosins and their assembly into filaments are affected by phosphorylation of their 20,000-Da light chains. We have previously shown that the actin-activated ATPase activities of filamentous, unphosphorylated and phosphorylated thymus myosins have the same maximum rates. While phosphorylation does cause a decrease in K_{app} , in the presence of tropomyosin the decrease in K_{app} appears to be too small for this phosphorylation to be an effective regulatory system. These assays were performed under conditions where both the unphosphorylated and phosphorylated myosins were filamentous. We have now examined the effects of light chain phosphorylation on the actin-activated ATPase activity and filament assembly of thymus myosin under a variety of conditions. Under conditions where phosphorylation increased filament formation, there were large increases in actin-activated ATPase activity upon LC20 phosphorylation, but under conditions where phosphorylation had only a small effect on filament assembly, it had only a small effect on actin-activated ATPase activity. By varying the myosin concentration, it was possible to have under the same assay conditions, either predominantly monomeric, unphosphorylated myosin which was not activated by actin or predominantly filamentous, unphosphorylated myosin which was activated by actin. These results suggest that phosphorylation may regulate actomyosin based motile activities in vertebrate nonmuscle cells by regulating myosin filament assembly. However, if the unphosphorylated myosin in vivo is filamentous, there must be some other mechanism for regulating its interaction with actin.

W-PM-D8 PROTEIN KINASE C CAN PHOSPHORYLATE MYOSIN HEAVY AND LIGHT CHAINS IN INTACT HUMAN PLATELETS. Sachiyo Kawamoto, A. Resai Bengur, James R. Sellers and Robert S. Adelstein. (Intr. by: Alan N. Schechter) NHLBI, NIH, Bethesda, MD 20892

When human platelets were treated with 12-O-tetradecanoylphorbol 13-acetate (TPA) The 20-kDa myosin light chain (MLC) as well as the myosin heavy chain (MHC) were found to be phosphorylated. The phosphorylation of the MHC was localized by two-dimensional peptide mapping to a serine site in a single tryptic peptide. This phosphopeptide comigrated with a peptide that was produced following *in vitro* phosphorylation of platelet MHC using protein kinase C and had been localized to the light meromyosin region of the MHC. The phosphorylatable MLCs were found to consist of two isoforms present in approximately equal amounts, but with different isoelectric points. Following TPA treatment monophosphorylated and diphosphorylated forms of each MLC were identified. While the monophosphorylated form was found to be phosphorylated at a serine site known to be phosphorylated by protein kinase C (corresponding to ser-1 or 2 in gizzard MLCs) the diphosphorylated form was found to be phosphorylated at two serine sites, one known to be phosphorylated by MLC kinase (corresponding to ser-19 in gizzard MLCs) and the other by protein kinase C (ser-1 or 2). Following TPA treatment phosphate incorporation rose from negligible levels to 1.2 mol P/mol MLC and 0.7 mol P/mol MHC. These results suggest that protein kinase C can phosphorylate both MHCs and MLCs in intact platelets.

W-PM-D9 COOPERATIVE DEPENDENCE OF THE ACTIN-ACTIVATED Mg^{2+} -ATPase ACTIVITY OF ACANTHAMOEBA MYOSIN II ON THE EXTENT OF FILAMENT PHOSPHORYLATION. Mark A.L. Atkinson, and Edward D. Korn, LCB, NHLBI, NIH, Bethesda, Md 20892.

The actin-activated Mg^{2+} -ATPase of myosin II from *Acanthamoeba castellanii* is regulated by phosphorylation of three serine residues at the tip of the tail of each of its two heavy chains; only dephosphorylated myosin II is active. We have chemically modified dephosphorylated myosin II with N-ethyl maleimide (NEM). The modification occurs primarily at a single site within the NH_2 -terminal 73,000 Da of the globular head of the heavy chain. NEM modification had no effect on the ability of the myosin to bind to F-actin or to form filaments but inhibited the Ca^{2+} -ATPase, Mg^{2+} -ATPase and actin-activated Mg^{2+} -ATPase activity of the dephosphorylated myosin II. Native phosphorylated myosin II regained actin-activated Mg^{2+} -ATPase activity when copolymerized with NEM-inactivated dephosphorylated myosin II and the increase in activity was cooperatively dependent on the fraction of NEM-dephosphorylated myosin II in the filaments. From this result, we conclude that all heads within a filament are equivalent, irrespective of the state of phosphorylation of the tails to which they are linked, and that the specific activity of each molecule is highly cooperatively dependent upon the global state of phosphorylation of the filament. This enables the actin-activated Mg^{2+} -ATPase activity of myosin II filaments to respond rapidly and extensively to small changes in the level of their phosphorylation.

W-PM-D10 REGULATION OF DICTYOSTELIUM MYOSIN ASSEMBLY BY ACTIN FILAMENT NETWORKS. J.D. Pardee, K.T. Vaughan, R.K. Mahajan, and J.A. Johns. Dept. of Anatomy and Cell Biology, Cornell University Medical College, New York, NY. 10021.

Since *Dictyostelium* myosin thick filaments are located in the actin-rich cortex of motile cells, we have examined the effects of actin filament networks on *Dictyostelium* myosin assembly. As evidenced by fluorescence energy transfer (FET) and light scattering spectroscopy, myosin assembly is accelerated approximately 5 fold by actin filaments when 1 mM ATP is present. Assembly rates are linearly dependent on F-actin concentration between 0 - 1 μ M, with a stoichiometric ratio of approximately 10 moles actin / mole myosin giving maximum assembly acceleration. Mixtures of 1mM AMPPNP with 1 μ M F-actin also cause accelerated thick filament formation, although the assembly rate does not reach that achieved by ATP. In contrast, actin filaments in the presence of ADP abolish myosin assembly. Addition of severin to mixtures of actin filaments and assembling myosin causes immediate fragmentation of actin filaments and an immediate cessation of accelerated myosin assembly. FET assays employing donor-labeled myosin and acceptor-labeled F-actin demonstrate that individual myosin molecules associate with actin filaments at a rate equivalent to the accelerated myosin assembly rate, suggesting myosin to actin binding before thick filament formation. Electron microscopic examination of myosin thick filament formation in the presence of actin filaments supports a model of actin filament mediated myosin assembly. In ADP, myosin monomers rapidly decorate F-actin, preventing self-association of myosin. During AMPPNP accelerated assembly, thick filaments are positioned axially along the length of actin filaments and organize randomly arranged actin networks into cylindrical arrays. ATP accelerated assembly results in formation of contracted actomyosin filament complexes. These results suggest a significant regulatory role for actin cytoskeletal structures in non-muscle myosin assembly. Supported by NIH Grant GM32458.

W-PM-D11 CONCENTRATION DEPENDENCE OF FLUORESCENCE BEHAVIOR FOR THE Ca(2+) INDICATOR FURA2 by Stefan Highsmith and Kenneth W. Snowdowne, Department of Biochemistry, University of the Pacific, San Francisco, CA 94115.

The Ca(2+) indicator FURA2 has a linear increase in fluorescence intensity in solution for increasing [FURA2] up to 4 μ M. Above 4 μ M, in the presence or absence of Ca(2+), the observed fluorescence intensity is substantially quenched. Above 30 μ M FURA2, the observed intensity decreases with increasing [FURA2]. Excitation spectra of FURA2 with and without Ca(2+), at the high concentrations (>50 μ M) typically used in fluorescence ratio determinations of changes in intracellular [Ca(2+)], are strikingly different from those at 1 μ M FURA2. At 60 μ M, the -Ca(2+) spectrum has its maximum shifted to 328 from 360 nm, while the +Ca(2+) spectrum has two peaks at 361 and 312 nm, instead of one at 340 nm.

Including sucrose up to 40% (w:v) in 10 μ M FURA2 solutions decreased the fluorescence intensity from 36% (0% sucrose) to 51% (40% sucrose) of the value expected if quenching were absent. The same range of sucrose increased the steady-state polarization five-fold. These results and the appearance of new bands in the excitation spectrum suggest that FURA2 aggregates substantially in aqueous solutions of greater than 4 μ M FURA2.

(Supported by N.I.H. Grants DK 37729 and AM 25177 and A.H.A. California Affiliate Grants to S.H. and K.W.S.)

W-PM-E1 CHARACTERIZATION OF PHOSPHATIDYLINOSITOL 4,5-BISPHOSPHATE PRODUCTION IN SKELETAL MUSCLE TRIADS. Scott D. Jay and Kevin P. Campbell, Department of Physiology and Biophysics, University of Iowa, Iowa City, IA 52242.

It has been proposed that inositol 1,4,5-trisphosphate (InsP₃) may be the messenger responsible for excitation-contraction (E-C) coupling in skeletal muscle. Work by Hidalgo et al. (FEBS LETTERS 202(1):69, 1986) supported this hypothesis by showing that phosphatidylinositol (PtdIns) is phosphorylated to PtdIns 4-P and PtdIns 4,5-P₂ in isolated transverse tubular vesicles. It is our aim to examine the potential role of phosphoinositides in E-C coupling using isolated triads which are enriched in both dihydropyridine and ryanodine binding. Skeletal muscle membrane fractions were phosphorylated with γ -³²P-ATP and assayed for the production of labeled PtdIns 4-P and PtdIns 4,5-P₂. PtdIns 4,5-P₂ production was specific for isolated triads and T-system membranes prepared from French-press treated triads, as compared with sarcoplasmic reticulum and surface membrane vesicles, thus indicating that this phosphorylation reaction is enriched in the junctional T-system. The phosphorylation was rapid ($t_{1/2} < 30$ s), and is independent of calmodulin and cAMP-dependent protein kinase. There appears to be regulation by divalent cations with millimolar Mg²⁺ producing a maximal stimulatory effect on the phosphorylation, and micromolar free Ca²⁺ having an inhibitory effect. Future experimental goals include: the study of the hydrolysis of PtdIns 4,5-P₂ to InsP₃, the identification/purification of the kinase, and examination of possible phosphoinositide specific protein interactions in isolated triads. (Work supported by NIH HL37187 & Lutheran Brotherhood Fellowship).

W-PM-E2 INOSITOL (1,4,5)-TRISPHOSPHATE ACTIVATES A CALCIUM CHANNEL IN ISOLATED SARCOPLASMIC RETICULUM (SR) MEMBRANES. Benjamín A. Suárez-Isla, Verónica Irribarra, Ricardo Bull, Andrés Oberhauser, Laura Larralde, Enrique Jaimovich, and Cecilia Hidalgo. Centro de Estudios Científicos de Santiago, P.O. Box 16443, Santiago 9, and Department of Physiology and Biophysics, Faculty of Medicine, University of Chile, P.O. Box 70055, Santiago 7.

We report here that inositol (1,4,5)-trisphosphate (InsP₃), a proposed internal agonist of EC coupling (1,2), activates a high conductance calcium channel present in highly purified SR membrane vesicles from frog skeletal muscle (*C. caudiverbera*; see Irribarra et al., this meeting), by increasing channel fractional open time (P_o) without effect on the single channel conductance. SR vesicles were fused into neutral (POPE/PC 4:1) or charged (POPE/PS 1:1) planar bilayers and the single channel conductance was ca. 100 pS with 37 mM trans Ba or Ca.

In charged bilayers formed by POPE/PS, addition of 10 μ M InsP₃ (cis) in the presence of 40 μ M cis Ca increased P_o from 0.10 ± 0.01 (mean \pm S.E.M.) in the control to 0.18 ± 0.02 ($p < 0.01$); P_o evaluated from records of 280 seconds). Further additions of InsP₃ brought P_o up to 0.85 ± 0.02 at 50 μ M InsP₃ in an approximately sigmoidal fashion, indicating an apparent half-maximal activation at 15 μ M InsP₃. In neutral POPE/PC bilayers, addition of 13.5 μ M InsP₃ in the presence of 10 μ M cis Ca produced a significantly greater increase in P_o from 0.01 to 0.75, suggesting that InsP₃ responses are induced at lower agonist concentration in neutral as compared to charged artificial membranes. The agonistic effect of InsP₃ was also seen in the presence of high cis Mg (8 mM). These results are consistent with the proposed role of inositol (1,4,5)-trisphosphate as a physiological agonist of EC-coupling. 1. Vergara et al. PNAS 82, 6352 (1985). 2. Volpe et al. Nature, 316, 347 (1985). Supported by NIH Grants GM35981 and HL23007, FONDECYT 598, MDA, DIB and Tinker Foundation.

W-PM-E3 INOSITOL (1,4,5) TRISPHOSPHATE INDUCES CALCIUM RELEASE FROM SKINNED FROG SKELETAL MUSCLE. Cecilia Rojas, Eduardo Rojas, Manuel Kukuljan and Enrique Jaimovich. Department of Physiology and Biophysics, Faculty of Medicine, University of Chile. P.O. Box 70055 Santiago.

As controversial evidence on the effect of inositol trisphosphate (InsP₃) on calcium release in skeletal muscle has been presented, we tested the effect of InsP₃ and other compounds on the aequorin light signal using mechanically skinned fibre bundles from sartorius muscle of the frog *C. caudiverbera*. After skinning, fibre bundles were loaded with 0.1 mM Ca²⁺ for 120 min and incubated in a medium containing 130 mM sodium glutamate, 2.5 mM ATP, 3 mM Mg²⁺, and were placed in a dark chamber in front of a photomultiplier window. Micromolar concentrations of InsP₃ induce a release of Ca⁺⁺ on the order of 5 nmoles/g wet weight; the release signal being comparable to that induced by caffeine (7 mM). Unlike caffeine, the effect of InsP₃ is dependent on Ca²⁺ concentration and buffer capacity of the incubation media. Time to peak of the signals, largely determined by mixing, is between 100 and 150 ms. Financed by NIH Grant 35981, Muscular Dystrophy Association, FONDECYT, Univ. de Chile DIB 2123.

W-PM-E4 TRANSVERSE TUBULE VOLTAGE CONTROL OF INOSITOL-TRISPHOSPHATE-INDUCED Ca^{2+} RELEASE IN PEELED SKELETAL MUSCLE FIBERS. Sue K. Donaldson, Nelson D. Goldberg, Timothy F. Walseth, and Daniel A. Huetteman. University of Minnesota, Minneapolis, MN 55455.

Inositol-trisphosphate (IP_3) stimulates sarcoplasmic reticulum (SR) Ca^{2+} release in skeletal muscle fibers but its role in excitation-contraction (EC) coupling is questioned, in part due to concerns regarding time required for IP_3 production and diffusion to SR. Here we demonstrate that transverse tubule (TT) voltage controls SR sensitivity to IP_3 . Single rabbit adductor magnus fibers were mechanically peeled and all fibers responded to TT depolarization with Ca^{2+} releases (Cl^- -induced), as described previously (Donaldson, *JGP*, 86:501-525, 1985). IP_3 was microinjected (pipette concentration $0.5\mu\text{M}$) into peeled fibers in oil, using 10mM procaine in all solutions to block Ca^{2+} -induced Ca^{2+} release (Donaldson et al, *BBA*, 927:92-99, 1987). TT potential was set by bathing solution ionic composition ($[\text{K}^+] \times [\text{Cl}^-] = 264\text{mM}^2$) and only paired data were analyzed. IP_3 ($0.5\mu\text{M}$) elicited a maximum IP_3 -induced Ca^{2+} -activated tension transient with depolarized TTs (66mM Cl^-) every time it was microinjected (#fibers=8). However, many of the same fibers failed to respond to $0.5\mu\text{M IP}_3$ when their TTs were polarized (4mM Cl^-) and the mean IP_3 -induced tension transient was significantly smaller with polarized versus depolarized TTs. The effect of TT potential was reversible and independent of order of microinjection or solvent for IP_3 . These data indicate that the TT membrane potential may control response of SR to resting sarcoplasmic IP_3 , rather than IP_3 production, thus eliminating problematic delays. Negative results for IP_3 stimulation may be due to lack of TT-SR functional integrity in other preparations or polarized TTs. Supported by grants from NIH (AR 35132, GM 28818).

W-PM-E5 PROTEIN KINASE C (PKC) MODULATORS INFLUENCE E-C COUPLING STEPS IN SKINNED MUSCLE FIBERS. E.W. Stephenson and S.S. Lerner*. Dept. of Physiology, NJ Medical School, Newark, NJ.

We recently reported (1987. *J. Gen. Physiol.* 90:39a) that diacylglycerol (DAG) inhibits and sphingosine (SPH) potentiates the stimulation of Ca release by depolarizing ion gradients, which appear to act on sealed transverse (T) tubules. DAG (+ cofactor phosphatidylserine (PS)) promotes and SPH inhibits activation of PKC's; DAG is a polyphosphoinositide metabolite and T tubule membranes have high sphingomyelin and PS contents. Mechanically skinned segments of frog semitendinosus fibers were stimulated by submaximal ion gradients (70 mM choline Cl replaced K methanesulfonate at constant $[\text{K}^+][\text{Cl}^-]$) or by low caffeine (1.5-2.5 mM), at 5 mM MgATP; isometric force and ^{45}Ca efflux were measured simultaneously. Synthetic DAG (75 μM 1,2-dioctanoyl-sn-glycerol + 200 μM PS, 1.5 μM BSA) or SPH (15 μM SPH + BSA) were added after ^{45}Ca loading. Test and control ^{45}Ca release (with 5 mM EGTA addition after a few s) were compared on segments from the same fiber. Control ^{45}Ca release with the submaximal ionic stimulus varied between fibers; SPH-potentiated ^{45}Ca release was linearly related to submaximal paired control release ($P < 0.01$) with slope 4.94. The regression and final pre-stimulus efflux suggested a small basal SPH effect. 100 μM PS antagonized SPH potentiation, consistent with a PKC mechanism. Contrary to its inhibition of ionic stimulation, DAG potentiated submaximal caffeine stimulation, increasing stimulated ^{45}Ca release ~ 2 -fold. SPH had similar effects. These results suggest that E-C coupling steps preceding SR Ca release are down-regulated by DAG and potentiated by SPH, while SR Ca release itself is potentiated by DAG, each presumably via a PKC-mediated phosphorylation. Similar effects of endogenous DAG and SPH would be important in E-C coupling. Supported by NIH AR30420.

W-PM-E6 INOSITOL 1,4,5 TRISPHOSPHATE (IP_3) HAS NO EFFECT ON THE CONTRACTILE APPARATUS OF SKINNED CARDIAC MUSCLE FIBERS. T.M. Nosek, P.D. Clein & R.E. Godt. Dept. of Physiol. & Endo., Medical College of GA, Augusta, GA 30912.

Blinks & Endoh (*Circ.* 73:III85, 1986) find that alpha stimulation appears to increase the Ca^{2+} sensitivity of the contractile apparatus in rabbit hearts. Since Thieleczek & Heilmeyer (*BBRC* 135:662, 1986) report that IP_3 increases the Ca^{2+} sensitivity of skinned rabbit skeletal muscle, IP_3 may be involved in this phenomenon. While we have found no effect of IP_3 on Ca^{2+} sensitivity of skinned guinea pig papillary muscle (Nosek et al. *Am. J. Physiol.* 250:C807, 1986), this may be associated with the low alpha receptor density in guinea pig relative to rabbit hearts. We investigated this further by comparing the effects of 30 $\mu\text{M IP}_3$ on the Ca^{2+} sensitivity of skinned (Triton X-100) papillary muscles from animals with high (rabbit & rat) and low (guinea pig & dog) alpha receptor densities. We found that IP_3 had no effect on either the Ca^{2+} sensitivity or maximum Ca^{2+} -activated force of any of the cardiac muscles. On the contrary, when we replicated the exact ionic conditions of Thieleczek & Heilmeyer, we did observe a slight increase in Ca^{2+} sensitivity of rabbit psoas fibers (but not, however, of skinned rabbit papillary muscles). If, on the other hand, we used our standard bathing solutions (Nosek et al, 1986), no effect of IP_3 was observed. These solution dependent differences in skeletal muscle are at present unexplained. (Support: Dean's Res. Fellow., NIH (HL/AR 37022 & AR 31636) and GA Heart Assoc.).

W-PM-E7 BIOCHEMICAL AND IMMUNOLOGICAL EVIDENCE FOR A 52,000 DA SUBUNIT OF THE 1,4-DIHYDROPYRIDINE RECEPTOR FROM RABBIT SKELETAL MUSCLE. Albert T. Leung, Toshiaki Imagawa and Kevin P. Campbell. Dept. of Physiology and Biophysics, University of Iowa, Iowa City, IA 52242.

The 1,4-dihydropyridine receptor purified from rabbit skeletal muscle has been shown to contain four polypeptide components of 175,000 Da (nonreduced)/150,000 Da (reduced), 170,000 Da, 52,000 Da and 32,000 Da when analyzed by SDS-PAGE (Leung, A.T., Imagawa, T. and Campbell, K.P. (1987) *J. Biol. Chem.* 262, 7943-7946). A monoclonal antibody specific to the 52,000 Da polypeptide component of the dihydropyridine receptor has been produced. Immunoprecipitation experiments with [³H]PN200-110-labeled and ³²P-labeled dihydropyridine receptor have demonstrated a tight association between the 170,000 Da dihydropyridine binding subunit and the 52,000 Da polypeptide of the dihydropyridine receptor. Immunoblotting experiments have shown that the 52,000 Da polypeptide co-purifies with the 175,000/150,000 Da and 170,000 Da subunits of the dihydropyridine receptor at all stages of the purification, using either digitonin or CHAPS for the solubilization of the dihydropyridine receptor. Peptide mapping experiments with ³²P-labeled dihydropyridine receptor have indicated that the 52,000 Da polypeptide is distinct from and not a proteolytic fragment of the 170,000 Da subunit. Densitometric scanning of Coomassie Blue stained SDS-polyacrylamide gels of the dihydropyridine receptor purified from either digitonin or CHAPS-solubilized triads has shown that the 52,000 Da polypeptide exists in a 1:1 stoichiometric ratio with the 175,000/150,000 Da, 170,000 Da and 32,000 Da subunits of the dihydropyridine receptor. In summary, our results demonstrate that the 52,000 Da polypeptide is an integral subunit of the 1,4-dihydropyridine receptor from rabbit skeletal muscle. (Supported by NIH HL-37187 and MDA.)

W-PM-E8 IMMUNOLocalIZATION OF THE 52-kDa AND 170-kDa SUBUNITS OF THE 1,4-DIHYDROPYRIDINE RECEPTOR IN RABBIT SKELETAL MUSCLE. Annelise O. Jorgensen*, Wayne Arnold*, Albert T. Leung⁺, Alan H. Sharp⁺ and Kevin P. Campbell⁺, (Intr. by Robert E. Fellows). *Dept. of Anatomy, University of Toronto, Toronto, Canada M5S 1A8 and ⁺Dept. of Physiology and Biophysics, University of Iowa, Iowa City, IA 52242.

The intracellular distribution of the 1,4-dihydropyridine receptor in rabbit skeletal muscle was determined by the indirect immunofluorescence labeling technique. Cryosections (5-8 um) of unfixed rabbit gracilis muscle were labeled with monoclonal antibodies (mAb) specific to either the 52-kDa or 170-kDa subunit of the dihydropyridine receptor. In transverse sections, specific labeling with the mAb's showed a hexagonal staining pattern within each myofiber. However, the relative intensity of labeling of the Type II (fast) fibers was judged to be 3 to 4-fold higher than that of the Type I (slow) fibers. In longitudinal sections, specific labeling was present only near the interface between the A- and I-band regions of the sarcomeres where the transverse tubular membranes form junctions with the terminal cisternae of the sarcoplasmic reticulum. In contrast, specific labeling of the sarcolemma was not observed. The results are consistent with the idea that the 52-kDa and 170-kDa subunits of the dihydropyridine receptor in skeletal muscle are densely distributed in the transverse tubular membrane but apparently absent from the sarcolemma. Immunoelectron microscopic studies with mAb's to the 52-kDa and 170-kDa subunits of the dihydropyridine receptor are currently in progress to determine more precisely the relative distribution of the dihydropyridine receptor in skeletal muscle. (Supported by MRC and NIH.)

W-PM-E9 PURIFICATION, PHOTOAFFINITY LABELLING, STRUCTURE AND FUNCTIONAL RECONSTITUTION OF THE Ca²⁺ RELEASE CHANNEL FROM SKELETAL SARCOPLASMIC RETICULUM. F. ANTHONY LAI, HAROLD P. ERICKSON*, ERIC ROUSSEAU, QI-YI LIU, AND GERHARD MEISSNER. Department of Biochemistry, University of North Carolina, Chapel Hill, NC 27599 and *Department of Anatomy, Duke University Medical Center, Durham, NC 27710.

The neutral plant alkaloid, ryanodine, specifically interacts with the Ca²⁺ release channel of skeletal and cardiac sarcoplasmic reticulum (SR) (Rousseau *et al. Am. J. Physiol.* 253, C368, 1987). Employing ryanodine as a channel-specific ligand, the Ca²⁺ release channel from rabbit skeletal muscle SR has been purified on sucrose density gradients as a complex of apparent sedimentation coefficient 30S. SDS-polyacrylamide gel electrophoresis under reducing and non-reducing conditions showed the channel to comprise polypeptides of apparent relative molecular mass (M_r) 360,000. Photoaffinity labelling of the purified channel and heavy SR membranes with 8-azido-[α-³²P]ATP resulted in specific labelling of the M_r 360,000 protein, consistent with the observation that SR Ca²⁺ release is stimulated by adenine nucleotides (Meissner *et al. Biochemistry* 25, 236, 1986). Negative stain electron microscopy of the channel revealed the four-leaf clover (quatrefoil) structure previously described for the "feet" that span the transverse tubule (T)-SR junction (Ferguson *et al. J. Cell Biol.* 99, 1735, 1984). The purified 30S complex, upon incorporation into planar lipid bilayers, displayed properties characteristic of the SR Ca²⁺ release channel (Smith *et al. J. Gen. Physiol.* 88, 573, 1986). These results indicate that the SR ryanodine receptor, "feet" structures, and Ca²⁺ release channel are synonymous. This further implies that SR Ca²⁺ release, induced by T-system depolarization during excitation-contraction coupling in muscle, may be effected through a direct association of the T-system with SR Ca²⁺ release channels. Supported by Fellowships from MDA(FAL) and CHF(ER) and NIH grant AR 18687.

W-PM-E10 IDENTIFICATION OF THE TRIAD AND ISOLATION OF THE RYANODINE RECEPTOR FROM THE THERMOGENIC MUSCLE TISSUE OF FISH. Barbara A. Block, C. Franzini-Armstrong,⁺ F. Anthony Lai,^{*} and Gerhard Meissner.^{*} Departments of Biology and Anatomy,⁺ University of Pennsylvania, Philadelphia, PA 19104 and Department of Biochemistry,^{*} University of North Carolina, Chapel Hill, NC 27514.

An unusual tissue modified for heat production is found beneath the brain of several large oceanic fish. The extraocular muscle associated with thermogenesis is primarily composed of cells that lack contractile proteins but are enriched with sarcoplasmic reticulum (SR), transverse (T) tubules and mitochondria. Although we have recently identified the T network in heater cells using a modified Golgi stain, it has remained a challenge to characterize the junction between the T system and the SR due to the complicated morphology of these membrane systems. Using tannic acid and glutaraldehyde fixed tissues we have morphologically identified triads with EM and biochemically confirmed the presence of the feet by isolating the protein using the Ca^{2+} release channel probe [^3H]ryanodine. In the heater cells, closely apposed SR and T membranes are occasionally held together by small rows of evenly spaced feet. The center to center spacing between the feet is similar to the 30 nm spacing normally found in skeletal muscle. Heavy SR fractions from heater tissue were used to isolate the junctional feet-ryanodine complex. For comparison heavy SR fractions were also prepared from toadfish swim bladder and shark white muscle. We observed a small single peak of specifically bound [^3H]ryanodine after centrifugation through a linear sucrose gradient in all three fish tissues. SDS-PAGE analysis indicated that a 350K protein comigrated with the ryanodine receptor peak. Negative staining of the ryanodine peak fractions revealed a few junctional feet-like structures composed of four subunits surrounding a central opening. Supported by MDA and NIH grant AM18687, and MDA fellowships to BAB and FAL.

W-PM-E11 THE PURIFIED CARDIAC MUSCLE RYANODINE RECEPTOR FROM SARCOPLASMIC RETICULUM (SR) IS A Ca^{2+} -ACTIVATED OLIGOMERIC Ca^{2+} CHANNEL. Lin Hymel¹, Hansgeorg Schindler¹, and Makoto Inui², Kazuo Nagasaki², Sidney Fleischer² (Intr. by John H. Venable). ¹Institute for Biophysics, University of Linz, A-4040 Linz, Austria and ²Department of Molecular Biology, Vanderbilt University, Nashville, TN 37235.

The purified ryanodine receptor protein (Mr 340,000) from canine cardiac muscle SR was incorporated into vesicle-derived planar bilayers and found to induce Ca^{2+} channel activity. A multiplicity of conductance states was observed, the smallest of which (unitary conductance) was about 4 pS (50 mM Ca^{2+} on the trans side). Mean channel conductance increased with age of the bilayer, diagnostic of the formation of cooperative channel associates. The channels were selective for Ca^{2+} over K^+ ($P_{\text{Ca}}/P_{\text{K}} \sim 20$) and activated by Ca^{2+} in the nM concentration range and mM ATP. Ryanodine (10 μM) stabilized the open state of the channel and reduced the flickering frequency. Ruthenium red (30 μM) or Mg^{2+} (5 mM) blocked channel activity. We suggest that the ryanodine receptor protein, which has been demonstrated to form the "feet structures" located at the triad junction *in situ* (M. Inui, A. Saito, S. Fleischer (1987) J. Biol. Chem. *in press*), forms oligomeric, Ca^{2+} -activated Ca^{2+} channels identical to the Ca^{2+} release channels of the terminal cisternae of cardiac sarcoplasmic reticulum vesicles. [Supported in part by NIH grant HL 32711 and Investigatorship from the American Heart Association (M.I.).]

W-PM-E12 THE PURIFIED RYANODINE RECEPTOR OF SKELETAL MUSCLE (SM) SARCOPLASMIC RETICULUM (SR) FORMS Ca^{2+} ACTIVATED Ca^{2+} CHANNELS IN PLANAR BILAYERS. Lin Hymel¹, Hansgeorg Schindler¹, and Makoto Inui², Kazuo Nagasaki², Christopher Chadwick², Sidney Fleischer². ¹Institute of Biophysics, University of Linz, A-4040 Linz, Austria and ²Department of Molecular Biology, Vanderbilt University, Nashville, TN 37235.

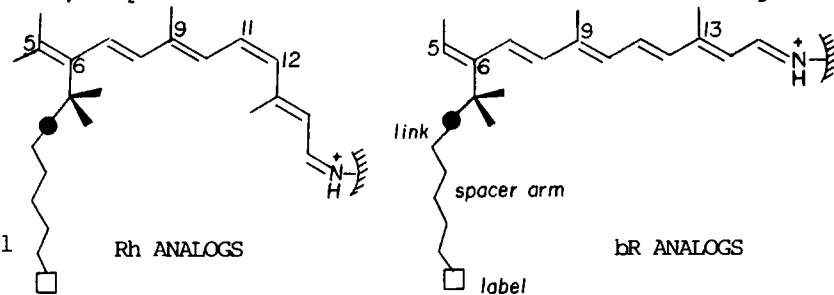
The ryanodine receptor of SR from fast twitch SM has been purified and by electron microscopy found to be equivalent to the feet structures which *in situ* are involved in the junctional association of transverse tubules with terminal cisternae (TC) of SR [Inui, Saito and Fleischer (1987) J. Biol. Chem. 262, 1740-1747]. We now find that when the purified receptor is incorporated into vesicle-derived planar bilayers, it forms Ca^{2+} -specific channels which are dependent on sub-micromolar [Ca^{2+}] for activity. In the presence of 1 mM ATP, the channel becomes highly activated at 50 nM Ca^{2+} and can be blocked by ruthenium red and Mg^{2+} . Ryanodine stabilizes the open state of the channel, and blocks the action of ruthenium red to close the channel. Sublevel gating is observed for the purified Ca^{2+} channel as well as for that obtained by fusion of TC with the bilayer. For the latter the gating is less frequent, with less flicker and the conductance state lifetime is much longer on the average. Thus, the purified ryanodine receptor incorporated into a bilayer has the Ca^{2+} channel characteristics consistent with the calcium release observed in isolated TC vesicles. The purified receptor is an oligomer of a single size high molecular weight polypeptide (Mr ~ 360 KD) which forms the square rectangles diagnostic of the feet structures. We conclude that the identity of the Ca^{2+} release channel of SR is the foot structure. (Supported by NIH AM 14632 and the Muscular Dystrophy Association.)

W-PM-F1 SYNTHETIC PROBES OF RHODOPSIN, BACTERIORHODOPSIN AND THEIR PHOTOACTIVATED FORMS.

Valeria Balogh-Nair and Wei-Xing Li, Department of Chemistry, City College, New York 10031

The interaction of photoactivated rhodopsin (Rh) with transducin (G protein) triggers a sequence of events which culminate in vision. Similarly the photoactivated M intermediate of bacteriorhodopsin (bR) cycle triggers proton pumping across the purple membrane. In order to further the elucidation of the tertiary structure of Rh, bR and their photoactivated forms, retinal analogs having truncated ring binding sites were synthesized. Spacer arms of varying lengths were then attached to the ring sites via ester and ether linkages. These spacer arms will enable introduction of cross-linking, fluorescent and spin labels, at predetermined and variable distances from the ring binding site. The interaction of these synthetic probes with the retinal binding sites will reveal the structural features of bovine and bacteriorhodopsin crucial for their function at their photoactivated stages.

Supported by NSF grant BNS 851363 and the American Chemical Society PRF grant 17797-AC1.

**W-PM-F2 4-HYDROXY ANALOGS OF 9 & 11-CIS RETINAL EXCITE ROD PHOTORECEPTORS IN THE DARKNESS**

FOLLOWING MODERATE OR BRIGHT LIGHTS. D. Wesley Corson,^{1,2} M. Carter Cornwall³, Rosalie K. Crouch² & Venkatchalam Mani². Departments of ¹Pathology & ²Ophthalmology, Medical University of South Carolina & ³Department of Physiology, Boston University School of Medicine.

Photon shot noise in isolated photoreceptors provides a sensitive bioassay for photoactivation of rhodopsin. We have used this assay to seek evidence for chemical activation of rhodopsin by analogs of 11-cis retinal in darkness as a means of exploring the initiation of transduction under physiological conditions. Extracellular membrane current was recorded from the inner segments of a total of 24 rods mechanically isolated from the tiger salamander *A. tigrinum* in a search for chromophore-induced spectral shifts and membrane activation. An estimated 90% of the native chromophore of 9 cells was removed by bleaching (3 log units sensitivity loss) and replaced by addition of retinal analogs in lipid vesicles. All of these cells recovered sensitivity and those exposed to 4-hydroxy analogs displayed spectral sensitivity maxima shifted to 471 ± 0 nm (n=2) for 11-cis 4-hydroxy retinal and 462 ± 3 nm (n=3) for 9-cis 4-hydroxy retinal. Fifteen cells were exposed to vesicles containing 11-cis 4-hydroxy retinal (2 after bleach, 7 in darkness) or 9-cis 4-hydroxy retinal (3 after bleach, 3 in darkness). All produced excess noise similar to photon shot in darkness. No similar noise was observed in 15 control measurements in cells exposed to 11-cis retinal (n=9), 9-cis retinal (n=2), all-trans retinal (n=1) or all-trans 4-hydroxy retinal (n=3). 4-hydroxy and other retinal analogs provide a useful tool for exploring the initial events in transduction.

Funded by grants MUSC 22450CR07 to DWC, NIH EY04939 to RKC & NIH EY01157 to MCC.

W-PM-F3 LIPID INFLUENCES ON RHODOPSIN CONFORMATIONAL STATES IN VISUAL EXCITATION.

Robert D. Pates, Timothy S. Wiedmann, James M. Beach, Amir Salmon, Theresa A. Bens, and Michael F. Brown. Department of Chemistry, University of Arizona, Tucson, AZ 85721.

We have identified those molecular features of recombinant membranes containing rhodopsin which are implicated in its photochemical function as defined by the MI-MII transition. The influences of the membrane lipid acyl chain length, degree of unsaturation, and polar head group composition have been investigated systematically. Three types of experiments were conducted; namely flash photolysis studies of the decay of MI, scanning spectrophotometry, and photobackreaction of MII to yield rhodopsin + isorhodopsin. In each case, the results were compared to control studies of native rod disk membranes. The results demonstrate that both the head group and acyl chain compositions of the rod membrane phospholipids are important for the photochemical behavior of rhodopsin, suggesting a role in visual excitation. The composition of the rod disk membranes is such that the lipids may be near a lamellar (L_a) to hexagonal (H_{II}) phase boundary under physiological conditions (1,2). The influences of membrane phospholipids on the energetics of the MI and MII states of rhodopsin can be formulated in terms of the average hydrocarbon thickness, area (or thickness) compressibility modulus, and curvature modulus of the bilayer. (1) A. J. Deese et al., *FEBS Lett.* 124, 93 (1981). (2) L.C.P.J. Mollevanger and W. J. De Grip, *FEBS Lett.* 169, 256 (1984). Supported by Postdoctoral Fellowships from the American Heart Association (R. D. P.) and NIH (T. S. W. and J. M. B.), an NSF Predoctoral Fellowship (A. S.), a Research Career Development Award from the NIH (M.F.B.), and NIH Grant EY03754.

W-PM-F4 AS MEASURED BY FAST MICROCALORIMETRY, BOUND GTP IN TRANSDUCIN IS HYDROLYSED WITHIN 3 SECONDS IN CATTLE RODS AT 23°C. T. Minh VUONG and Marc CHABRE, Biophysique Moleculaire et Cellulaire (U.A.520 CNRS), DRF-LBio, CENG, BP 85X, 38041 Grenoble France.

As measured in vitro by steady state methods, the transducin GTPase turn over rate in illuminated cattle ROS membranes is 3 min^{-1} at 25°C. This seems to imply a half-life of about 20 seconds for the active $T\alpha$ -GTP state, much too long to account for a rapid inactivation of the cGMP cascade, as required by the fast turn-off of the physiological response. A full GTPase cycle includes however the time needed for the newly formed $T\alpha$ -GDP (from the soluble $T\alpha$ -GTP) to re-bind to the membrane and reassociate with $T\beta\gamma$ before a new GTP can be loaded by the R^* -catalysed GTP/GDP exchange. In vitro, due to dilution of $T\alpha$ in the bulk solution, this re-binding step might be slow and account for a large part of the 20 seconds. Using time resolved microcalorimetry we have devised a kinetic measurement of GTP hydrolysis in a population of $T\alpha$ -GTP formed by a short time pulse of R^* activation. The heat detector is a pyroelectric film of PVDF, sandwiched between a 40 Kg brass heat sink and a layer of ROS suspension ($4 \times 4 \text{ cm}^2$, 0.4 mm thick, 4-8mg rhod./ml) which is illuminated through a thin teflon cover. The sensitivity of the device is 5 μcal and its impulse response FWHM is 0.75sec. As in vitro R^* is not quenched fast enough by the diluted kinase and arrestin, we limited the R^* half-life to below 1 sec by adding 40mM NH_2OH . In the presence of GTP, a heat pulse resulting from GTP hydrolysis is triggered by a light flash ($R^*/R=10^{-4}$) and decays with a time constant of less than 3 sec at 23°C. This can be repeated (after a 20 sec delay) until exhaustion of GTP. If the half life of $T\alpha$ -GTP is less than 3 sec at 23°C, it may be in the subsecond range at 37°C. -T.M.V. is a fellow of the Helen-Hay Whitney foundation.

W-PM-F5 pH DEPENDENCE of CYCLIC GMP-ACTIVATED CHANNEL CONDUCTANCE IN PATCHES of ROD OUTER SEGMENTS from the SALAMANDER.

Brian J. Nunn*, Anna Menini, & Vincent Torre, Dept. of Physiology, Duke Univ. Durham, N.C. 27710 and Dept. di Fisica, Univ. di Genova, 16100 Genova, Italy. (Intr. by John W. Moore)

From the current-voltage relationship for the cGMP-activated channels, we measured the conductance of excised, inside-out patches of salamander rod outer segment membrane. The pipette solution contained: 110mM NaCl, 0.1mM EDTA/TMAOH, 10mM HEPES/TMAOH, pH 7.6. The bathing solution contained: 110mM NaCl, 0.1mM EDTA/TMAOH, 10mM of different buffers covering the range of pH from 9.0 to 4.0.

Cyclic GMP-activated currents were measured over membrane potentials ranging from -70mV to +70mV as the difference in the current flow in the presence and absence of 0.5 mM cGMP. The solution on the cytoplasmic side was changed rapidly by moving the patch across the boundary between two flowing solutions.

The amplitude of the activated current and the shape of the I-V relationship were essentially unchanged over the range of pH from 6.7 to 8.2. However, the conductance increased at a pH of 9.0 and was depressed by a pH of 5.7. At pH values below 5, the membrane became so labile that it was difficult to obtain reliable data. * Deceased Sept. 18 1987

W-PM-F6 IONIC PERMEATION IN THE cGMP-ACTIVATED CHANNEL OF RETINAL RODS. A.L. Zimmerman and D. A. Baylor. Neurobiology Department, Stanford Medical School, Stanford, CA 94035. (A.L.Z. is now at Brown University, Providence, R.I.)

We have studied the ionic dependence of macroscopic currents through the cGMP-activated channels in excised, inside-out membrane patches from salamander rod outer segments. Steady-state current-voltage relations and conductance-ion concentration curves were compared with the predictions of a 1-well, 2-barrier model based on Eyring rate theory. The main assumptions of the model are: 1) only one cation occupies the well at a time, 2) divalents occupy the well longer than monovalents, 3) the well and barriers are not located symmetrically with respect to electrical distance through the channel.

With suitable parameters the model satisfactorily reproduced: 1) the mild outward-rectification and large currents observed in symmetrical Na-only solutions, 2) the stronger outward rectification and very small currents in symmetrical Ca- or Mg-only solutions, 3) the saturation of the outward current with increasing internal Na, 4) block of the Na current by internal Mg or Ca, and the voltage dependence of block, 5) the form of the current-voltage relations in symmetrical Na solutions also containing Mg or Ca on the inside, outside, or both.

Voltage-dependent block of the Na current by external divalents is probably a primary determinant of the rectification of the light-sensitive conductance under physiological conditions. Modulation of the conductance by changes in internal divalents seems unlikely because of the channel's low sensitivity to internal Ca and Mg. (Supported by NIH grant EY01543.)

W-PM-F7 cGMP-DEPENDENT CATION CHANNELS AND Na-Ca-EXCHANGING PROTEINS OF RETINAL ROD OUTER SEGMENTS ARE MOST LIKELY LOCALIZED IN THE PLASMA MEMBRANE. Paul J. Bauer, Inst. f. Biol. Information Processing, D-5170 Jülich, FRG

Rod outer segments contain two species of membranes: one species which contains cGMP-dependent channels and Na-Ca-exchangers and another one which contains neither of these proteins (Bauer P.J. (1987) Biophys. J. 51, 16a). - I attempted to estimate the surface fractions of these two membrane species from the fractions of Ca releasable with cGMP or Na. Mild sonication in the presence of 15mM Ca was used to transform the membranes into small vesicles of similar size. With increasing sonication time, the fractions of Ca which could be released upon addition of cGMP or Na decreased from ca. 23% to final values of 2.5% for cGMP and 7% for Na. Assuming that inside-out and right-side-out vesicles occur with equal probability, only half of the cGMP-sensitive vesicles should display a Ca-release upon addition of cGMP. Thus, 5-7% of the membranes are likely to contain both cGMP-dependent channels and Na-Ca-exchangers. This fraction is identical with the fraction of plasma membrane present in this membrane preparation.

Fusion of disk and plasma membrane was carried out in order to spread cGMP-dependent channels and Na-Ca-exchangers throughout all membranes. In fact, cGMP- as well as Na-induced Ca-releases from such preparations were now up to 60% of the total releasable Ca. Furthermore, sonication had no significant influence on the Na-induced Ca-release and reduced the cGMP-induced Ca-release only to about 60% of its initial value.

W-PM-F8 SODIUM-DEPENDENT CALCIUM EFFLUX AT THE OUTER SEGMENT OF THE RETINAL CONE. K.-W. Yau and K. Nakatani, Howard Hughes Medical Institute and Department of Neuroscience, Johns Hopkins University School of Medicine, Baltimore, MD 21205.

We have studied the efflux of Ca^{++} from the outer segment of a single tiger salamander cone using the suction pipet method. After the outer segment of a cone was loaded with Ca^{++} , a transient inward current was observed in the presence of external Na^+ . This current was not observed if external Li^+ or guanidinium was substituted for Na^+ , suggesting that it was associated with an electrogenic Na^+ -dependent Ca^{++} efflux. The stoichiometry of the exchange was estimated to be near $3\text{Na}^+ : 1\text{Ca}^{++}$. The decline of this exchange current was about 3 times as fast as that previously observed in rods, suggesting a more rapid decline of the internal free Ca^{++} concentration in the cone outer segment caused by the exchanger. This faster rate of decline seemed to arise mostly from a smaller cytosolic volume of the cone outer segment, because the number of exchange sites did not appear to differ significantly in the two types of receptors (as suggested by similar maximum exchange currents). The flash sensitivity of a cone measured in the absence of external Na^+ , and hence without any Ca^{++} efflux, was up to several times higher than control, suggesting that the Ca^{++} efflux in cones, as that in rods, has a role in regulating light sensitivity. Since, however, a rather similar increase in flash sensitivity was observed for rods under the same conditions, we conclude that the negative feedback regulation produced by the Ca^{++} efflux has little to do with the ca. 100-fold difference in light sensitivity between rods and cones. The faster decline in Ca^{++} concentration in cones may simply serve to match the faster transduction kinetics in these cells.

W-PM-F9 CYTOSOLIC FREE $[\text{Ca}^{2+}]$ OF RODS IN THE BULLFROG RETINA MEASURED WITH FURA2. G. M. Ratto, R. Payne, W. G. Owen and R. Y. Tsien*. Departments of Biophysics & Medical Physics and *Physiology/Anatomy, University of California, Berkeley, CA 94720.

Retinae from the bullfrog, *Rana catesbeiana*, were loaded with fura2 by incubation. By two independent techniques we determined that, on average, two-thirds of the loaded dye was trapped in the rod outer segments, (ROS), at a cytosolic concentration of 40 - 80 μM . Loaded retinae were mounted receptor-side up and perfused with media containing 10 mM Na-aspartate to eliminate responses of proximal neurons as confirmed by recording the pIII component of the electroretinogram. Fluorescence was stimulated from 24 mm^2 of retina by rapidly alternating 340/390 nm light, delivered from above. Fluorescence was collected from above and measured by a cooled photomultiplier. Due to the experimental configuration and rhodopsin screening, most of the collected fluorescence emanated from the ROS.

Exposure of loaded retinae to 0.5 mM IBMX caused $[\text{Ca}^{2+}]_i$ to rise, saturating the dye. Light caused a marked fall in $[\text{Ca}^{2+}]_i$. In normal Ringer's, free $[\text{Ca}^{2+}]_i$ was found to fall from a resting, (dark), level of ~220 nM to ~140 nM during exposure to lights which bleached ~75 rhodopsin molecules/rod/sec. The fall was exponential with a time constant of 1.6 secs. Reducing $[\text{Ca}^{2+}]_o$ with EGTA caused a marked reduction in free $[\text{Ca}^{2+}]_i$ in darkness. Bright light then elicited a light response but no measurable change in free $[\text{Ca}^{2+}]_i$.

These findings can be explained in terms of a model in which Ca^{2+} enters the ROS through the light-sensitive channels and is expelled by the Na/Ca exchanger. Initiation of a light response does not depend upon a change in free $[\text{Ca}^{2+}]_i$.

Supported by Grant EY04372 from the National Eye Institute.

W-PM-F10 TRANSDUCTION BY CONES IN THE GOLDEN-MANTLED GROUND SQUIRREL, CITELLUS LATERALIS.

Timothy W. Kraft (Intr. by D.A. Baylor) Department of Neurobiology, Stanford Medical School, Stanford, CA 94305.

Transduction by mammalian cones is particularly accessible in the cone dominant retina of the ground squirrel. Suction electrodes were used to measure photocurrents from individual cones in small pieces of isolated retina.

The response to a brief flash consisted of a transient reduction of the dark current. The undershoot present in the recovery phase of flash responses in primate cones was usually absent in squirrel cones, although in about 1/3 of the cells a small undershoot developed during recording. The time to peak of the flash response was about 20 msec; the form of the response was well-fitted by a model with five delays of time constant 5 msec. Background lights did not appreciably effect the time to peak, but increased the speed of recovery, thus reducing the integration time. The flash sensitivity ($0.002 \text{ pA photon}^{-1} \mu\text{m}^2$) and half-saturating flash strength ($11,000 \text{ photon } \mu\text{m}^{-2}$) at the optimum wavelength showed that sensitivity was tenfold lower than that of primate cones.

Spectral sensitivity measurements demonstrated two classes of cones with peak sensitivities near 520 nm and 430 nm. The kinetics and sensitivity of flash responses from these two cone types were distinguishable. The form of the spectral sensitivity curves were similar when plotted on a log-wavenumber axis, but differed significantly from similar plots of monkey and human cone spectra. Supported by grants EY05750 and EY05956.

W-PM-F11 ACCELERATION OF PHOSPHODIESTERASE-GUANYL CYCLASE CYCLE MAY MEDIATE ROD LIGHT-ADAPTATION.

H. Kondo & W.H. Miller, Department of Ophthalmology and Visual Science, Yale Medical School, New Haven, CT 06510

We compare inner-segment, suction current responses to light of larval-salamander retinal rods before and after introduction of the hydrolysis-resistant GTP analog 5'guanylylimidodiphosphate (GppNHp) into outer segments using the whole-cell patch clamp technique. GppNHp prolongs cyclic GMP hydrolysis by transducin-mediated phosphodiesterase activation. Cyclic GMP maintains a cationic current in darkness. The hydrolysis of cyclic GMP causes the light response, a decrease in dark current. Cyclic GMP is required for recovery, yet the response recovers from a bright flash after introduction of GppNHp. Hence recovery requires activation of guanyl cyclase.

GppNHp mimics light adaptation by desensitizing the rod and speeding the response to a dim flash. A faster rising phase can be explained by GppNHp or light adaptation increasing phosphodiesterase activity. Faster recovery then requires increased guanyl-cyclase activity which desensitizes the rod by response truncation. We conclude that transducin, activated by photolyzed rhodopsin, controls rod-response recovery, sensitivity and adaptation by accelerating the phosphodiesterase-guanyl cyclase cycle.

W-PM-F12 CALCIUM, MAGNESIUM, AND SENSITIVITY ADAPTATION IN THE ROD CELL James L. Miller and Burton J. Litman, University of Virginia, School of Medicine, Charlottesville, VA 22908

Changes in the calcium ion activity in the rod cell influence the response of the cell to light. In order to determine whether calcium activity can modulate the processes that couple light absorption and cGMP hydrolysis, we have examined the effects of calcium on (1) G-protein activation, (2) rhodopsin and G-protein coupled phosphodiesterase (PDE) activation, and (3) cGMP hydrolysis by purified PDE. In rod outer segment membranes, decreasing the calcium activity from $10E-6 \text{ M}$ to ca. $10E-8 \text{ M}$ increases the rhodopsin bleach necessary to produce comparable levels of PDE and G-protein activation by 8 - 10 fold and decreases the efficiency of rhodopsin catalyzed binding of [^3H]GMP P(NH)P by G-protein by 50%. When purified PDE and G-protein were combined with urea - stripped rod disc membranes or rhodopsin containing, mixed phosphatidylcholine-phosphatidylserine (4:1) vesicles, the calcium dependence of the PDE and G-protein activation are preserved, although the range of calcium activities that affect PDE activation is slightly shifted towards increased calcium levels. The cGMP turnover rate for purified PDE is half maximally supported by a magnesium ion concentration of $300 \mu\text{M}$, but is unaffected by changes in the calcium ion activity that modulate light coupled PDE activation. Additional evidence suggests that calcium may modulate the efficiency of the G-protein-PDE interaction. These data are consistent with the notion that a decrease in the calcium ion activity in the rod cell in the presence of background light may be coupled to the desensitization of the rod cell during light adaptation. Supported by NIH Grant EY00548.

W-PM-G1 A NEW DESIGN FOR A RAPID MULTIMIXING CHEMICAL QUENCH-FLOW APPARATUS.

Frederic Mandel, Cardiovascular Diseases Research, The Upjohn Company, Kalamazoo, MI 49001, and Richard J. Kinney, Commonwealth Technology Inc., Alexandria, VA 22304.

This new design for a chemical quench-flow apparatus is based on modifications of a quench-flow device designed by Froehlich, Sullivan and Berger and built by Commonwealth Technology. The modifications are based on experience gained by many years of quench-flow equipment usage. The salient features of this design are a modular construction which allows the device to be configured with as many or as few syringes as required. Such modular construction also results in significant savings in manufacturing costs. Other features include individual motors for each syringe and adjustable diameter interchangeable syringes. These latter two modifications result in the ability to mix components in volume ratios as high as 50:1. Finally, some modifications have been made to minimize the dead volume in the system, thereby minimizing enzyme usage.

W-PM-G2 GEL ELECTROPHORESIS OF DNA. Anil R. Diwan and Todd M. Schuster, Molecular and Cell Biology, University of Connecticut, Storrs, CT 06268.

The mathematical theory of gel electrophoresis of DNA presented by Lumpkin, De'jardin and Zimm (Biopolymers 24:1573-93, 1985) explains the observed electrophoretic mobility of medium sized DNA molecules at moderate electric field strengths and low gel concentrations. We have extended this theory by taking into account the rigidity of the gel, which contributes a mechanical kinetic friction in addition to the hydrodynamic sliding friction considered by Lumpkin *et al.* This extension results in a correction factor α_m to the equation for electrophoretic mobility μ derived by Lumpkin *et al.* Our model thus predicts that μ decreases more than linearly as the reciprocal chain length ($1/L$) decreases. Further, the μ -intercept can appear to become negative using a linear fit under certain conditions, because of the nonlinearity. Thus our model is able to explain the comprehensive data of Stellwagen (1985) at higher molecular weights, higher gel concentrations, and both lower as well as higher electric field strengths, E , in contrast to the original treatment of Lumpkin *et al.* The value of the parameter J which determines the sensitivity of the mobility to electric field strength obtained by fitting the data of Hervet and Bean (1985) was found to be half the value calculated in the model of Lumpkin *et al.* Our model predicts that the value of J obtained using a linear best fit in a μ vs. $1/L$ plot can underestimate the true value by more than 50% due to the curvature in the plot. The new mathematical model and its predictions will be discussed in light of the available experimental data. (Supported by NIH grant AI-11573.)

W-PM-G3 UNDERSTANDING AND IMPROVING DNA PULSED FIELD ELECTROPHORESIS USING THE BIASED REPTATION

MODEL.— Gary W. Slater, Jaan Noolandi, Jean Rousseau, Xerox Research Centre of Canada, Mississauga, Canada, and Chantal Turmel and Marc Lalonde, Biotechnology Research Institute, Montreal, Canada.

The biased reptation model provides an adequate framework to discuss the physical mechanisms involved in the electrophoretic separation of DNA in agarose gels, both in continuous and pulsed field conditions. Using this model, one can provide qualitative and quantitative explanations to why crossed fields, field gradients, single pulsed fields, and reverse fields all improve the separation of large DNA fragments. In particular, one can calculate the pulse times and field intensities needed to optimize the various experimental techniques relying on pulsed fields. Computer simulations can be used to predict the outcome of experiments, and to study the problems of band inversion and band compression often encountered experimentally. The model helps to rationalize the experimental observations made in the last 4 years with the many set-ups now in use, and lead to some suggestions as to what modifications might be needed to separate DNA fragments of increasingly larger sizes.

W-PM-G4 SELF-TRAPPING AND ANOMALOUS MIGRATION OF DNA IN ELECTROPHORESIS. -Jaana Noolandi, Jean Rousseau, Gary W. Slater, Xerox Research Centre of Canada, Mississauga, Canada, and Chantal Turmel and Marc Lalonde, Biotechnology Research Institute, Montreal, Canada. The electrophoresis of DNA in agarose gels is one of the most powerful tools of molecular genetics research. Among other applications, this technique is routinely used to obtain size estimates of DNA molecules. We have predicted theoretically and verified experimentally that linear DNA fragments can display anomalous mobilities under certain conditions of continuous field electrophoresis. A non-monotonic electrophoretic mobility versus DNA fragment size relationship, which might lead to serious errors in the estimation of DNA fragment lengths, was predicted using the equations of the biased reptation model of electrophoresis. The theory shows that during their migration, DNA fragments can get trapped for long periods of time in near-zero-velocity, loop-like compact conformations. Here we demonstrate, by analyzing the experimental mobilities of DNA fragments in continuous and pulsed field electrophoresis, that the anomalous behavior, which has been termed DNA self-trapping, is proportional to the lifetime and the probability of occurrence of compact chain conformations, both of which are strongly dependent on the agarose gel concentration, electric field intensity, pulse times and molecular size. Anomalous mobility of DNA is related to the dynamics of chain stretching and relaxation, and is adequately described by the high-field biased-reptation theory for the size range of DNA fragments (4.4 to 170 kbp) discussed here.

W-PM-G5 POSITRON ANNIHILATION LIFETIME SPECTROSCOPY OF PROTEINS

Roger B. Gregory, Department of Chemistry, Kent State University, Kent, Ohio 44242

Positrons emitted from radioactive nuclides, such as ^{22}Na , rapidly lose their kinetic energy by collision until they reach thermal energies where they combine with electrons to form e^-e^+ bound states (Positronium or Ps). Of the two ground states of Ps, most interest has focused on the triplet o-Ps species which has a free-space lifetime of 140 ns. The o-Ps lifetime is reduced to a few nanoseconds in condensed matter as a result of "pick-off" annihilation, in which a second electron of appropriate spin is captured resulting in subsequent rapid annihilation. o-Ps lifetimes are therefore sensitive to electron density and polarizability and reflect the probability of Ps-electron encounters. Because of this sensitivity to the local molecular environment, o-Ps lifetimes have been widely used to monitor defects in solids, micelle formation phase transitions and conformational changes in macromolecules. However, use of the approach in studies of systems of the complexity of proteins has been greatly limited because of the difficulties associated with analyzing multiple-lifetime spectra. A new method of analyzing positron annihilation lifetime data employing numerical Laplace inversion techniques will be described. The approach avoids any prior specification of the number of components in the system and generates continuous positron annihilation rate spectra which represent the best compromise between stability to noise and an adequate model. The results of a positron annihilation lifetime study of lysozyme will be presented. (Supported by NSF grant DMB-18941 and by Research Corporation).

W-PM-G6 LASER-EXCITED Eu^{3+} LUMINESCENCE AS A PROBE OF Ca^{2+} BINDING SITES: TIME RESOLUTION AND ENERGY TRANSFER STUDIES OF CALMODULIN AND ITS TARGETS. W. DeW. Horrocks, Jr., J. M. Tingey, B. C. Thompson and D. T. Cronce, Department of Chemistry, The Pennsylvania State University, University Park, PA 16802.

Laser-excited lanthanide ion luminescence techniques have been used in this laboratory to probe the Ca^{2+} binding sites of proteins including calmodulin, CaM, (Mulqueen *et al.*, *Biochemistry* **1985**, *24*, 6639; Horrocks *et al.* *Recl.: J. R. Neth. Chem. Soc.* **1987**, *106*, 261). The four metal binding sites of calmodulin cannot be distinguished in the frequency domain of the excitation spectrum of the $^7\text{F}_0 \rightarrow ^5\text{D}_0$ transition of Eu^{3+} , but different classes of sites can be resolved using time resolution techniques. In D_2O solutions the excited state lifetimes of Eu^{3+} bound to calmodulin distinguish three classes of sites. The two tight Ln^{3+} binding sites (in domains I and II) have indistinguishable lifetimes, τ , of 2.50 ms, while the weaker sites (in domains III and IV) have τ values of 1.70 and 0.63 ms. These correspond to time-resolved peaks in the excitation spectrum at 579.20, 579.40, and 579.32 nm, respectively. The order of filling of the sites can be followed during the course of a titration with Eu^{3+} from the amplitude of each of the luminescent decay components. Förster-type energy transfer ($\text{Eu}^{3+} \rightarrow \text{Nd}^{3+}$) measurements yielded distances of 12.1 ± 0.5 and 11.6 ± 0.8 Å between sites I and II and between sites III and IV, respectively. The accessibility of the various Eu^{3+} binding sites to the solvent is assessed by means of diffusion-enhanced energy transfer to small energy acceptor ions, e.g. $[\text{Co}(\text{NH}_3)_6]^{3+}$ free in solution. Experiments were carried out both in the presence and absence of the calmodulin antagonists melittin, trifluoperazine, and fluphenazine. (Supported by NIH grant GM23599 and NSF grant CHE-8504256.)

W-PM-G7 CHARACTERIZATION OF MICROSCOPIC LASER BEAMS BY TWO-DIMENSIONAL SCANNING OF FLUORESCENCE EMISSION. A.H. Stolpen, C.S. Brown, and D.E. Golan. Dept. of Biological Chemistry and Molecular Pharmacology, Harvard Medical School, Boston, MA.

Accurate determination of the laser beam profile and radius at the sample plane of a fluorescence microscope is critical for the analysis of fluorescence photobleaching recovery (FPR) experiments. We have developed a rapid, accurate, and reproducible method for calibrating microscopic laser beams. Fundamental mode (TEM_{00}) output from an argon ion laser is focused on a thin ($<0.5 \mu\text{m}$), aqueous fluorescein solution located at the sample plane. The image of the resulting two-dimensional fluorescence intensity profile is scanned at the emission diaphragm of the microscope by a computer-driven X-Y scanning mirror. Such scans demonstrate that the profile of the microscopic laser beam is Gaussian in two dimensions. The Gaussian ($1/e^2$) beam radius is obtained by non-linear least squares analysis. For Gaussian beams typically used in FPR experiments (i.e. for beam radius \gg the diffraction limit), we show that the accuracy of beam calibration is not adversely affected by beam divergence within the fluorescein solution. Further, we present experimental and theoretical evidence, the latter based on the contrast transfer function of an objective lens, that the fluorescent images of these beams are not significantly distorted by diffraction effects or by out-of-focus planes within the fluorescein solution.

W-PM-G8 LOW TEMPERATURE TRANSMISSION ELECTRON MICROSCOPY OF VESICULAR AND MICELLAR SYSTEMS.

J.R. Bellare, H.T. Davis, L.E. Scriven and Y. Talmon*, Dept. Chem. Engng. & Mat. Sci. U. Minnesota, Minneapolis, MN 55455 and *Dept. Chem. Engng. Technion, Haifa 32000, Israel (Intr. by P. Dragsten)

Vesicular and liposomal dispersions and micellar solutions of organic and synthetic amphiphiles are thermally fixed into thin ($<0.5 \mu\text{m}$) layers of transmission electron microscope specimens from a controlled environment, assuring fixed temperature and humidity around the sample prior to fixation. Ultra-rapid cooling by propelling the specimen into liquid ethane at its melting point, using a spring-loaded plunger, leads to vitrification of the liquid components of the specimen, thus preserving the original fluid microstructure. Temperature control makes it possible to quench fluid microstructures that exist only at temperatures below or above room temperature, and to study temperature-induced phase transformations. Humidity control prevents loss of volatiles from the thin liquid film before thermal fixation, or may be used to induce controlled concentration of the solution. After thermal fixation the specimen is transferred under liquid nitrogen to a cold-stage of a transmission electron microscope, where it is examined at about -160°C . Alternatively, the specimen is fractured, the fracture surface is replicated, and the metal-carbon replica is examined in the microscope at room temperature. Technical details of the technique including the Controlled Environment Vitrification System (CEVS) are given by Bellare et al. [1]. Examples of applications in the study of the microstructure of micellar solutions and vesicular dispersion will be given. The study of the dynamics of phase transformation of phospholipid liposomes by this technique is described separately [2].

[1] J.R. Bellare et al., *J. Electron Microsc. Tech.* (submitted). [2] Y. Talmon et al., this volume.

W-PM-G9 VIBRATIONAL CIRCULAR DICHROISM STUDIES OF THE SOLUTION CONFORMATION OF (-)-EPINEPHRINE & (-)-NOREPINEPHRINE. Teresa B. Freedman, Nam-Soo Lee and Laurence A. Nafie (Intr. by Jeffrey C. Freedman). Department of Chemistry, Syracuse University, Syracuse, New York 13244-1200.

Vibrational circular dichroism (VCD), the differential absorbance of left vs. right circularly polarized infrared radiation during vibrational excitation, is a new spectroscopic probe of the solution conformations of chiral molecules. VCD intensity is particularly sensitive to the presence of intramolecular hydrogen bonds. According to the ring current mechanism for VCD, nuclear oscillation adjacent to a heteroatom in a hydrogen-bonded ring can initiate oscillating electronic current in the ring at constant electron density. The current gives rise to a magnetic dipole transition moment, \mathbf{m} , perpendicular to the ring. If the electric dipole transition moment, $\boldsymbol{\mu}$, for the driving oscillation has a component out of the ring plane, the VCD intensity, proportional to the rotational strength $R = \text{Im}(\boldsymbol{\mu} \cdot \mathbf{m})$, is enhanced. The CH_2 -stretching VCD spectrum of (-)-epinephrine·HCl consists of a negative band at 2962 cm^{-1} , assigned to the antisymmetric methylene stretch, and a positive band at 2884 cm^{-1} , corresponding to the symmetric methylene stretch. Based on the ring current interpretation, the signs of these bands are consistent with an excess of the intramolecularly $\text{NH} \cdots \pi$ hydrogen-bonded rotameric conformation. In contrast, in (-)-norepinephrine·HCl, the methylene stretches exhibit little or no VCD intensity, implying nearly equal populations of $\text{NH} \cdots \text{O}$ and $\text{NH} \cdots \pi(\text{phenyl})$ forms, which will have oppositely signed CH_2 -stretching VCD signals. The structures deduced from the VCD spectra provide insight into the differences in the mode of interaction of these species with surfaces, as reflected in their distinct surface enhanced Raman spectra. (Supported by NIH Grant GM-23567).

W-PM-G10 MOLECULAR AGGREGATION CHARACTERIZED BY HIGH ORDER AUTOCORRELATION IN FLUORESCENCE CORRELATION SPECTROSCOPY. Arthur G. Palmer III and Nancy L. Thompson, Department of Chemistry, University of North Carolina at Chapel Hill, Chapel Hill, NC 27599-3290

The use of high order fluorescence fluctuation autocorrelation in fluorescence correlation spectroscopy for investigating aggregation in a sample that contains fluorescent molecules is described. Theoretical expressions for the fluorescence fluctuation autocorrelation functions defined by $G_{m,n}(\tau) = [\langle \delta F^m(t+\tau) \delta F^n(t) \rangle - \langle \delta F^m(t) \rangle \langle \delta F^n(t) \rangle] / \langle F \rangle^{m+n}$, where $\delta F(t)$ is the fluorescence fluctuation at time t , $\langle F \rangle$ is the average fluorescence, and m and n are integers less than or equal to 3, are derived. Methods for determining the number densities and relative fluorescence yields of aggregates of different sizes from a series of $G_{m,n}(0)$ values are outlined. The method is applied to 1,1'-dioctadecyl-3,3,3',3'-tetramethylindocarbocyanine perchlorate (diI) suspended in solutions of water and ethyl alcohol, and to systems with defined distributions of fluorescent molecules. The technique presented may prove useful in detecting and characterizing aggregates of fluorescent-labeled biological molecules such as cell-surface receptors. This work was supported by NIH grant GM-37145 and NSF grant DCB-8552986.

W-PM-G11 PERTURBATION OF TRP RESIDUES IN BACTERIOPHAGE T4 LYSOZYME BY POINT MUTATIONS STUDIED BY OPTICAL DETECTION OF TRIPLET STATE MAGNETIC RESONANCE (ODMR) SPECTROSCOPY. L.-H. Zang, S. Ghosh, and A.H. Maki (Intr. by C.F. Meares), Department of Chemistry, University of California, Davis, CA 95616.

We have investigated changes in the triplet state properties of Trp residues in T4 lysozyme caused by the point mutations, Gln 105 \rightarrow Ala, or Ala 146 \rightarrow Thr, by low temperature phosphorescence and ODMR spectroscopy. The mutation Gln 105 \rightarrow Ala eliminates the hydrogen bond between the γ carbonyl of Gln 105 and Trp 138. We find that the phosphorescence 0,0-band of Trp 138 is strikingly red-shifted relative to its position in the wild type protein¹; a strong wavelength dependence of the D and E parameters and broadening of the ODMR transitions of Trp 138 result. In contrast, the mutation Ala 146 \rightarrow Thr, which places a bulkier group near Trp 138, shifts the 0,0-band of Trp 138 to the blue, but a similar wavelength dependence of D and E, and ODMR linewidth broadening occur. This behavior suggests that Trp 138 is shifted to a more solvent exposed position. The red shift of the 0,0-band of Trp 138 by the Gln 105 \rightarrow Ala mutation, however, is inconsistent with a solvent exposed location. No significant spectroscopic changes in Trp 126 or 158 were found in either mutant, so perturbations are probably localized near Trp 138. Specifically, their relative orientation appears to be unchanged, since efficient Trp 126 \rightarrow Trp 158 energy transfer in the wild type lysozyme¹ is retained in both mutants. We thank Dr. L. McIntosh for the mutated T4 lysozymes. Research supported in part by a NSF grant.

1. S. Ghosh, L.-H. Zang and A. H. Maki, *J Chem. Phys.*, submitted.

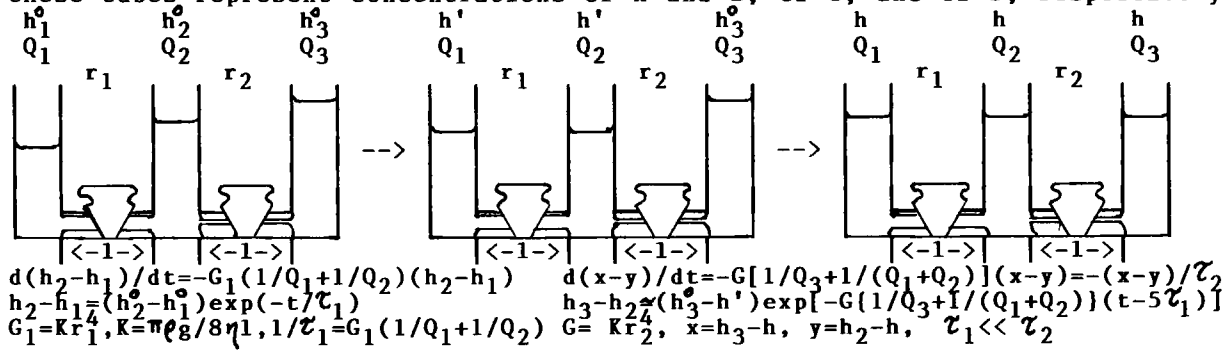
W-PM-G12 FT-IR MICROSCOPIC INVESTIGATION OF ENDOCHONDRAL OSSIFICATION AT 20 μ SPATIAL RESOLUTION. Richard Mendelsohn* and Adele Boskey#, *Dept. of Chemistry, Rutgers University, Newark, NJ, 07102; #Dept. of Ultrastructural Biochemistry, Hospital for Special Surgery, Cornell University Medical College, New York 10021.

The coupling of an FT-IR spectrophotometer with an optical microscope permits the acquisition of infrared data with a spatial resolution of 20 μ . Our initial biophysical application of this device is to the study of endochondral ossification in the femur of normal and rachitic (Vitamin D deficient) rats. Thin (5 μ) longitudinal sections of femurs, which had been fixed in PMMA, were mounted on BaF₂ windows and the PMMA partially removed with EtOH. High quality spectra (S/N of 50:1) were obtained in a short time (2 min.) with adequate spectral (4 cm⁻¹) and spatial (20 μ) resolution from a variety of physical regions within the tissue. The 900-1200 cm⁻¹ spectral region, containing vibrations from the hydroxyapatite constituent, was sensitive to the extent and structure of the calcifying phase. Rachitic tissue showed significantly reduced levels of calcification compared with corresponding zones in normal animals, both within and without the growth plate.

The calcifying material was shown to contain mostly a poorly crystallized, probably carbonate-substituted phase of hydroxyapatite, although occasional spectra revealed patterns not resembling any model compounds. These possibly arise from mineral structures altered through interaction with collagen.

W-PM-G13 A SIMPLE HYDRAULIC ANALOG FOR CHEMICAL RELAXATION. Gerson Kegeles, Emeritus Professor, Univ. CT. RD1, Box 156, Groveton, NH 03582.

The analogy between fluid flow and chemical kinetics has been used as a laboratory teaching device (D. Davenport, J. Chem. Educ. 52, 379, 1975). Starting in 1968, I used the present material as an analog computer to explain relaxation kinetics in the coupled processes $A + B \rightleftharpoons C \rightleftharpoons D$. Tubes 1, 2 and 3 are connected through capillaries of unequal radii, and liquid heights in these tubes represent concentrations of A and B, of C, and of D, respectively.



W-Pos1 **DECOMPOSITION OF MICROCALORIMETER THERMOGRAMS IN THE 100 MICROJOULE RANGE.** Courtney P. Mudd¹, Robert L. Berger², David P. Remeta³, and Kenneth J. Breslauer³. ¹ Biomedical Engineering and Instrumentation Branch, DRS, NIH, Bethesda, MD 20892 ² Laboratory of Technical Development, NHLBI, NIH, Bethesda, MD 20892 ³ Department of Chemistry, Rutgers University, Piscataway, NJ 08854

An all tantulum stopped-flow microcalorimeter, previously reported at these meetings [49 (1986) p. 87a ; 51 (1987) p. 443a], has now been used extensively to study the binding enthalpies of DNA-drug interactions. Decomposition of the measured thermograms yields reconstructed thermograms with a time constant of approximately three seconds. Two schemes have been used to reconstruct the measured thermograms. The finite element method of Davids and Berger [*J. Biochem & Biophys Methods*, 6 (1982) p. 205-217] requires a knowledge of the physical construction of the calorimeter. The iterative method adapted by Schuette and Mudd [*J. Biochem & Biophys Methods*, 14 (1987) p. 167-175] requires only that the impulse response be known and digitized at the same rate as the measured thermogram. Results employing both deconvolution methods will be presented. The microcalorimeter is capable of measuring binding enthalpies of 30 microjoules with a standard deviation of 3 microjoules. A reaction requires 80 microliters of each reagent and is completed within 200 seconds thus allowing a typical throughput of 120-150 runs per day. The high resolution of this instrument has permitted accurate measurement of reaction heats at extremely dilute reagent concentrations thereby precluding the need to correct the binding enthalpies for drug and/or DNA aggregation. Specific details and results of our DNA-drug binding studies on the complexation of daunomycin, an anthracycline antibiotic, with a series of DNA host duplexes are presented in an accompanying poster in this session. This research was supported in part by NIH grant GM 34469.

W-Pos2 **APPLICATION OF STOPPED-FLOW MICROCALORIMETRY FOR THE DETERMINATION OF DAUNOMYCIN:DEOXYPOLYNUCLEOTIDE BINDING ENTHALPIES.** David P. Remeta¹, Courtney P. Mudd², Robert L. Berger³, and Kenneth J. Breslauer¹. ¹ Department of Chemistry, Rutgers University, Piscataway, NJ 08854 ² Biomedical Engineering and Instrumentation Branch, DRS, NIH, Bethesda, MD 20892 ³ Laboratory of Technical Development, NHLBI, NIH, Bethesda, MD 20892.

The interaction of the anthracycline antibiotic daunomycin with synthetic deoxypolynucleotides has been the subject of numerous investigations involving a variety of experimental and instrumental techniques. The thermodynamic binding profiles gleaned from such studies were derived in part via spectroscopic determinations of van't Hoff enthalpies or calorimetric measurements of drug binding enthalpies, the latter requiring extensive correction for binding induced disruption of aggregated drug species. The accuracy of the measured enthalpies has been further compromised by the need to assume a model depicting the aggregation process. By employing a stopped-flow microcalorimeter recently developed at the NIH (refer to the companion poster in this session), we report the first calorimetric determination of binding enthalpies for the interaction of a series of deoxypolynucleotides with daunomycin in a *non-aggregated* state. The enhanced resolution and sensitivity of this instrument permits the measurement of drug binding enthalpies for daunomycin concentrations in the 10 - 20 μ M range, at which the monomeric form of the drug predominates. In conjunction with our microcalorimetric studies, we have employed UV/Vis and fluorescence spectroscopy to derive binding free energies for the daunomycin-DNA complexes. The deoxypolynucleotides examined to date include six alternating copolymers [poly d(AT) • poly d(AT); poly d(GC) • poly d(GC); poly d(AU) • poly d(AU); poly d(IC) • poly d(IC); poly d(AC) • poly d(GT); and, poly d(AG) • poly d(CT)] and four homopolymers [poly d(A) • poly d(T); poly d(G) • poly d(C); poly d(A) • poly d(U), and poly d(I) • poly d(C)]. Complete thermodynamic binding profiles will be presented and discussed in terms of the influence of nucleic acid composition, base sequence, and helical conformation on the binding affinity and specificity of daunomycin. This research was supported in part by NIH grant GM 34469.

W-Pos3 **DEGRADATION OF DNA BY BLEOMYCIN STUDIED BY VISCOSITY AND DYNAMIC LIGHT SCATTERING.** S. A. Allison, J. L. Mokrosz, L. Strekowski, A. Strekowski and W. D. Wilson, Department of Chemistry and Laboratory for Microbial and Biological Sciences, Georgia State University, Atlanta, GA. 30303.

Bleomycin, an anticancer drug, binds with and degrades DNA in the presence of ferrous ion and molecular oxygen. The activity of bleomycin can be enhanced by certain compounds that alone may have no activity. One class of amplifiers bind to DNA by intercalation and stimulate directly the drug induced fragmentation of DNA [L. Strekowski et. al., *J. Medicinal Chem.* 30, 1415 (1987)]. The techniques of laser light scattering and viscosity are used to study the fragmentation of DNA by bleomycin in the absence and presence of various amplifiers. The light scattering intensity autocorrelation function is analyzed by an inverse Laplace transform algorithm [N. Ostrowsky et. al., *Optica Acta* 28, 1059 (1981)]. From this analysis, the size distribution of DNA during the course of the reaction can be estimated. Experiments have been carried out on sonicated calf thymus DNA as well as a plasmid DNA (pRR322). We also report on an improved method for synthesizing pRR322 DNA. SUPPORT: DMB-8451873 from NSF and CH-383 from the American Cancer Society.

W-Pos4 THE BINDING OF INTERCALATORS TO NUCLEIC ACID DUPLEXES: THE INFLUENCE OF A CHARGED SIDE CHAIN ON THE BINDING THERMODYNAMICS. WanYin Chou and Kenneth J. Breslauer. Department of Chemistry, Rutgers, The State University of New Jersey, New Brunswick, NJ 08903.

Ethidium and propidium cations are DNA binding ligands which exhibit important biological effects. Both drugs contain an aromatic phenanthridinium ring system, but differ by the nature of the substituent group attached to the ring system. Propidium contains a large, charged side chain in contrast with the neutral ethyl group of ethidium. Both drugs bind to DNA and RNA by intercalation of their aromatic rings. To investigate the influence of side chain size and charge on the binding affinity and specificity of these two intercalators, we have determined and compared the thermodynamic binding profiles of each drug to several synthetic DNA and RNA duplexes. Specifically, we have used a combination of temperature-dependent uv/vis spectroscopy as well as batch and differential scanning calorimetry to characterize thermodynamically the binding of each drug to alternating sequences of deoxy and ribo host duplexes. These studies were conducted in 10mM phosphate buffer, pH=7.0. We obtained the following thermodynamic binding profiles at 25°C:

| | ΔG^* (kcal/mol) | | ΔH^* (kcal/mol) | | $T\Delta S^*$ (kcal/mol) | |
|-----------------|-------------------------|-----------|-------------------------|-----------|--------------------------|-----------|
| | ethidium | propidium | ethidium | propidium | ethidium | propidium |
| polydAU•polydAU | -8.2 | -9.2 | -9.9 | -7.3 | -1.7 | +1.9 |
| polyrAU•polyrAU | -9.0 | -9.7 | -7.1 | -7.3 | +1.9 | +2.4 |
| polydIC•polydIC | -9.3 | -9.9 | -9.2 | -7.8 | +0.1 | +2.1 |
| polyrIC•polyrIC | -8.9 | -9.2 | -4.5 | -4.2 | +4.4 | +5.0 |

Based on the above results, we can draw the following conclusions: 1) Propidium always binds more strongly than ethidium to both the DNA and RNA duplexes. 2) With one exception, the binding of both drugs is overwhelmingly enthalpically driven. 3) Both drugs exhibit a more favorable binding enthalpy when they complex with DNA compared with RNA. 4) With one exception, the DNA binding of both drugs is accompanied by a positive entropy change. We now are studying the binding of these two drugs with DNA and RNA homopolymers to evaluate the influence of homo versus alternating sequences in the host duplexes. This work was supported by NIH Grant 34469.

W-Pos5 BROWNIAN DYNAMICS SIMULATIONS OF A THREE-SUBUNIT AND A TEN-SUBUNIT WORMLIKE CHAIN-- COMPARISON OF RESULTS WITH TRUMBELL THEORY AND WITH EXPERIMENTAL RESULTS FROM DNA. Roger J. Lewis¹, Stuart A. Allison², Don Eden³, and R. Pecora¹, ¹Stanford Univ., ²Georgia State Univ., ³San Francisco State Univ.

Brownian dynamics simulations of a three-bead and a ten-bead model of a flexible linear macromolecule in solution are performed. Dynamic forward depolarized light scattering autocorrelation functions are calculated from these dynamic simulations to a delay time of 30 microseconds and are analyzed by the program CONTIN, [S. W. Provencher, Comp Phys Comm 27 213 and 229 (1982)], yielding the simplest distribution of decay times that is consistent with the simulated data. The distribution of decay times obtained from the simulations of the three-bead model are compared with those obtained from the calculations of Roitman and Zimm [D. B. Roitman and B. H. Zimm, J. Chem. Phys. 81, 6333, 6348, and 6356 (1984)] on the dynamic behavior of a three-bead trumbell. The simulations and the theory of Roitman and Zimm show excellent agreement. The distribution of decay times obtained from the simulations of the ten-bead model with a persistence length of 600 Å is compared with previously published transient electric birefringence data from a 367 base pair monodisperse DNA fragment, [R. J. Lewis, R. Pecora, and D. Eden, Macromolecules 19, 134 (1986)], again showing excellent agreement. Results from dynamic simulations of the ten-bead model with varying persistence length are then favorably compared with new transient electric birefringence data from the 367 base pair DNA fragment, obtained with ionic strengths of 1.4 and 4.4 mM. Simulations of ensembles of rigid three-bead and ten-bead models yield dynamics quite different from their flexible counterparts. This raises concerns about the use of ensembles of rigid shapes as models for rotational dynamics of flexible molecules.

W-Pos6 NOVEL PHASE BEHAVIOUR OF CONCENTRATED DNA SOLUTIONS AT LOW IONIC STRENGTHS. Teresa E. Strzelecka and Randolph L. Rill, Department of Chemistry and Institute of Molecular Biophysics, Tallahassee, Florida 32306.

Phosphorus-31 and sodium-23 NMR, together with polarized light microscopy, were used to determine the phase diagram for transitions between liquid-crystalline phases in aqueous solutions of DNA in low ionic strength (10 mM Na+) buffer. The range of DNA concentrations was 100-290 mg/ml. A new anisotropic, weakly birefringent phase was observed in samples with DNA concentrations of 110-150 mg/ml. This phase coexisted with the isotropic and cholesteric phases until the DNA concentration reached 230 mg/ml, forming a triphasic solution. In samples above 230 mg/ml DNA only cholesteric and isotropic phases existed. This phase behaviour has not been observed in DNA solutions of higher ionic strengths (>0.3 M).

The behaviour of the Na+ atmosphere was monitored by ²³Na NMR for samples with DNA concentrations of 10-290 mg/ml. Quadrupole splitting was observed in samples with concentrations exceeding 160 mg/ml DNA. The temperature dependence of T₁ relaxation time and quadrupole splitting suggested that the exchange between free and condensed counterions is fast and that the condensed ions tumble rapidly in the vicinity of the DNA helix. The quadrupole splitting decreased with increasing DNA concentration, indicating that a rearrangement of the counterion atmosphere takes place when DNA helices are brought close together in solution. Supported by NIH Grant GM37098.

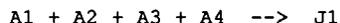
W-Pos7 NEUTRAL FILTER ELUTION (pH 9.6) OF SMALL INTACT GENOMES REVEALS ANOMALOUS BEHAVIOR OF KNOWN MOLECULAR WEIGHT DNA Peter J. Mayer and Christopher S. Lange, Department of Radiation Oncology, SUNY Health Science Center, Brooklyn, NY 11203

In attempting to validate and calibrate the neutral filter elution (NFE) technique, we used intact genomes of known molecular weight, i.e., *E. coli* ($M_r=2.7 \times 10^9$) and coliphage T4c ($M_r=1.15 \times 10^8$) in conjunction with polycarbonate filters of varying pore size (0.03-3.0 μm). T4c or *E. coli* containing radiolabelled DNA (^{14}C -thymidine) were mixed with a tritiated sucrose (5%) solution, gently layered onto the filters and lysed. Released DNA was eluted (pH 9.6) for 120-180 or 960 min and radioactivity per elution fraction determined by scintillation counting; sucrose eluted prior to DNA.

NFE at all pore sizes consistently discriminates the two genomes as measured by %DNA retained on the filter. However semi-log plots of %DNA retained on the filter vs. time reveal a discontinuity: as pore size decreases the expected linear slope becomes an anomalous two-component curve. This discontinuity occurs between pore size 2.0 and 1.0 μm for *E. coli* and between pore size 0.1 and 0.08 μm for T4c. For *E. coli* DNA rate of elution increases slightly with increased pore size from 0.05 to 1.0 μm and substantially (47%) for pore size 2.0 and 3.0 μm ; for T4c DNA rate of elution is constant for pore sizes 3.0 to 0.2 μm and decreases as pore size decreases from 0.2 to 0.03 μm . Elution rate of intact DNA appears related to pore size per se and not to pore density or "open area" per filter. Mathers Fdn. funded.

W-Pos8 THEORY OF THERMAL TRANSITIONS IN DNA JUNCTIONS. Luis A. Marky, Nadrian C. Seeman, and Neville R. Kallenbach. Department of Chemistry, New York University, New York, NY 10003.

DNA junctions are complexes made of complementary oligonucleotide strands designed to create branched DNA structures. These molecules provide stable models for normally unstable transient states of DNA such as arise in recombination. We have investigated the thermal stability of J1, a complex composed of four hexadecamer strands which combine with 1:1:1:1 stoichiometry to form a Holliday structure in which the branch point is immobile. A combination of UV absorbance, circular dichroism, and differential scanning calorimetry to estimate the thermodynamic parameters for forming a tetrameric junction from the free strands, according to the scheme:



which assumes an all-or-none mechanism. While the results are consistent with overall two-state behavior in J1, to include the effects of sequence and chain-length on the thermal transitions of DNA junctions in general, one must take into account the multistate nature of the transition. We have derived general expressions applicable to the analysis of equilibria in junctions of N strands, including contributions from all paired states that exist as the transition occurs. This general treatment requires evaluating the statistical weights corresponding to unusual configurations of the strands. We have used computer simulations to approach this problem. Supported by grants GM-29554, ES-00117 and CA-24101 from the NIH.

W-Pos9 AN APPARENT PERMANENT DIPOLE MOMENT IN DNA DUE TO LIGAND BINDING. G. Eric Plum and Victor A. Bloomfield, (Intr. by C.K. Woodward) Department of Biochemistry, University of Minnesota, St. Paul, Minnesota 55108

Double stranded B-form DNA is an antiparallel double helix and, therefore, is expected to exhibit no permanent dipole moment. Transient electric birefringence and dichroism experiments have revealed an apparent permanent dipole moment which is thought to be due to polarization of the DNA counterion atmosphere. We propose that a second contribution to the apparent permanent dipole moment may come from site binding of charged ligands. Since the distribution of a few randomly placed ligands will likely be asymmetrical with respect to the center of mass of the rod, a dipole moment will be found. The mean dipole moment over the population will vanish. However, the root-mean-squared dipole moment is nonvanishing.

We have developed a simple theory, based on the Kirkwood-Shumaker fluctuating dipole model, to calculate this contribution to the apparent permanent dipole moment from ligand binding. Calculated curves will be presented to evaluate the magnitude of this phenomenon.

W-Pos10 A THEORY OF SEQUENCE-DEPENDENT FLEXIBILITY IN DNA

Robert C. Hopkins, University of Houston - Clear Lake, Houston, Texas 77058

A quantitative theory consistent with the observed base-sequence dependence of DNA persistence lengths (1) is presented. It assumes that DNA in solution consists of stiff segments punctuated by bends, as suggested by the Configuration II DNA models in which the backbones appear hinged between adjacent base pairs (2). Thus, a bend in the molecule requires overcoming the specific stacking energy of the base pairs adjacent to the bend, plus a smaller, constant energy for opening the chain "hinges". Equations incorporate the probability of each possible 5'-MN-3' doublet occurring in one strand, the Boltzmann probability that such a doublet will be in a bent or unstacked state, and two empirical constants allowing a least-squares fit to the observed data. Using calculated (corrected optimized potential) stacking energies (3), the standard deviation of predicted versus observed persistence lengths for data from seven different oligonucleotides (1) is only 33 bp. The theory predicts that 1.) there should be an increase in persistence length with increasing GC content, 2.) a contour-length dependence of persistence length should be observable for short lengths (< 2000 bp.), 3.) there should be a decrease in persistence length with increased temperature, and 4.) fragmented genomic DNA (e.g., chicken DNA) is significantly stiffer than predicted for random sequence DNA having the same average GC content. Supported by grant BC-889 from the Robert A. Welch Foundation.

1. Hogan M., LeGrange, J., & Austin B. (1983) *Nature* 304, 752.2. Hopkins, R.C. (1981) *Science* 211, 289; Hopkins, R.C. (1983) *Cold Spr. Harb. Symp. Quant. Biol.* 47, 129; Hopkins, R.C. (1987) Abstracts, 5th Conversation on Biomolecular Stereodynamics, Albany, N.Y., p. 143.3. Ornstein, R.L., Rein, R., Breen, D.L., & MacElroy, R.D. (1978) *Biopolymers* 17, 2341.**W-Pos11** SIZE DISTRIBUTION OF DNA PARTICLES CONDENSED WITH MULTIVALENT CATIONS. Victor A.

Bloomfield, Patricia G. Arscott, and An-Zhi Li, Department of Biochemistry, University of Minnesota, 1479 Gortner Avenue, St. Paul MN 55108.

DNA is condensed by multivalent cations into toroidal and rodlike particles. We have previously shown that the size distribution of such particles is relatively narrow and independent of the length of the DNA molecules of which they are composed. A theory that accounts for these observations should shed light on the forces stabilizing condensed DNA. We have used the successive association formulation developed for micelle formation by Tanford (PNAS 71:1811-1815, 1974) to compute the mole fraction X_m of m-mers:

$$\ln X_m = -m\Delta G_m^0/kT + m \ln X_1 + \ln m$$

The free energy change for incorporating m random coil DNA molecules of length L into a condensed m-mer was taken as

$$m\Delta G_m^0/kT = -A(mL)^2/(1 + \beta mL) + BmL + CmL \ln m.$$

This expression is intended to take into account saturation of short-range attractive and repulsive interactions, bending and/or kinking, entropy loss upon chain collapse, and electrostatic interactions (Riener and Bloomfield, *Biopolymers* 17:785-794, 1978). Plausible choices of the parameters produce good agreement with electron microscopic measurements on 1350 bp and 2700 bp plasmid DNA molecules.

W-Pos12 MONTE CARLO SIMULATIONS OF COUNTERION DISTRIBUTIONS NEAR DNA IN MIXED SALT SOLUTIONS

M.D. Paulsen, C.F. Anderson and M.T. Record, Jr., Departments of Chemistry and Biochemistry, University of Wisconsin-Madison, Madison, Wisconsin 53706

For a model of DNA having a helical charge distribution, radial distribution functions are calculated from canonical Monte Carlo simulations for systems containing more than one type of counterion. These results are compared with the predictions of the PB cell model and with the results of NMR experiments. Using both theoretical approaches, an ion exchange parameter, D, and an exchange stoichiometry, n^* , are calculated. These coefficients are found to be relatively independent of the bulk salt concentration. The variation in n^* and D with the size and charge of the competitor cation have been investigated. MC simulations and PB calculations of the dependence of D on ion size and ionic charge yield qualitatively similar results, although consistently smaller values of D are predicted by the MC simulations than by the PB equation.

W-Pos13 ELECTROPHORESIS OF DNA MULTIMER LADDERS ON AGAROSE AND POLYACRYLAMIDE GELS. Nancy C. Stellwagen, Department of Biochemistry, University of Iowa, Iowa City, IA 52242.

One of the most obvious differences between polyacrylamide and agarose gels is that some DNA fragments exhibit anomalously slow electrophoresis in polyacrylamide gels but not in agarose gels of comparable pore size. In an effort to determine the basis of this effect, the electrophoresis of multimer ladders of two 147 base pair restriction fragments of plasmid pBR322 was studied in various gel media. One of these fragments exhibits an anomalously slow electrophoretic mobility in polyacrylamide gels; the apparent lengths of trimers of these fragments differ by 25-50%, depending on the polyacrylamide concentration and temperature. In 4.0% agarose gels no difference in the mobility of the multimers is observed, even though the apparent absolute mobility is the same as in the polyacrylamide gels. A systematic investigation of various parameters in the gel electrophoresis experiment was undertaken, including gel concentration and type, pore size, charge density, and mixed gel media. Supported by Grant No. 29690 of the National Institute of General Medical Sciences.

W-Pos14 A SITE SPECIFIC PROBE FOR DUPLEX DNA DYNAMICS. A. Spaltenstein, B.H. Robinson*, P.B. Hopkins, Department of Chemistry, University of Washington, Seattle, WA 98195

We have recently synthesized a spin-labeled derivative of thymidine, T*, capable of being incorporated into oligomers via phosphoramidite synthesis. Characterization of the self-complementary DNA dodecamer, 5'-d(CGCGAATT*CGCG) by NMR, UV-melting, and CD demonstrated that the probe is non-perturbing. A hydrodynamic model of this dodecamer as a rigid cylinder, predicts that helical DNA will have two rotational correlation times of 4 and 7 nanoseconds at 0 C, and twice that at -5 C. Experimental EPR spectra are indicative of an object rotating at 5 and 10 nanoseconds at 0 C and -5 C respectively. Therefore the experimentally determined correlation times indicate an absence of internal probe dynamics. Differential line broadening of imino proton resonances due to the presence of the electron spin supports the model of a spin probe localized with respect to right handed duplex DNA.

We have incorporated the T* probe into the hexadecamer 5'-d(GCGAATT*CGCGCGCGC), which is self-complementary in the center with 6 bases unpaired on either end. Without ligation, the EPR spectra of this material are indicative of immobilization well beyond what could be accounted for by a 16-mer in solution. Ligated multimers are being studied individually. The EPR-monitored thermal denaturation profiles will be compared to the UV-monitored profiles. The study of these extended DNA systems is in progress and will be discussed.

W-Pos15 FLUORINATED NUCLEIC ACIDS: SENSITIVITY TO LIGHT AND PHOTOPRODUCT DISTRIBUTION. J.L. Alderfer, S.D. Soni, J.C. Wallace and G.L. Hazel; Biophysics Department, Roswell Park Memorial Institute, Buffalo, NY 14263.

Radiation of nucleic acids with light can produce photoproducts. Variations of experimental conditions such as radiation wavelength, solvent composition, and the presence or absence of oxygen, produce photodimers, photoadducts, and photohydrates. In the experiments reported here, a series of dinucleoside monophosphates (d-NpN; N = Thymine or 5-Fluorouracil), in aqueous phosphate buffer with acetone as a photosensitizer, were irradiated with a sunlamp (UV-B) at 4°C, under nitrogen. The major photoproduct formed during irradiation of d-TpT is the *cis*,*syn* cyclobutane-type dimer. Formation of such photoproducts can be followed by the disappearance of uv absorbance of starting material with dose, which usually follows pseudo first-order rate kinetics. Using this assay, the sensitivity to light of d-TpT was compared to d-TpF, d-FpT, and d-FpF, in the pH range 6.0-10.5. All the fluorinated compounds are more sensitive to light than d-TpT and are degraded in the order d-TpF < d-FpT < d-FpF. At pH 6.0, the photodimer is also the major photoproduct of the fluorinated compounds, but as pH is increased (with simultaneous reduction of degradation rate), a photoproduct which lacks fluorine is observed, and a concomitant formation of F⁻ is observed in the solution. At a given pH the relative amount of this product follows the order d-TpF < d-FpT < d-FpF. The structure of this photoproduct is tentatively identified as a "5-5 adduct". (Supported by NIH.)

W-Pos16 PYRUVATE KINASE ISOZYMES: ARE THEY REGULATED BY A COMMON MECHANISM? Thomas G. Conslor, Suzanne H. WOODARD AND James C. Lee. Department of Biochemistry, St. Louis University School of Medicine, St. Louis, MO 63104

Pyruvate kinase (PK) is an important glycolytic enzyme which is expressed differentially in a tissue specific manner. There are four distinct isozymes, namely, liver (L), erythrocyte (R), skeletal muscle (M_1), and kidney (M_2). The reaction catalyzed by PK is also regulated in a tissue specific manner. Those found in gluconeogenic tissues, e.g. kidney, have been described as being under allosteric control and the isozymic form exhibits sigmoidal kinetics. In contrast, the muscle isozyme is not generally regarded as allosteric since it exhibits hyperbolic kinetic properties. Hence, are these isozymes regulated by different molecular mechanisms? To provide insights to this aspect of PK, distance matrix analysis was employed to locate the intersubunit contact sites of muscle isozyme based on the crystallographic data of Muirhead and co-workers (private communication). The common structural features are the N-terminal domain and the Ca1-Ca2 helical region of the C domain. The primary sequences of the M_1 and M_2 isozymes (Noguchi et al., JBC 261, 13807, 1986) show that the only difference is at the Ca1-Ca2 region. In addition, kinetic studies under a wide spectrum of conditions showed that both isozymes exhibit the same regulatory properties. Thus, it leads to the proposal that both isozymes are regulated by a common mechanism similar to that shown for the M_1 system. The enzyme can exist at least in two states which are in equilibrium. It is the nature of this equilibrium which determines the characteristic properties exhibited by each isozyme. The primary sequence of the Ca1-Ca2 region apparently influences this equilibrium between states.

W-Pos17 INVESTIGATION OF THE ACTIVE SITE OF MONOAMINE OXIDASE B BY SPIN LABELED SUBSTRATE TRYPTAMINE

HENRY M. ZEIDAN* and SHARUNDA DANIEL
ATLANTA UNIVERSITY, CHEMISTRY DEPARTMENT
ATLANTA, GA 30314

ABSTRACT:

The spin label substrate tryptamine was used as a structural probe of the active site of bovine liver monoamine oxidase B. When the reaction was monitored by electron spin resonance (ESR), line broadening effects indicative of binding with an apparent relation to substrate specificity of the highly purified enzyme was observed. The spectrum indicates relatively fast and isotropic motion of the spin label. The dissociation constant of binding is 36 μ M. The environment surrounding the catalytic site and the mobility of the label are both characterized and discussed.

This work was supported by NIH, RCM Grant #1G 12-RR03062, NIH Grant #RR08247 to (HZ) and NSF Grant #R11855438.

W-Pos18 A FLUORESCENT METHOD TO STUDY INTERACTION OF INHIBITORS WITH PHOSPHOLIPASE A₂
B. S. Vishwanath*, A. A. Fawzy*, T. V. Gowda†, and R. C. Franson*. *Department of Biochemistry and Molecular Biophysics, P.O. Box 614, Medical College of Virginia, Richmond, VA 23298, U.S.A. †Department of Biochemistry, University of Mysore, Manasaganqotri, Mysore - 570 006, India.

To develop enzyme-directed inhibitors of phospholipase A₂ (PLA₂) methods are needed to assess the interaction of potential inhibitors with the protein. In this study a fluorescent approach is probed. Aristolochic acid, quercetin and retinol inhibit in vitro activity of purified snake venom (Naja mossambica mossambica) PLA₂, and highly purified PLA₂ isolated from human synovial fluid. Excitation of the Naja venom PLA₂ at 280 nm results in a broad fluorescent peak ranging from 300 nm to 400 nm with maximal emission at 342 nm. Aristolochic acid, quercetin and retinol quenched the fluorescence of the Naja venom PLA₂ at 342 nm indicating formation of an enzyme inhibitor complex. With all the three inhibitors the relative intensity decreased in a dose dependent manner to reach a maximum that varied from drug to drug. Molar binding ratios of aristolochic acid, quercetin, and retinol to the Naja PLA₂ was 34, 30, and 36 respectively. These studies indicate that three inhibitors of in vitro PLA₂ activity interact directly with the protein. This method may therefore be useful to assess stoichiometry and relative affinities of binding of venom inhibitors to isolated PLA₂s.

W-Pos19 ENTHALPIC AND ENTROPIC CONTRIBUTIONS TO THE ADP ACTIVATION OF NAD-DEPENDENT ISOCITRATE DEHYDROGENASE Marina M. Symcox and Gregory D. Reinhart, Dept. of Chemistry, Univ. of Oklahoma, Norman, OK 73019.

The allosteric activation of beef heart mitochondrial NAD-dependent isocitrate dehydrogenase (ICDH) by ADP was investigated. ADP (not MgADP) allosterically activates ICDH by increasing the apparent affinity of the enzyme for its substrate Mg-isocitrate (MgIC) rather than by increasing turnover per se. This activation is well characterized by the linked-function equation:

$$K_{1/2} = K_a^0 \frac{K_{ix}^0 + [\text{ADP}]}{K_{ix}^0 + Q \cdot [\text{ADP}]}$$

where $K_{1/2}$ = [MgIC] producing half-maximal velocity, $K_a^0 = K_{1/2}$ when [ADP] = 0, K_{ix}^0 = the apparent dissociation constant of ADP when [MgIC] = 0, and Q is equal to the ratio of $K_{1/2}$ when [ADP] = 0 to $K_{1/2}$ when [ADP] is fully saturating. The influence of temperature on Q was evaluated between 10 and 45°C. A van't Hoff plot of $\log(Q)$ vs. $1/T$ is straight and indicates that $\Delta H = -10$ kcal/mol and $T\Delta S = -8.8$ kcal/mol at 25°C. If MgIC achieves a rapid binding equilibrium in the steady-state, then these data imply that the coupling between ADP and MgIC on ICDH results from large, opposing enthalpic and entropic contributions with the entropic contribution serving to substantially mitigate the enthalpically driven activation. The data further suggest that the origin of the entropic contribution does not primarily involve changes in protein/ligand solvation. Supported by NIH grant GM 33216.

W-Pos20 PURIFICATION AND CHARACTERIZATION OF THE Mg^{2+} -ATPase FROM RABBIT SKELETAL MUSCLE. T.L. Kirley, Department of Pharmacology and Cell Biophysics, University of Cincinnati, Cincinnati, Ohio 45267-0575.

There is a Ca^{2+} , Mg^{2+} -ATPase (hereafter, Mg^{2+} -ATPase) associated with transverse tubule (t-tubule) membranes in rabbit skeletal muscle. This enzyme is dissimilar to the sarcoplasmic reticulum (SR) Ca^{2+} -ATPase in many functional properties including: (1) an apparent lack of phosphorylated intermediate, (2) relative insensitivity to inhibition by vanadate, FITC and sulfhydryl group reactive reagents, (3) nucleotide specificity, (4) pH and temperature dependence, (5) susceptibility to inactivation by detergents, and (6) lack of activation by micromolar Ca^{2+} . The Mg^{2+} -ATPase is a glycoprotein whose activity is modulated by Concanavalin A.

The Mg^{2+} -ATPase activity has been solubilized with lysolecithin and digitonin and purified by a combination of lectin affinity chromatographies, ion exchange chromatography and native gel electrophoresis. The purified enzyme preparation always contains a ~105 kDa protein (α subunit) and various amounts of ~70 kDa (putative β subunit) and ~45 kDa (putative γ subunit) proteins, which are not disulfide linked. The ~105 kDa α subunit glycoprotein was subjected to CNBr peptide mapping, amino acid analysis and microsequencing. In contrast to published reports (see Damiani et al. (1987) *J. Cell Biol.* 104, 461-472), the purified Mg^{2+} -ATPase is not structurally similar to the SR Ca^{2+} -ATPase as shown by very different peptide maps. The Mg^{2+} -ATPase also has a lower percentage of cysteine and methionine, consistent with the chemical reactivity and peptide mapping data. The t-tubule Mg^{2+} -ATPase α (105 kDa) subunit appears to have a blocked N-terminus. (Supported by Southwest Ohio American Heart Association grant #SW-86-15).

W-Pos21 PHYSICAL METHODS FOR THE DETERMINATION OF COENZYME B-12 ENZYME MECHANISMS. Mark R. Chance, Department of Chemistry, New York University, 4 Washington Place, NY, NY 10003.

Cobalt chemistry performed by the coenzyme B-12 dependent enzyme systems has proven to be exceedingly complex and sophisticated. The maintenance of the stable organometallic bond between cobalt and the adenosyl carbon is unique among metalloenzymes. Yet, it is generally accepted that the breaking of this bond is the necessary first step for all B-12 catalysis. It is clear that the competing influences of the corrin macrocycle, the dimethyl-benz-imidazole base, the sixth ligand, and the protein serve to regulate the stability of the bond and the structure and oxidation state of cobalt. The mechanisms of B-12 coenzymes have been demonstrated in some cases to proceed via $\text{Co}(+2)$ intermediates accompanied by substrate free radical rearrangements which may or may not involve direct participation by the metal. Physical methods for examining: 1) the cobalt-ligand distances, 2) the oxidation state and coordination number of cobalt, 3) the corrin macrocycle and the peripheral groups, and 4) the axial ligands, are necessary to solve the questions of B-12 reactivity and mechanism. Direct and precise measurement of cobalt-ligand interatomic distances using Extended X-ray Absorption Fine Structure (EXAFS) spectroscopy is shown to be quite feasible. The estimates of metal-ligand distances provided by EXAFS are shown to closely agree with crystallographic results. Examination of x-ray absorption edge spectra also provides information on the oxidation state and coordination number of cobalt. Resonance Raman techniques are also well suited to B-12 structural characterization because of its strong and complex chromophore. Several vibrational modes have been assigned to the corrin macrocycle and others may be responsive to peripheral groups and the axial ligands.

W-Pos22 INDUCTION OF A LATENCY PHASE DURING ACTION OF PHOSPHOLIPASE A₂ ON DIPALMITOYLPHOSPHATIDYLCHOLINE LIPOSOMES IN THE GEL PHASE.

Marco T. González-Martínez* and Marta S. Fernández, Dept. of Biochemistry - Centro de Investigación del I.P.N., P. O. Box 14-740, 07000 México City.

The hydrolysis of dipalmitoylphosphatidylcholine liposomes by pig pancreatic phospholipase A₂, was studied at 31°C i.e., with the substrate in the gel phase. It has been found that addition of fatty acid - free bovine serum albumin to the assay medium, induces the appearance of a latency phase in the time course of the enzymatic action; the more albumin added, the longer the latency. The lag period can be reduced and finally abolished, by addition of increasing concentrations of free palmitic acid whereas no reversal is found by addition of lysolecithin. At the concentrations that induce a lag period, bovine serum albumin does not shift the phase transition temperature of the liposomes employed in this study. This is important since even in the absence of albumin, a lag period appears both in the phase transition temperature range and in the liquid crystalline state but not in the gel phase of dipalmitoylphosphatidylcholine liposomes. Thus, the generation of a latency period by albumin appears to be due to its ability to sequester the palmitic acid produced by the phospholipase A₂ catalysis. These results point to the essential role of the fatty acid released by the enzyme, in the regulation of the time course of the hydrolytic action.

*Present address: Dept. of Pharmacology, same Institution.

W-Pos23 OXIDATION INCREASES THE PROTEOLYTIC SUSCEPTIBILITY OF THE INTERDOMAIN TETHER IN RHODANASE.

Paul Horowitz and Steven Bowman, Department of Biochemistry, The University of Texas Health Science Center, San Antonio, Texas 78284

The enzyme rhodanase has been proteolytically cleaved to give species that most likely correspond to individual domains, indicating cleavage in the interdomain tether. The conditions for cleavage show that availability of the susceptible bond(s) depends on conformational changes triggered by oxidative inactivation. Rhodanase, without persulfide sulfur (E), was oxidized consequent to incubation with phenylglyoxal, NADH, or hydrogen peroxide. The oxidized enzyme (Eox) was probed using the proteolytic enzymes endoproteinase glutamate C (V8), trypsin, chymotrypsin, or subtilisin. The proteolytic susceptibility of Eox, formed using hydrogen peroxide, was compared with that of E and the enzyme containing transferred sulfur, ES. ES was totally refractory to proteolysis, while E was only clipped to a small extent by trypsin or V8 and not at all by chymotrypsin or subtilisin. Eox was susceptible to proteolysis by all the proteases and, although there were some differences among the proteolytic patterns, there was always a band on SDS PAGE corresponding to MW=16,500. This was the only band observed in addition to the parent species (MW=33,000) when Eox was digested with chymotrypsin, and conservation of total protein was observed after digestion up to 90 min. No additional species were observable on silver staining, although there was some indication that the band at 16,500 might be a doublet. The results indicate a conformational change after oxidation that results in increased exposure and/or flexibility of the interdomain tether which contains residues that meet the specificity requirements of the proteases used. (Supported by NIH grant GM25177 and Welch grant AQ723.)

W-Pos24 ANALYSIS OF THE INTERACTION OF REPAIR PROTEINS AND ENZYMES WITH RANDOMLY DAMAGED DNA

Sharlyn J. Mazur, Department of Biochemistry
The Johns Hopkins University School of Hygiene and Public Health,
615 N. Wolfe St., Baltimore MD 21205

Many types of damage in DNA are repaired by specific DNA repair enzymes. Randomly damaged DNA is often used in characterizing the interactions of these enzymes with their substrates *in vitro*. In randomly damaged DNA, there is a distribution in the number of damaged sites per DNA molecule as well as variation in the sequence in which the damage is located. Both of these factors must be considered in analyzing equilibrium and kinetic data. Theoretical descriptions of many aspects of the interaction of proteins with nucleic acids can be extended to sites which are randomly located. Expressions are derived for the equilibrium distribution of protein at randomly located specific sites, including the effects of site overlap and site heterogeneity. The effects of the random location of specific sites on association and dissociation kinetics are considered. Since one-dimensional diffusion is a component in the mechanism of many site-specific DNA binding proteins, a description of sliding-assisted association and dissociation to randomly located sites is developed. In addition, expressions describing the rate of repair of randomly located damage by DNA repair enzymes are derived. The effect of the random location of sites in processive and distributive mechanisms of repair are considered.

W-Pos25 THE GAMMA SUBUNIT OF NA,K-ATPASE IS A SMALL, AMPHIPATHIC PROTEIN WITH A UNIQUE AMINO ACID SEQUENCE. John H. Collins and John D. Leszyk, Dept. Biol. Chem., Univ. Maryland Sch. Med., Baltimore, MD 21201.

The gamma subunit, or "proteolipid" of cell membrane Na,K-ATPase is a small, membrane-bound protein which copurifies with the alpha and beta subunits of this enzyme, and may be involved in forming a receptor for cardiac glycosides. We have determined the sequence of the N-terminal half of gamma, and the remainder will be deduced from its cDNA. The sequence is unique, proving that gamma is not a breakdown product of the larger subunits. Gamma is not a true proteolipid, but rather has an N-terminal hydrophilic domain which must be extracellular, and a short C-terminal domain which traverses the cell membrane once. The hydrophilic domain is probably extracellular, and includes a cluster of aromatic residues which may be involved in glycoside binding. Supported by NIH grant AR35120.

W-Pos26 TIME-VARYING MAGNETIC FIELD CAUSES CELL TRANSFORMATION:

A. H. Parola^{a,b}, N. Porat^b, and L. A. Kiesow^a ^aNaval Medical Research Institute, Bethesda, MD 20814, USA, and ^bDepartment of Chemistry, Ben-Gurion Univ of the Negev, Beer-Sheva, ISRAEL

Chick embryo fibroblasts (CEF) have undergone malignant transformation when exposed for 24 hr to a sinusoidal electromagnetic field (100 Hz, 7 G). This was evident from reduced adenosine deaminase (ADA) specific activity (a malignancy marker), from an ~100% increased rate of cell growth and from increased membrane lipid microfluidity, as measured by fluorescence polarization and by the single photon correlation lifetime studies of 3 lipophilic probes. Using continuous frequency phase modulation spectrofluorimetry, rotational relaxation motion of the complex formed between the small subunit ADA labeled by pyrene sulfonyl chloride and its membrane binding protein on the intact cells, normal CEFs could be distinguished from electromagnetically transformed CEFs. Plots of phase angle vs. frequency of the latter were identical with those of RSV transformed CEFs, for which ADA activity is 10-fold reduced. Viral and electromagnetic transformation resulted in increased rotational relaxation motion of the ADA complex which is consistent with fluidization of membrane lipids. Using CEFs infected with the temperature sensitive mutant RSV-Ts68 the electromagnetic effect was shown not to be thermal. CEFs grown at 41° showed the fingerprint profile of phase angle vs. frequency characteristics of normal cells while CEFs grown at 36° had the profile of transformed cells. Ts68 transformed cells when grown at 36° in the magnetic field showed a profile identical to that of RSV transformed cells, and not the profile of cells grown at 41° indicating a magnetic rather than a thermal effect.

W-Pos27 CYTOCHROME C INDUCED FORMATION OF LARGE PHOSPHOLIPID DOMAINS AND PARTITIONING OF MEMBRANE PROTEINS. Doris M. Haverstick and Michael Glaser, Department of Biochemistry, University of Illinois, Urbana, IL 61801

A fluorescence microscope attached to a charge-coupled-device camera and a digital image processor was used to visualize the distribution of labelled phospholipids in large unilamellar vesicles. The phospholipids were covalently labelled with either the NBD (4-nitrobenzo-2-oxa-1,3-diazolyl) or dansyl (5-dimethylaminonaphthalene-1-sulfonyl) fluorophore on the fatty acid chain. In vesicles composed of 95% phosphatidylcholine (PC) and 5% phosphatidic acid (PA), cytochrome c at low ionic strength bound to the PA and caused it to be sequestered into large domains. The number and size of the domains depended on the cytochrome c concentration. The formation of the domains was not reversed by 0.1 M NaCl, but pretreatment of the vesicles with 0.1 M NaCl prevented cytochrome c binding and phospholipid reorganization. In vesicles containing NBD-PA on the inner leaflet and dansyl-PA on the outer leaflet of the bilayer, the addition of cytochrome c to the outside of the vesicle induced sequestering of PA on the outer leaflet but it did not induce reorganization of the phospholipids on the inner leaflet. Inclusion of 5% of the channel forming peptide gramicidin did not interfere with the cytochrome c induced phospholipid reorganization. Gramicidin partitioned preferentially into the PC-enriched area of the vesicle and was excluded from the PA-enriched domain. This work was supported by NIH Grant GM 21953.

W-Pos28 INVESTIGATION OF CHAIN CONFORMATION AND MOBILITY OF DISULFIDE POLYMERIZED PHOSPHATIDYLCHOLINES. Tracy M. Handel¹, Jack Blazyk² and John D. Baldeschwieler¹. ¹Division of Chemistry and Chemical Engineering, California Institute of Technology, Pasadena, CA 91125 and ²Chemistry Dept., Ohio University, Athens, Ohio 45701.

The potential of polymerizable thiol-containing phospholipids as constituents of drug delivery vehicles has been under investigation in our laboratory. Of particular interest has been the correlation between lipid structure and the physical properties of the liposomes. In this study, FT-IR and Raman spectroscopy have been utilized to probe the conformation and degree of motion in the hydrocarbon chains of monomeric and polymeric A-THIOLS and T-THIOLS (thiol at C-2 and the terminal carbon, respectively). For the A-THIOLS, temperature-dependent changes in the bandwidth and peak position of the IR symmetric methylene C-H stretch suggests polymerization induces a broadening of the phase transition with little shift in temperature and an increase in the disorder of the hydrocarbon chains. Raman C-H and C-C stretching vibrations of gel state lipids also indicate the polymers are more disordered than the monomers, largely due to the presence of more gauche rotomers. T-THIOLS have a distinctly different behavior. The vibrational spectra and DSC indicate a large increase in the phase transition and membrane order upon polymerization as well as a highly trans chain conformation. Additional properties pertinent to drug delivery applications will be discussed. This work was supported by an NRS award (T32 GM07616) from NIH, a grant (DAAG-29-83-K-0128) from ARO and gifts from Monsanto.

W-Pos29 INTERACTION OF MEMBRANE BOUND CARBOHYDRATES WITH DRY LIPID HEAD GROUPS
RAYMOND P. GOODRICH, JOHN H. CROWE*, LOIS M. CROWE*, AND JOHN D. BALDESCHWIELER.
CALIFORNIA INSTITUTE OF TECHNOLOGY, 127-72, PASADENA, CA 91125. *UNIVERSITY OF CALIFORNIA, DAVIS, CA 95616.

FT-IR has been utilized by Crowe, et al. to examine the interaction of free carbohydrates with dry lipid membranes.¹ We have utilized the same techniques to examine the behavior of membrane bound carbohydrates in the form of synthetic glycolipids. Dry samples composed primarily of DPPC with various amounts of the derivatives were examined in the P=O stretching region. Samples were also prepared using derivatives lacking the carbohydrate (TEC) and with cholesterol (CHOL). Pure DPPC, DPPC:TEC (7:3), and DPPC:CHOL (7:3) yielded a broad band centered at 1252 cm⁻¹. Samples containing the derivatives with a galactose or maltose unit exhibited a band centered at 1238 cm⁻¹. Upon heating to 40°C, a second band at 1252 cm⁻¹ appeared which increased in intensity upon heating to 65°C. This band disappeared upon cooling the sample to room temperature. This behavior was unique to samples containing the carbohydrate derivatives. Such behavior is believed to be characteristic of H-bonding interactions of the carbohydrate with the P=O segment of the phospholipids in a manner similar to that induced by hydration. This work was supported in part by a National Research Service Award (T32 GM07616) from the National Institute of General Medical Sciences, grant no. DAAG-29-83-K-0128 from the ARO, and a gift from Monsanto.

¹Archives of Biochemistry and Biophysics, Vol. 236, No. 1, 289-296 (1985).

W-Pos30 PHASE MODULATION ANALYSIS OF FLUOROPHORE ROTATIONAL HETEROGENEITY IN SYNTHETIC AND BIOLOGICAL MEMBRANES. N.P. Illsley and A.S. Verkman, Cardiovascular Research Institute, University of California, San Francisco, CA 94143.

Differential polarization measurements of DPH in simple solvents, sonicated phosphatidylcholine (PC) vesicles, hepatic plasma membranes (HPM) and placental microvillous vesicles (MVV) were performed using a multi-frequency phase-modulation fluorimeter. DPH fluorescence was excited using a He-Cd laser and measurements were made using >15 modulation frequencies (1-210 MHz). Fluorescence lifetime and differential phase and modulation data were fitted to a series of anisotropy decay models including (1) anisotropic rotation, (2) isotropic hindered rotation with ground state rotational heterogeneity and (3) isotropic hindered rotation with continuous distributions in limiting anisotropy (r_{∞}) and/or rotational correlation time (ϕ). In non-viscous solvents (ethanol, chloroform, hexadecane) the data fitted well ($\chi^2 < 2$) to a single unhindered rotator. DPH in mineral oil fitted best to an anisotropic rotator with 2 correlation times (0.4, 2.8 ns). In PC vesicles and in the biological membranes, the data fitted best to a double, hindered rotator model with χ^2 values <2, >25-fold lower than the best χ^2 for an anisotropic rotator, single hindered rotator or r_{∞} and ϕ rotational distributions. The r_{∞} values in PC vesicles (0.02, 0.03) were lower than those in HPM (0.11, 0.18) or MVV (0.11, 0.28). The ϕ values in PC vesicles (.4, 4.7 ns) were similar to ϕ in HPM (.1, 6.3) and MVV (.1, 6.1). The best distribution model, although a poorer fit, was a uniform distribution in ϕ , however asymmetric distribution analyses may provide a better anisotropy decay model. These results indicate that an adequate description of fluorophore rotation in biomembranes requires inclusion of ground state rotational heterogeneity, likely because of distinct solid and fluid phase lipid domains.

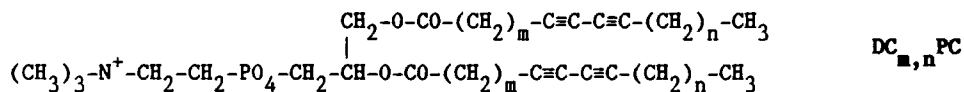
W-Pos31

STRUCTURES OF TWO 27-CARBON DIACETYLENIC PHOSPHATIDYLCHOLINE ISOMERS

William Morris¹, Paul Schoen², Paul Yager³, Alok Singh⁴ and David G. Rhodes⁵

1. U.Conn. Dept. of Chemistry, Storrs, CT 06268, 2. Code 6190, Bio/Molecular Engineering Branch, Naval Research Laboratory, Washington, DC 20375-5000, 3. Bioengineering, FL-20, U. of Washington, Seattle, WA 98195, 4. Geo-Centers, Inc., Fort Washington, MD 20744, 5. Biomolecular Structure Analysis Center, Dept. of Radiology, U. Conn. Health Center, Farmington, CT 06032

DC_{8,13}PC and DC_{9,12}PC were investigated using low-angle x-ray diffraction. Bilayers of these diacetylenic phosphatidylcholine derivatives were highly ordered, typically yielding at least 16 orders of lamellar diffraction. The unit cell repeat is very small for a lipid of this size, even considering previously published data for DC_{8,9}PC. Electron density profiles of bilayers of both 27 carbon derivatives have double peaks in the acyl chain region, corresponding to the diacetylene positions, at approximately 10 Å and 17 Å from the bilayer center. At equal resolution, the doublet is less well resolved for DC_{9,12}PC than for DC_{8,13}PC. As expected, the electron density profile for DC_{8,13}PC is similar to that of DC_{8,9}PC, except that the extent of the distal acyl chain region is larger in the case of DC_{8,13}PC. Model structures inferred from the electron density maps feature tilted acyl chains which are interdigitated at the termini.



W-Pos32

STRUCTURES OF POLYMERIZABLE THIOL-SUBSTITUTED PHOSPHATIDYLCHOLINE BILAYERS

David G. Rhodes¹, Tracy M. Handel² and J. D. Baldeschweiler²

1. Biomolecular Structure Analysis Center, Dept. of Radiology, U. Conn. Health Center, Farmington, CT 06032 2. Chemistry Department, California Institute of Technology, Pasadena, CA 91125

Low-angle x-ray diffraction was used to investigate the structures of two thiol-derivatives of dipalmitoyl phosphatidylcholine (DPPC). The thiol was located at either the first methylene carbon (α -thiol) or at the terminal carbon (T-thiol). Profile structures were determined for bilayers of these derivatives in both polymerized and unpolymerized forms, and in most cases, above and below T_m . Unit cell repeats of both derivatives were somewhat smaller than might be expected, based on data from DPPC, but the apparent reasons for the smaller repeats were different. Based on the electron density profiles calculated for the α -thiol lipids, the bilayer interior is relatively disordered, consistent with its low T_m . This disorder results in decreased bilayer thickness, like that observed upon melting of conventional bilayers. The electron-dense sulfur atoms on the T-thiols are confined to a relatively narrow region of the bilayer center. Our best model to date which explains the observed electron density distribution as well as calorimetric and Raman data would require that the acyl chains of the T-thiols be tilted. The structure of monomer bilayers does not appear to differ significantly from that of polymer bilayers.

DGR was supported by the Defense Advanced Research Projects Agency and R.J.R. Nabisco, Inc.

TMH and JDB were supported by NRS Award (T32 GM07616) from NIH, DAAG-29-83-K-0128 from ARO and gifts from Monsanto.

W-Pos33

A CONVECTION-FREE MONOLAYER TROUGH FOR FLUORESCENCE MICROSCOPY AND PHOTOBLEACHING MEASUREMENTS AT THE AIR-WATER INTERFACE. F. Mojtabai and D. Axelrod, Biophysics

Research Division and Department of Physics, University of Michigan, Ann Arbor, Michigan 48109.

A new circular trough with radial motorized barriers and a clear glass or fused silica bottom has been developed for fluorescence microscopy of lipid/protein monolayers at an air-water interface. Very shallow depths of water (less than 0.5 mm) can be used, thus minimizing convection and flow of the monolayer. The entire area of the monolayer is accessible for scanning, thereby permitting tracking of distinct features in the monolayer as the area is changed. Possible edge effects are minimized by the large open area. This trough allows for conventional focusing by vertical motion of the microscope stage rather than by adjustment of the water level to the objective's focal plane as required in some other systems. The monolayer trough is easily adaptable onto the stage of any inverted microscope, compatible with epi- and total internal reflection illumination, and easily demountable for cleaning. Leakage problems around the sides of the barriers are avoided by making the barriers from Kalrez instead of Teflon. With this trough, we have successfully observed by fluorescence: (1) the formation of 2-D crystals in DPPC monolayers doped with 1 mole % of the fluorescent probe NBD-egg-PE; and (2) the diffusion coefficient (measured by photobleaching recovery) of NBD-egg-PE in such monolayers as a function of temperature through the phase transition. Supported by a Swiss National Science Foundation Postdoctoral Fellowship, the University of Michigan Protein Structure and Design Program and NIH grant NS14565.

W-Pos34 PHOSPHOLIPASE A₂ AND NBD-PHOSPHOLIPIDS AS PROBES OF MEMBRANE LIPID SURFACE MODIFICATIONS INDUCED BY CHRONIC ETHANOL INTOXICATION.

C.D. Stubbs, B.W. Williams and E. Rubin. Department of Pathology and Cell Biology, Thomas Jefferson University, Philadelphia PA 19107

Previous studies have established that the consumption of chronic ethanol leads to a development in membranes of a resistance to lipid fatty acyl chain disordering by ethanol and other hydrophobic agents. The techniques used (fluorescence and ESR spectroscopy) do not, however, reveal any structural basis for the effect such as an alteration in the lipid order parameter in the absence of the added ethanol. The implication is that the modification induced by chronic ethanol consumption resides elsewhere in the membrane such as in the lipid head group region. We have therefore used phospholipase A₂ as a probe for the chronic ethanol induced alterations since it interacts with the membrane surface. The substrate for the phospholipase A₂ was NBD-PC (1-palmitoyl, 2-N-(4-nitrobenzo-2-oxa-1,3-diazole) amino caproyl-PC). The advantages of using NBD-PC are a rapid uptake into natural membranes, the ease of quantification of the released NBD-hexanoic acid by measurement of fluorescence, and the lack of re-acylation of the NBD-hexanoic acid. It was found that the rate of hydrolysis of NBD-PC by phospholipase A₂ (*Crotalus Durissus Terrificus*) was significantly reduced in liver microsomal membranes from ethanol-treated rats as compared to controls. This was not only found in intact membranes but also in vesicles of the phospholipids extracted from the microsomes showing that the ethanol induces an alteration to a phospholipid(s) which modifies the membrane structure.

W-Pos35 OUTER MEMBRANE FLUIDITY IN SMOOTH AND ROUGH STRAINS OF SALMONELLA TYPHIMURIUM AND THEIR SUSCEPTIBILITY TO ANTIMICROBIAL PEPTIDES.

Fazale Rana and Jack Blazyk, Chemistry Department and College of Osteopathic Medicine, Ohio University, Athens, Ohio 45701.

Although the outer membrane (OM) of gram-negative bacteria has been studied extensively, its molecular architecture is not well characterized. Lipopolysaccharide (LPS) is an unusual glycolipid which is a major component of the outer monolayer of the OM and is responsible for much of the surface character of the gram negative bacterial cell. In an effort to better understand the structure and dynamics of the OM of these microorganisms, membrane fluidity changes in three strains of Salmonella typhimurium which differ in LPS structure were measured by differential scanning calorimetry and FT-IR spectroscopy. The three strains which were examined are: (a) a smooth strain (SL3770) which contains LPS containing both the core region and O-antigen sugars; (b) a rough strain (SL3749) of R_a chemotype in which the LPS lacks the O-antigen region; and (c) a rough strain (SL1102) of R_e chemotype where the LPS lacks both the O-antigen sugars and the entire core region except for the 2-keto-3-deoxyoctonate residues. As the hydrophilic portion of the LPS molecule is reduced, the organism becomes increasingly more susceptible to the bactericidal effects of a variety of naturally occurring antimicrobial peptides, such as defensins, cecropins and magainins. Using FT-IR spectroscopy, the thermotropic phase behavior of the OM, extracted LPS and lipid A (a derivative of LPS from which all of the core and O-antigen sugars have been hydrolyzed) from these organisms was determined by monitoring changes in the peak position and bandwidth of the symmetric methylene stretching band as a function of temperature. These data, combined with calorimetric results, provide insight into the effects of altered LPS structure on the structural and functional properties of the OM of gram-negative organisms.

W-Pos36 DPH FLUORESCENCE LIFETIME DISTRIBUTIONS IN CHOLESTEROL-EGG LECITHIN MULTILAMELLAR LIPOSOMES.

R.Fiorini, G.Curatola, E.Bertoli and E.Gratton*. Biochemistry Institute, University of Ancona, ITALY; *Department of Physics, University of Illinois, Urbana, IL

The fluorescence decay of 1,6-diphenyl-1,3,5-hexatriene (DPH) in egg lecithin multilamellar liposomes with varying concentrations of cholesterol was studied using multifrequency phase fluorometry. The data were analyzed in terms of both sums of exponentials and continuous distributions of lifetime values. In egg lecithin with and without cholesterol, DPH showed a double exponential decay with a long component which represents the principal fraction in both analyses. Cholesterol has been shown to affect both the lifetime value and the width of the distribution, causing an increase of the lifetime value and a narrowing of the distribution width. The effect of cholesterol on the distribution width appears to be relevant even at low cholesterol-phospholipid concentrations (5 to 100 molar ratio). Moreover at high concentrations, such as 40-50 to 100 molar ratio, a better fit of the DPH fluorescence decay data is obtained by a unimodal distribution analysis. This correlation between the DPH lifetime and the distribution width, and the molecular environment of the DPH molecule has been used to investigate the role of cholesterol in modifying membrane water permeability and membrane structural heterogeneity.

Supported by Regione Marche Ricerca Sanitaria Finalizzata n.7005 del 22/12/86 and G.C.40, M.P.I., Rome (Italy); IHS-IP41RR03155.

W-Pos37 KINETIC AND MAGNETIC RESONANCE STUDIES OF CHEMICALLY MODIFIED D-3-HYDROXYBUTYRATE DEHYDROGENASE (BDH). Lauraine A. Dalton, Department of Molecular Biology, Vanderbilt University, Nashville, TN 37235.

BDH is a lipid-requiring enzyme purified from the mitochondrial inner membrane. The apoenzyme, devoid of lipid, is inactive but can be reactivated by insertion into phospholipid vesicles containing lecithin. BDH in the membrane is a tetramer with two sulfhydryl groups (SH1 and SH2) per monomer (31 kD). SH1 and/or SH2 have been selectively alkylated with maleimide spin label (MSL) (irreversible) and/or diamide (reversible) and the function (by enzyme kinetics) and distance from the surface (by EPR methods) of the derivatized enzyme have been correlated. Modification of SH1 with either diamide or MSL diminishes V_{max} and increases the K_m for 3-hydroxybutyrate (BOH) ~50-fold but has little or no effect on the K_m for the NAD^+ cofactor. Alkylation of SH2 with MSL reduces V_{max} to ~25% of its original value, but does not affect the K_m for BOH or NAD^+ . Derivatization of both sulfhydryls markedly decreases V_{max} to <10% of its original value and increases K_m for BOH ~100-fold. SH1 has been demonstrated, by the spin label-spin probe method, to be at least 9 Å from the surface of the membrane [Dalton et al., *Biochemistry* (1987) 26, 2117-2130]. The EPR spectrum of MSL on SH2 is markedly broadened (2-fold increase in linewidth) by titration with paramagnetic ions indicating that, for this site, Heisenberg spin exchange is the dominant mechanism of relaxation. The nitroxide on SH2 is directly accessible to paramagnetic ions, and close to the membrane surface (<5 Å) whereas SH1 is more distal and located in the immediate vicinity of the substrate binding site of BDH. [Supported in part by NIH grants AM 21987 and AM 14632 to Sidney Fleischer; advice from SF and J. Oliver McIntyre is appreciated.]

W-Pos38 STRUCTURE OF THE ACETYLCHOLINE RECEPTOR IN THE RESTING AND DESENSITIZED STATES

Chikashi Toyoshima, Elizabeth Kubalek and Nigel Unwin*.

Dept. of Cell Biology, Stanford Univ. School of Medicine, Stanford, CA. *Present address: MRC Lab. of Molecular Biology, Cambridge, England

Three-dimensional structures of nicotinic acetylcholine receptor in the native and desensitized states have been studied by cryo-electron microscopy of frozen hydrated tubular crystals. In order to examine the differences between the two states the data were collected to 18 Å resolution, higher than in the previous study (Brisson & Unwin (1985) *Nature*:315, 474). The structures show significant differences suggesting a transition involving small rearrangements of the subunits.

W-Pos39 FREEZE-FRACTURE OF PROTEIN CRYSTALLINE ARRAYS IN MITOCHONDRIAL OUTER MEMBRANES.

Lorie Thomas, Marco Colombini and Eric Erbe*, Labs. of Cell Biology, Dept. of Zoology, Univ. of Maryland, College Park, MD 20742 and *USDA, Beltsville Agricultural Research Center, Beltsville, MD 20705. (Intr. by Lynn M. Amende)

The mitochondrial outer membrane contains large channel-forming proteins called VDAC. These channels form aqueous pores with a radius of 1.3 to 2 nm. In the outer membrane of *Neurospora crassa* mitochondria these proteins are often ordered into crystalline arrays. These arrays have been extensively studied in negatively stained outer membranes by Mannella and coworkers. They report a basic repeating unit of six channels within a parallelogram with dimensions of 12.6 by 11.1 nm and a tilt angle of 109°. Here we report results from freeze-fracture studies on these membranes. We see particles in ordered hexagonal arrays. Each hexagon is 6.7 nm on a side. These structures compare favorably with an entire six channel unit as opposed to one individual channel, implying the intimate structural association of six channels. Our results differ in two ways: 1) the hexagons observed with freeze-fracture have a six-fold axis of symmetry compared to the distorted hexagons seen with negative staining 2) the areas of the former are 13% smaller. Results of structural studies with treatments which induce channel closure in planar phospholipid membranes (in the absence of an applied electric field), will be presented. This work was supported by ONR grant N00014-85-K-0651.

W-Pos40 ROLES OF LIPIDS AND PROTEINS IN ION BINDING TO ISOLATED CARDIAC SARCOLEMMA VESICLES. Kenneth S. Leonards and Corina Dhers, Dept. of Physiology and Cardiovascular Research Laboratories, UCLA School of Medicine, Los Angeles, Ca. 90024.

Numerous studies suggest that cation/sarcolemmal interactions play an essential role in the excitation/contraction/relaxation cycles of cardiac cells. The identity of the membrane components involved in these interactions, however, remain completely unknown. It is also unknown whether cation binding to the sarcolemma is due to the primary independent binding of cations to individual membrane components, or a secondary function of molecular interactions between sarcolemmal components. To investigate these issues the cation-induced aggregation behavior of isolated rat, rabbit, and canine cardiac sarcolemmal vesicles (SLves), biochemically modified SLves, and SUVs generated from SLves lipid extracts were examined. Our results indicate that the binding of cations, such as Ca^{2+} , to the sarcolemma involves two or more interacting sites in the membrane, and is not the result of the independent binding of cations to individual membrane components. We also found that this binding does not involve the membrane proteins, but instead is due to lipid/lipid or lipid/carbohydrate interactions within the plane of the bilayer. In addition, our results indicate that while the basic characteristics of the cardiac sarcolemmal surface are similar from species to species, the particular interactions involved have been modified in a species specific manner. Finally, the selectivity series for this binding is the same as that which uncouples excitation from contraction in cardiac cells suggesting that these interactions could be involved in regulating the activities of the ion transport/channel proteins of the cardiac sarcolemmal membrane. (Supported by NIH grant HL 34517, AHA(GLAA) grant #843 G1, and Laubisch and Tuchbreiter endowments.)

W-Pos41 DATA ACQUISITION AND PROCESSING FOR DOUBLE-LABELED MEMBRANE SPLITTING. Knute A. Fisher and Kathleen C. Yanagimoto, Dept. Biochem. Biophys. & CVRI, Univ. of Calif., San Francisco, Calif. 94143-0130.

Double-labeled membrane splitting (DBLAMS) is a physical fractionation technique that can be used to analyze transbilayer distributions of hydrophobic molecules. In DBLAMS, planar freeze-fracture of intact red cell membranes is quantified by measuring concentrations of hemoglobin, a native marker for the cytoplasmic leaflet, and fluorescein concanavalin A, a marker for the extracellular leaflet. DBLAMS utilizes three conventional methods: liquid scintillation counting, absorbance spectroscopy, and fluorescence spectroscopy. Data sets are large and require multiple corrections. To improve the accuracy and efficiency of data acquisition and computation, the HP 85 computer resident in an HP 8451 diode array spectrophotometer was interfaced with a Beckman LS7000 scintillation counter and a home-built fluorometer. Programs were written for sample identification; signal averaging; sample averaging with statistics; background, quench, and enhancement corrections; file storage; and file transfer between the HP 85 and an IBM PC/XT. Programs were written for the IBM PC/XT for analyzing and displaying data and used to analyze the transbilayer distributions of tritiated derivatives of cholesterol, dipalmitoylphosphatidylcholine (DPPC), and the phorbol ester TPA in the red cell membrane at steady-state. All molecules distributed asymmetrically across the bilayer: the extracellular leaflet was enriched in cholesterol (outer:inner::2:1) and DPPC (4:1); the cytoplasmic leaflet enriched in TPA (1:2). The DBLAMS enhancements should facilitate analyses of the transbilayer distributions of other hydrophobic and amphipathic molecules. Supported by NIH GM31517.

W-Pos42 THE LOCATION OF THE HEME-Fe ATOMS WITHIN THE PROFILE STRUCTURE OF A MONOLAYER OF CYTOCHROME *c* BOUND TO THE SURFACE OF AN ULTRATHIN LIPID MULTILAYER FILM, James M. Pachence, Robert F. Fischetti, and J. Kent Blasie, Chemistry Dept., Univ. of PA., Phila., PA.

We have recently developed x-ray diffraction methods to derive the profile structure of ultrathin lipid multilayer films having 1 to 5 bilayers (eg., Skita, et al, J. Physique (1986) 47:1849). Furthermore, we have employed these techniques to determine the location of a monolayer of cytochrome *c* bound to the carboxyl group surface of various ultrathin lipid multilayer substrates via non-resonance x-ray diffraction (Pachence and Blasie, Biophys. J. (1987) 51:228). In this study, an intense tunable source of X-rays (beam line X9-A at the National Synchrotron Light Source at the Brookhaven National Laboratory) was utilized to measure the resonance x-ray diffraction effect from the heme-Fe atoms within the cytochrome *c* molecular monolayer located on the carboxyl surface of a 5 monolayer arachidic acid film. Lamellar x-ray diffraction was recorded for energies above, below, and at the Fe K-absorption edge ($E = 7112$ eV). An analysis of the resonance x-ray diffraction effect is presented, whereby the location of the heme-Fe atoms within the electron density profile of the cytochrome *c*/arachidic acid ultrathin multilayer film is indicated to ± 1 Å accuracy.

W-Pos43 PRESERVATION OF AN OPTIMAL MIXTURE OF LAMELLAR AND HEXAGONAL PHASE LIPIDS IN MODIFIED MYCOPLASMA CAPRICOLUM MEMBRANES. Sanda Clejan, Dept. Pathology, Mount Sinai School of Med. and City Hosp. Ctr at Elmhurst, NY.

When cultured in a media supplemented with an unsaturated phosphatidylethanolamine (PE) the cellular lipids of M. capricolum become highly enriched with the fed PE, but the ratio of the other major phospholipids phosphatidylglycerol (PG) and cardiolipin (DPG) changed in favor of PG. The ratio DPG + PE/PG was altered depending on temperature, configuration of fatty acids and membrane cholesterol. Synthesis of DPG was stimulated by low temperature and saturated fatty acids, whereas DPG was synthesized more in M. capricolum adapted to grow on very low cholesterol levels. Alteration of membrane lipid composition caused by hydrocarbons (HC), alcohols (AL) and detergents (DT), analyzed by a shift technique, showed more change in PE. M. capricolum counteracts the nonbilayer promoting ability of HC by lowering the ratio DPG + PE/PG. The same decrease was seen with addition of octanol and phenethylalcohol, but not with AL with higher chain length. With a growing number of oxyethylene units in the head group, DT acquire an increased tendency to shift phase equilibrium toward micellar phase. M. capricolum responded by raising the ratio DPG + PE/PG. Thus, factors beside the phase behavior and the hydrocarbon chain length of the participating molecule must be important when discussing the effect of perturbing molecules on this ratio.

W-Pos44 NUCLEAR MAGNETIC RESONANCE STUDY OF THE STRUCTURE OF MIXED DIACYLGLYCEROL/ PHOSPHATIDYL CHOLINE BILAYERS. H. DeBoeck and R. Zidovetzki, Department of Biology, University of California, Riverside, CA 92521.

We studied the effects of introducing four diacylglycerols (DAG) into bilayers of dipalmitoylphosphatidyl choline (DPPC) bilayers. The combination of ^{31}P - and ^2H nuclear magnetic resonance (NMR) allowed us to characterize the effects of DAGs on the macroscopic conformation of the mixed bilayers, orientation of DPPC headgroups and perturbation of the order parameters along the perdeuterated lipid side chains of DPPC. Two DAGs with saturated side chains, dipalmitin and distearin induce immobilization of the surrounding DPPC molecules at temperatures well above that of the temperature of gel to liquid crystalline phase transition (T_c) of pure DPPC. The amount of the immobilized DPPC is proportional to the amount of dipalmitin or distearin present. The ordering of the bulk DPPC molecules in such mixtures is the same as in control DPPC bilayers. Introduction of diolein or egg-DAG into DPPC bilayers results in a large increase of the order parameters of DPPC side chains which indicates stabilization of the bilayers by the DAGs with unsaturated side chains. At the same time, ^{31}P - but not ^2H NMR spectra of such mixed bilayers exhibit features characteristic of lipid polymorphism. Such behavior is consistent with the coexistence of regions with different average orientations of phospholipid headgroups, all in the basic bilayer conformation. The bilayer-stabilizing DAGs, diolein and egg-DAG, but not dipalmitin or distearin are known to be activators of phospholipases A and C in vitro.

W-Pos45 DEUTERIUM NMR SPECTROSCOPY OF SATURATED PHOSPHATIDYLCHOLINES IN THE LIQUID-CRYSTALLINE PHASE. Steven W. Dodd and Michael F. Brown (Intr. by W. R. Pearson). Department of Chemistry, University of Arizona, Tucson, AZ 85721.

^2H NMR studies of a homologous series of saturated phosphatidylcholines with perdeuterated acyl chains ranging in length from 12 to 18 carbons have been conducted [abbreviated di(n:0)PC where $n = 12, 14, 16, 18$]. The powder-type ^2H NMR spectra of randomly oriented dispersions in the L_α phase were deconvolved to yield subspectra corresponding to the director axis parallel to the magnetic field (de-Pakeing). Profiles of the bond order parameters $S_{CD}(i)$ and spin-lattice relaxation rates $R_{12}(i)$ as a function of chain segment position were derived. At the same absolute temperature, the length of the plateau in the $S_{CD}(i)$ profiles increases with the number of chain carbons; a small increase in their absolute values is observed. By contrast, at equivalent reduced temperatures, the absolute $S_{CD}(i)$ values decrease with increasing chain length. The average hydrocarbon thickness of the bilayer $2\langle L \rangle$ estimated from the order profiles increases with the number of chain carbon atoms; whereas the average lipid cross-sectional area $\langle A \rangle$ remains essentially constant. Thus, the surface area per molecule appears governed mainly by a balance of forces acting near the aqueous interfacial region of the bilayer. The $R_{12}(i)$ profiles depend on the square of the corresponding order profiles (1). This finding suggests that relatively slow bilayer fluctuations modulate the residual quadrupolar splittings left-over by faster motions, such as trans-gauche isomerizations. The relaxation contribution from the faster motions suggests the bilayer microviscosity is similar to that of a liquid paraffin with a bulk viscosity of 1-2 cP. (1) M.F. Brown, *J. Chem. Phys.* 77, 1576 (1982). Supported by an RCDA from the NIH (M.F.B.), NIH Grant EY03754, and the Sloan Foundation.

W-Pos46 POLYUNSATURATED LIPID BILAYERS STUDIED BY DEUTERIUM NMR. Theodore P. Trouard, Amir Salmon, Stuart S. Berr, and Michael F. Brown. Department of Chemistry, University of Arizona, Tucson, AZ 85721.

Polyunsaturated fatty acids are an interesting class of molecules which are found in nervous tissue and may play a role in cardiovascular disease. ^2H NMR studies of mixed-chain, saturated-polyunsaturated phosphatidylcholines have been performed [abbreviated (n:0)(22:6)PC where $n = 12, 14, 16, 18$]. In each case, the saturated chain at the $sn-1$ position was perdeuterated while the polyunsaturated, docosahexaenoic acyl chain (22:6 ω 3) at the $sn-2$ position was protiated (1). Measurements of the moments of the spectral lineshapes as a function of temperature were carried out to determine the order-disorder phase transition temperatures of dispersions containing 50 wt. % H_2O . Below the main transition temperature, to at least -70°C , significant disorder in the saturated $sn-1$ chain is observed, which is different from the behavior of the corresponding disaturated phosphatidylcholines. In the liquid-crystalline (L_α) phase at higher temperatures, ^2H NMR spectra of the polyunsaturated series are again different from their disaturated counterparts. The saturated acyl chain at the $sn-1$ position exhibits additional quadrupolar splittings intermediate between the largest and smallest values. The results suggest that a saturated chain has increased configurational freedom when esterified adjacent to a polyunsaturated acyl group in mixed-chain phospholipids, relative to bilayers of the corresponding disaturated phosphatidylcholines. (1) A. Salmon et al., *J. Am. Chem. Soc.* 109, 2600 (1987). Supported by an NSF Predoctoral Fellowship (A.S.), an American Heart Association Postdoctoral Fellowship (S.S.B.), an RCDA from the NIH (M.F.B.), the Jeffress Trust, and NIH Grant EY03754.

W-Pos47 DEUTERIUM NMR SPECTROSCOPY OF POLYUNSATURATED PHOSPHATIDYLCHOLINES IN THE LIQUID-CRYSTALLINE STATE. Amir Salmon and Michael F. Brown (Intr. by J. F. Ellena). Department of Chemistry, University of Arizona, Tucson, AZ 85721.

Mixed-chain, polyunsaturated phosphatidylcholines in the liquid-crystalline (L_α) phase were investigated using ^2H NMR. Phospholipids were synthesized with a perdeuterated, saturated acyl chain of variable length at the glycerol sn-1 position and a protiated, docosahexaenoic acyl chain (22:6 ω 3) at the sn-2 position [abbreviated (n:0)(22:6)PC where n = 12,14,16,18]. ^2H NMR spectra of multilamellar dispersions were acquired and deconvolved (de-Paked) to yield subspectra corresponding to the director parallel to the magnetic field. The de-Paked ^2H NMR spectra differ from those of the corresponding disaturated phospholipids in that the sn-1 acyl groups exhibit additional quadrupolar splittings with intermediate values (1). Profiles of the order parameters $S_{\text{CD}}(i)$ and spin-lattice relaxation rates $R_{1Z}(i)$ as a function of chain segment position were derived. At the same absolute temperature, the sn-1 saturated acyl chains of the polyunsaturated bilayers are more disordered relative to disaturated phosphatidylcholines; whereas the opposite is true at the same reduced temperature. The increased configurational freedom of the saturated chains evident from the order profiles is not due solely to the different transition temperatures, however. For the (12:0)(22:6)PC bilayer in the L_α phase, the relaxation profile $R_{1Z}(i)$ of the saturated chain is proportional to the square of the corresponding order profile $S_{\text{CD}}(i)$, suggesting that the dynamics are influenced by relatively slow bilayer fluctuations (2). (1) A. Salmon et al., *J. Am. Chem. Soc.* 109, 2600 (1987). (2) M. F. Brown, *J. Chem. Phys.* 77, 1576 (1982). Supported by an NSF Predoctoral Fellowship (A.S.), an RCDA from the NIH (M.F.B.), the Jeffress Trust, NIH Grant EY03754, and the Sloan Foundation.

W-Pos48 THE INTERACTION OF n-ALKANES WITH LIPID BILAYER MEMBRANES: A ^2H -NMR STUDY. P.W. Westerman*, J.M. Pope†, and L. Littlemore.† *Dept. of Biochem., N.E. Ohio U. College of Med., Rootstown, Ohio 44272. †School of Physics, Univ. of N.S.W., Kensington, N.S.W. 2033 (Australia).

The interaction of six n-alkanes with dimyristoylphosphatidylcholine (DMPC), DMPC/cholesterol, egg yolk lecithin (EYL) and EYL/cholesterol bilayers has been studied by deuterium nuclear magnetic resonance (^2H NMR). Using perdeuterated n-alkanes the solubilities of the n-alkanes in each bilayer system has been measured by integration of the relative signal intensities of the ordered and isotropic components in the spectra. For DMPC/25H₂O/0.1 n-alkane bilayers in the absence of cholesterol a sharp drop or "cut-off" in the percentage of ordered spectral component occurs with increasing alkyl chain length at n-tetradecane. In bilayers consisting of DMPC/25-H₂O/0.3 cholesterol/0.1 n-alkane the "cut-off" is shortened to n-undecane. Increasing the n-alkane concentration (0.5 n-alkane) in the same system further shifts the "cut-off" to $\approx C_9$. In contrast, for EYL/0.1 n-alkane bilayers, even in the presence of cholesterol the "cut-off" occurs at a chain length $> C_{16}$. Thus our results show that the "cut-off" in alkane solubility in lipid bilayers is dependent on the lipid chain length and/or the degree of unsaturation, as well as on the presence of cholesterol in the bilayer.

W-Pos49 EXTENSIONAL FAILURE OF RED CELL MEMBRANE ENHANCES THE LATERAL MOBILITY OF INTEGRAL PROTEINS. D. A. Berk*, A. Clark, Jr.†, R. M. Hochmuth*. *Department of Mechanical Engineering and Materials Science, Duke University, Durham, NC 27706 and †Department of Mechanical Engineering, University of Rochester, Rochester, NY 14627.

A flow-channel apparatus is used to extract tethers (hollow filaments of membrane material) from red cells. The material constituting the tether undergoes extensional failure; it loses its shear rigidity and flows as a two-dimensional liquid. The lateral mobility of integral proteins within the tether membrane is measured using the technique of Fluorescence Recovery after Photobleaching. Tethers are extracted from red cells labeled with the protein dye DTAF. The entire tether is then photobleached and the fluorescence recovery monitored. An analytical solution for surface diffusion from a spherical shell to a cylinder has been developed to analyze the fluorescence recovery data. For tethers longer than 10 μm , recovery time is strongly dependent on the lateral diffusion coefficient of the tether material and only weakly dependent on the coefficient for normal membrane on the cell body. The calculated diffusion coefficient for tether membrane is greater than $1.5 \times 10^{-7} \text{ cm}^2/\text{sec}$, much greater than the coefficient for normal membrane ($4 \times 10^{-11} \text{ cm}^2/\text{sec}$) and comparable to other reported coefficients for unconstrained protein surface diffusion in erythrocytes and other cells. This enhanced protein mobility implies that the tether membrane is spectrin-deficient and that the extensional flow associated with tether formation involves the separation of lipid bilayer from the underlying membrane skeleton.

W-Pos50 **Solute Partitioning into Lipid Bilayer Membranes.** L.R. De Young and K.A. Dill (Intr. by N. Duzgunes), Department of Pharmaceutical Chemistry, School of Pharmacy, University of California, San Francisco, California 94143.

Lipid bilayer membranes are interfacial phases of matter. In contrast to amorphous bulk hydrocarbons, the phospholipid chains in a lipid bilayer are ordered to a degree which increases with the surface density of the chains. Structural differences between bilayers and bulk phases such as oil or octanol should be manifested as differences in the nature of solute partitioning into them; surface density should strongly influence the partitioning of solutes into the bilayer.

The membrane/water partition coefficients of solutes such as benzene and hexane, obtained through a gas phase equilibration of radiolabeled solute, have been correlated with phospholipid chain surface densities. We have developed a simple $^1\text{H-NMR}$ method for measurement of surface densities; results from this method agree with those obtained from more demanding x-ray diffraction measurements. The surface density was altered with temperature, phosphatidylcholine chain length and cholesterol incorporation into the membrane. We observe that phospholipid chain ordering causes solute exclusion; partitioning decreases with increasing surface density. The magnitude of this effect is large; benzene partitioning decreases an order of magnitude as surface density increases from 50% to 90% of its maximum value. The dependence of partitioning on surface density is independent of the nature of the agent used to control the surface density.

W-Pos51 **EVALUATION OF THE THERMAL COEFFICIENT OF THE RESISTANCE TO FLUOROPHORE ROTATION OF MODEL MEMBRANES.** S.F. Scarlata, Cornell University Medical College, New York, NY 10021.

The thermal coefficient of the frictional resistance to fluorophore rotation (b) was determined for anthroyloxy-fatty acid probes in micelles and dimyristoyl lecithin (DMPC) and dioleoyl lecithin (DOPC) unilamellar and multilamellar vesicles. The value of b and the percent change in anisotropy with temperature ($\%dA/dT$) remained surprisingly constant with membrane depth and only depended on composition. These parameters were also the same when either in-plane or out-of-plane fluorophore motions were observed. The magnitude of b was found to be primarily dependent on the packing of the hydrocarbon chains comprising the membrane with higher b values relating to more closely-packed chains. The value of b changed during the gel to liquid crystal phase transition of DMPC and the bilayer to hexagonal phase transition of egg phosphatidylethanolamine. When the enthalpy values for the fluorophore transfer from one lipid phase to another are calculated, the values are much larger than those measured by calorimetry and reflect a discrepancy between the microscopic enthalpy experienced by the fluorophore due to a change in environment versus the macroscopic enthalpy of the system as a whole.

W-Pos52 **GLYCEROPHOSPHOLIPID SYNTHESIS - IMPROVED GENERAL METHOD AND NEW PHOTOPOLYMERIZABLE LIPIDS.** Ulrich Liman and David F. O'Brien, Department of Chemistry, University of Arizona, Tucson, AZ 85721.

The synthesis of speciality lipids is crucial to the study of bilayer membranes by D-NMR, ESR, fluorescence spectroscopy and for membrane modification by polymerizable lipids. The incorporation of labels or reactive groups into phospholipid acyl chains is frequently accomplished by the method of Gupta, et al., PNAS 74, 4315 (1977). Glycerol-3-phosphorylcholine (GPC) is acylated with an excess of the desired fatty acid anhydride. Reported yields are 40 to 90% based on GPC, but only 15 to 35% based on the valuable fatty acid. This report introduces a new method to form phospholipids in 50 to 70% yield based on the fatty acid. An intermediate activated fatty acid ester is formed in dimethylformamide from the fatty acid (2 eq) and 4-hydroxybenzotriazole (1 eq), in the presence of GPC (1 eq) and 4-pyrrolidinopyridine. The reaction proceeds over a few hours at room temperature and under argon to give the desired lipid. The reaction conditions permit the reaction of sensitive fatty acids with lysolecithin as well as GPC. Mono- and disubstituted chain terminal sorbyl ($-\text{OCOCH}=\text{CH}-\text{CH}=\text{CHCH}_3$) phospholipids prepared by this method were hydrated. The resulting light sensitive liposomes are photopolymerizable with UV light (254 nm). The characteristics of the liposomes before and after polymerization will be described.

W-Pos53 THE INTERACTION OF ALCOHOLS WITH LIPID BILAYER MEMBRANES: A ^2H -NMR STUDY. N. Phokphok*, P.W. Westerman*, J.M. Popel†, J.W. Doane*, and D.W. Dubro†. *Dept. of Biochem., N.E. Ohio U. College of Med., Rootstown, Ohio 44272. †School of Physics, Univ. of N.S.W., Kensington, NSW 2033 (Australia), ‡Liquid Crystal Inst., Kent State Univ., Kent, Ohio 44242.

The interaction of eight n-alkanols with DMPC bilayers has been studied by ^2H NMR. Under comparable conditions, order parameters measured at the 1-methylene segment of the n-alkanols, and average order parameters for the whole alkyl chain, show a maximum for n-dodecanol. This maximum in ordering occurs at the levels of solute concentration which produce anesthesia. From n-octanol to n-tetradecanol, orientational ordering shows a maximum at the C-4 to C-7 methylene segments, with labels at both ends of each n-alkanol exhibiting reduced order. The ordering of n-butanol, however, decreases from the hydroxyl group end to the methyl group. Orientational ordering at nine inequivalent sites in DMPC, has been measured for bilayers containing n-butanol, n-octanol, n-dodecanol and n-tetradecanol. At the 3R,S sites on the glycerol backbone, n-butanol produces the largest disordering, probably reflecting the greater fraction of time spent by the -OH group of n-butanol in the vicinity of the lipid polar headgroup. It was found that n-octanol orders the acyl chains of DMPC, unlike n-butanol which disorders them, and the longer chain n-alkanols which have little effect. The influence of n-alkanols on DMPC ordering at twelve sites has been compared with cholesterol and dimyristin, which are shown to interact with DMPC bilayers in a distinctly different manner.

W-Pos54 MONITORING MEMBRANE DOMAINS USING EXCIMER FLUORESCENCE ENERGY TRANSFER. Kristen A. Rundell and T. Gregory Dewey, Department of Chemistry, University of Denver, Denver, Colorado 80208.

Fluorescence energy transfer was measured from pyrene excimers to lipid acceptors in phospholipid vesicles. Using pyrene labels with different length hydrocarbon tails, it was demonstrated that energy transfer from excimer states could be used to gain accurate information regarding the distance of closest approach of an excimer to an acceptor. A simple theory is presented which allows energy transfer from the excimer state to be calculated without interference from monomer energy transfer. Results for a variety of pyrene labels indicate similar membrane locations for both excimers and monomers. These results demonstrate the validity of the analysis. It was previously shown that the excimer to monomer intensity ratio can be used to assess the lateral distribution of pyrene in co-existing fluid and gel phases (Hresko et al., *Biochem.* 25, 3813). Using fluorescence energy transfer from excimer states, it is possible to determine the surface density of acceptor in regions containing excimers. Thus, when partitioning of pyrene labelled fatty acids occurs, it is also possible to assess partitioning of a second species. This technique could also be used to monitor the aggregation of membrane proteins.

W-Pos55 SHORT-CHAIN LECITHIN/LONG-CHAIN PHOSPHOLIPID UNILAMELLAR VESICLES: IN VITRO & IN VIVO STABILITY STUDIES. Gerard Riedy¹, Mary F. Roberts¹, and N. Elise Gabriel²,[†]Department of Chemistry, Boston College, Chestnut Hill MA 02167, and²Department of Chemistry, M.I.T., Cambridge MA 02139.

In vitro and in vivo integrity studies have been carried out with unilamellar vesicles that form spontaneously from suspensions of long-chain phospholipids (14 or more carbons per fatty acyl chain) when small amounts, typically 20 mol%, of micellar synthetic short-chain lecithin (fatty acyl chains 6-8 carbons) are added [Gabriel & Roberts, *Biochem.* 23, 4011 (1984); 25, 2812 (1986); 26, 2432 (1987)]. Sizes of these binary component vesicles can be biased toward small (200 Å) or large (1000 Å) distributions depending on the physical state (e.g., gel or liquid crystalline) of the long-chain phospholipid. Short-chain lecithin/long-chain phospholipid unilamellar vesicles (SLUVs) are nonlytic to human erythrocytes, implying that most of the short-chain lecithin is partitioned in the bilayer and not free in solution as monomer or micelle. C-13 NMR studies show that upon prolonged incubation some of the lipids in SLUVs are exchangeable with those of the erythrocyte without cell lysis. Serum albumin, which can bind short-chain lecithin, does not appreciably destroy the integrity of SLUVs as judged by H-1 NMR experiments. Gamma ray perturbed angle correlation (PAC) studies using In-111 loaded vesicles indicate that SLUVs are stable in the presence of serum and whole blood for several days. This technique has also been used to measure blood clearance and biodistributions of different SLUVs in mice. Comparisons are made to other unilamellar vesicles. (Supported by N.I.H. grant GM 26762.)

W-Pos56 MOLECULAR MODELING OF THE INTERACTION OF TREHALOSE, SUCROSE AND GLUCOSE WITH THE PHOSPHOLIPID BILAYER. Bruce P. Gaber and Barbara R. Rudolph. Bio/Molecular Engineering Branch, Code 6190, Naval Research Laboratory, Wash. DC 20375 and Dept. of Chemistry, Georgetown University, Wash. DC 20007.

Disaccharides are known to impart stability to phospholipid bilayers under conditions of extreme dehydration. Trehalose and sucrose protect both cells and liposomes against leakage and fusion when they undergo dehydration, lyophilization or cycles of freezing and thawing. Previously we presented an interactively-derived computer graphics model to represent a possible mode by which trehalose could function to stabilize a lipid bilayer (Biophys J (1986) **49**, 435). That model portrayed trehalose as contributing three hydrogen bonds to non-esterified phosphate oxygens of DMPC. Here we describe the further refinement of that model by use of energy minimization procedures. Using the molecular mechanics program AMBER, we have refined the model with the result that two additional hydrogen bonds are formed. The refinement relieves several overly-close van der Waals contacts and places the sugar in a more energetically favorable conformation. The process of interactive modeling and energy refinement has been applied as well to sucrose and glucose. (Supported in part by a contract from the Biophysics Program of the Biological Sciences Division, Office of Naval Research.)

W-Pos57 DETECTION OF A NOVEL ALCOHOL BINDING SITE ON THE SURFACE OF DPPC-GM₁ MODEL MEMBRANES BY DEUTERIUM NUCLEAR MAGNETIC RESONANCE. Cindy Graham-Brittain and George P. Kreishman, Department of Chemistry, University of Cincinnati, Cincinnati, Ohio 45221-0172 and Robert J. Hitzemann, Department of Psychiatry and Behavioral Sciences, S.U.N.Y.-Stoney Brook, Stoney Brook, New York 11794-8101.

Deuterium Nuclear Magnetic Resonance has been used to demonstrate that d₆-ethanol not only partitions to the interior of model (DPPC) and synaptic plasma membranes, it also binds in an apparently cooperative manner to the surface of these membranes. Each of the membrane domains has a unique pre-exchange lifetime. For the methylene deuterons of d₆-ethanol, the exchange processes for both domains are slow on the NMR time scale; the amount of d₆-ethanol at both sites can be determined from the decrease in the methylene resonance intensity in the presence of membrane. For the methyl deuterons of d₆-ethanol, surface binding is slow, but interior binding is fast on the NMR time scale; the amount of surface-bound d₆-ethanol can be determined from the decrease in the methyl resonance intensity when membrane is present. Subtraction yields the amount of d₆-ethanol that has partitioned to the interior of the bilayer. The effect on alcohol-binding of incorporation of monosialoganglioside (GM₁) in DPPC model membranes is currently being investigated, as GM₁ has been shown to sensitize membranes to the partitioning effects of alcohols (*Molec. Pharm.* **25**, 410-417, 1984). Quadrupolar splitting of the d₆-ethanol methylene resonance to a doublet indicates that a new, fast-exchange binding site at the membrane surface has been introduced by GM₁. The implications of binding of ethanol to this third site will be discussed.

W-Pos58 ALCOHOL-INDUCED CHANGES IN THE MOLECULAR ORDER OF MODEL MEMBRANE SYSTEMS AS DETECTED BY DELAYED FOURIER TRANSFORM PROTON NMR SPECTROSCOPY. Harold E. Schueler and George P. Kreishman, Department of Chemistry, University of Cincinnati, Cincinnati, Ohio 45221-0172 and Robert J. Hitzemann, Department of Psychiatry and Behavioral Sciences, S.U.N.Y.-Stoney Brook, Stoney Brook, New York 11794-8101.

Previous research concerning the mechanism of action of alcohols has focussed on the disordering effects of the alcohol on the membrane interior. However, recent NMR studies have demonstrated that ethanol not only binds to the interior, but also to the surface of the membrane (*Biochem. Biophys. Res. Commun.* **130**, 301-305, 1985). Delayed Fourier transform proton NMR is employed to investigate changes in the membrane order at various depths of the DPPC liposome bilayer. By monitoring the spectral intensities of the terminal methyl, methylene and choline methyl resonances, the order/disorder of both the interior and surface membrane domains can be observed simultaneously. A decrease or increase in the spectral intensity of a given resonance corresponds to an increase or decrease, respectively, in the membrane order in that domain. With increasing ethanol concentration, an increase in the terminal methyl resonance intensity is detected and this is interpreted as a decrease in the interior order. In addition, an ordering effect on the surface, as shown by a decrease in the spectral intensity of the choline methyl resonance, results from ethanol binding to this domain. Incorporation of monosialogangliosides, which are known to sensitize membranes to the effects of ethanol, into the DPPC liposomes alters the surface properties of the bilayer. The correlation between these changes at the membrane surface and the ordering/disordering effects of ethanol will be presented.

W-Pos59 NUMBER OF IONS IN A VOLUME ADJACENT TO A CHARGED MEMBRANE. Robert Renthal, Univ. of Texas at San Antonio, San Antonio, Texas 78285

When ion binding to membranes is measured by centrifugation or ultrafiltration methods, some ions within the diffuse double layer will be removed as if they are bound to the membrane. Similarly, when detectors in bulk solution, such as electrodes, are used to measure ion transport across charged membranes, some transported ions may remain undetected in the double layer. In order to assess the magnitude of these effects, I have derived equations for the number of moles of counter ions, N , within a volume extending to a distance r from a membrane surface of area A : $N = A \int C dr$ where C is the concentration of the ion in a volume element $A dr$. The Poisson-Boltzmann equation provides a change of variables, leading to analytical solutions for two cases: 1) monovalent ions, and 2) divalent cation with monovalent anion. For case 1):

$$N = (A C_b^{1/2} / \kappa) [2(C_m^{1/2} - C_r^{1/2}) - C_b^{1/2} \ln \left(\frac{(C_r^{1/2} - C_b^{1/2})(C_m^{1/2} - C_b^{1/2})}{(C_m^{1/2} - C_b^{1/2})(C_r^{1/2} - C_b^{1/2})} \right)]$$

where C_m , C_r and C_b are, respectively, the cation concentration at the membrane surface, at a distance r from the membrane, and in bulk solution; and κ is the reciprocal Debye length. Sample calculations with purple membrane from *H. halobium* suggest that H^+ binding in the double layer has no effect on H^+ transport measured by electrode, while Ca^{2+} binding measured by centrifugation is 10% high. (Supported by grants from NIH, American Heart Assoc. Texas Affiliate, and the Welch Foundation)

W-Pos60 EFFECTS OF ALCOHOLS AND STEROIDS ON PHOSPHATIDYLETHANOLAMINE PHASE TRANSITIONS

Timothy J. O'Leary, Armed Forces Institute of Pathology, Washington, DC 20306

We have investigated the effects of short chain alcohols and anesthetic steroids on both the gel to liquid crystalline and the unhydrated crystal to liquid crystalline phase transitions of dimyristoylphosphatidylcholine using high sensitivity differential scanning calorimetry. Varying concentrations of alcohol or alcohol/steroid solution were added to unhydrated dispersions of dimyristoylphosphatidylethanolamine in distilled water. The dispersions were then placed in the calorimeter and heated from $4^\circ C$ to $65^\circ C$, cooled to $4^\circ C$, then reheated to $65^\circ C$. Both heating and cooling were performed at a rate of $20^\circ C/hour$. Increasing alcohol concentrations appeared to result in a very small decrease in the calorimetric enthalpy of both phase transitions, and resulted in a substantial lowering of both gel to liquid crystalline and unhydrated crystal to liquid crystalline phase transition temperatures. The effect on the gel to liquid crystalline phase transition was substantially greater than the effect on the crystalline to liquid crystalline phase transition, however. The effect on each transition was directly related to anesthetic potency and to dose of the anesthetic, as expected. The anesthetic steroids pregnanedione, progesterone, and testosterone, in limited experiments, have had similar potency-related effects. The results suggest that these anesthetics have relatively little effect on the thermodynamics of lipid membrane hydration. Attempts to examine any effects on the kinetics of the hydrated gel to unhydrated crystal transition have been unsuccessful since, in contrast to experiments in which dimyristoylphosphatidylethanolamine dispersions have been removed from the calorimeter and incubated at low temperature, we have been unable to see formation of crystals at $4^\circ C$ in 72 hours.

W-Pos61 RAMAN STUDIES OF PHASE BEHAVIOUR OF LIPID BILAYERS OF CEREBROSIDE SULFATES

Nathan H. Rich and Christopher Stevenson, Department of Physics Memorial University of Newfoundland, St. John's Newfoundland, Canada

and

Joan M. Boggs, Department of Biochemistry, The Hospital for Sick Children, Toronto, Ontario, Canada.

(Introduced by K.R. Jeffrey)

Phase behaviour of several synthetic cerebroside sulfates, (CBS) with hydroxy and non-hydroxy fatty acids from 18 to 26 carbons in length, has been investigated by Raman spectroscopy to compare with measurements on the same lipids by differential scanning calorimetry and by ESR. Effects of Li^+ and K^+ buffers were examined to determine differences on the head groups. Interdigitation of the bilayers in species with asymmetric chain roles of these CBS species.

W-Pos62 SLOW MOLECULAR MOTIONS IN ORIENTED PHOSPHOLIPID BILAYERS *#Zheng-yu Peng, *Nico Tjandra, #Virgil Simplaceanu, §#Irving J. Lowe, and #Chien Ho. #Department of Biological Sciences, *Department of Physics, Carnegie Mellon University, Pittsburgh, PA 15213; §Department of Physics and Astronomy, University of Pittsburgh, Pittsburgh, PA 15260.

Slow molecular motions in oriented phospholipid bilayers have been investigated by using a fluorine-19 NMR rotating-frame spin-lattice relaxation experiment and ^{19}F -labeled dimyristoylphosphatidylcholines. The field and the orientation dependence of the rotating-frame relaxation rates can be well fitted by a superposition of two terms, one originating from a large-scale localized anisotropic reorientation, the other originating from the collective director fluctuations. The effects on slow motions of lipid molecules induced by adding cholesterol or gramicidin to the bilayer have also been studied. Our results show that cholesterol affects mainly the localized reorientation, and gramicidin affects mainly the director fluctuations, which is only observed if the spectroscopic label is near the lipid head group. In order to gain additional insight into the molecular mechanism involved in the fast and slow thermal fluctuations of the lipid bilayer system, we have carried out preliminary Monte Carlo simulations. The relationship between NMR and computer simulation results on the dynamic properties of model membranes will be discussed. [This work is supported by research grants from the NIH (GM-26874) and NSF (DMB-8512141)].

W-Pos63 INTERACTION OF 1-PALMITOYL LYSOPHOSPHATIDYLCHOLINE AND PALMITIC ACID IN PHOSPHOLIPID VESICLES. Shastri P. Bhamidipati and James A. Hamilton, Biophysics Institute, Departments of Medicine and Biochemistry, Housman Medical Research Center, Boston University School of Medicine, Boston, MA 02118

We have investigated the interactions of palmitic acid (PA) and 1-palmitoyl lysophosphatidylcholine (LPPC) in phospholipid bilayers using ^{13}C NMR spectroscopy. Small unilamellar vesicles were prepared by cosonication of egg PC, LPPC and PA. The lipid compositions (mol%) were 4-6% PA+LPPC/96-94% egg PC and LPPC/PA molar ratios of 1:1, 2:1 and 1:2. 90% ^{13}C enrichment at the carboxyl carbon permitted detection of the small amounts of PA present in these systems. PA titration curves were constructed from chemical shift measurements as a function of pH. The apparent pK_a (7.7 ± 0.1) was unaffected by the LPPC/PA ratios and was similar to that for PA alone in PC vesicles at comparable concentrations. All systems showed carboxyl carbon linewidth increases near the pK_a (± 1.0); the degree of broadening was dependent on the LPPC/PA ratio. The mixture with excess LPPC had the largest and that with excess PA, the smallest linewidth increase. These results suggest that the mobility of, and/or the exchange rate of protons with, the PA carboxyl group are altered by the presence of LPPC. However, the net electrical/magnetic environment, as reflected in chemical shift, is not affected by LPPC. Although the linewidth changes suggest some association of LPPC with PA, fatty acid (FA) was quantitatively extracted from LPPC/PA/PC vesicles by bovine serum albumin at pH 8.0. The pH dependent partitioning of FA in the presence of LPPC was similar to that for FA/PC vesicles.

W-Pos64 PLANAR PHOSPHOLIPID BILAYER MEMBRANES MADE FROM MONOLAYERS FORM BY A THINNING PROCESS. W.D. Niles, R.A. Levis, F.S. Cohen. Rush Medical College. Department of Physiology. Chicago, IL. 60612.

We have investigated the manner by which planar membranes form when monolayers are raised over a hole (coated with either petroleum jelly or squalene) in a partition separating two aqueous compartments. We observed the formation of the membrane with high magnification video microscopy and simultaneously measured the capacitance of the membrane. After both monolayers were above the hole, a thick film initially formed and the capacitance was small. As the coating hydrocarbon drained out, a front separating the thin from thick region advanced and the capacitance increased accordingly. When the membrane was fully thinned the capacitance was maximal and a Gibbs-Plateau border (torus) surrounded the thin membrane, allowing the area of the actual membrane to be determined. Thus, the traditional view that these membranes form by each of the monolayers making direct apposition with each other as they are raised over the hole is incorrect. The membranes form by a thinning process similar to that which occurs for BLMs. The amount of solvent that remains within the bilayer depends on the partition coefficient of the coating solvent. By using a wide-bandwidth voltage clamp designed to have frequency characteristics independent of the capacitance load, we measured the admittance of the bilayer and determined the specific capacitance of membranes made from several lipid mixtures. The membrane dielectrics were not lossy and the specific capacitance of solvent-free bare bilayer was typically on the order of $0.8 \mu\text{F}/\text{cm}^2$. Supported by NIH grants GM27367 and NS21111.

W-Pos65 CALCULATION OF THE HYDROSTATIC PRESSURE DEVELOPED IN OSMOTICALLY SWELLING VESICLES ADSORBED TO A PLANAR MEMBRANE. W.D. Niles & F.S. Cohen. Dept. of Physiology, Rush Medical Center, Chicago, IL 60612.

When the vesicle-containing compartment (*cis*) bathing one side of a planar membrane is made hyperosmotic by the addition of a solute termed an osmoticant, the adherent vesicles swell, develop a hydrostatic pressure (ΔP), and fuse with the planar membrane. We have calculated the steady-state ΔP by solving equations for the flows of water and solute given by irreversible thermodynamics. ΔP is determined by the permeabilities of the vesicle membrane to solute (ω) and water (L), as well as by the magnitude of the osmotic gradient. If the vesicle is devoid of open channels that allow the osmoticant to enter the vesicle, then $\Delta P = 0$. When channels are present, ΔP peaks at a channel density unique to the species of osmoticant. The optimum channel density is a function of its permeability properties. ΔP is largest for osmoticants which have small ω 's in the contact region, such as KCl and urea; they enter the vesicle through the channels but can't leak out through the region of vesicle-planar membrane contact because the channels do not couple the *cis* and *trans* compartments. Experimentally, when porin is the channel KCl > urea > glycerol > formamide \cong ethylene glycol in promoting fusion with KCl 10 to 20 times more effective than formamide. When the narrower channel nystatin is used, KCl is twice as effective as formamide. The model quantitatively predicts these results. When the ω of the channel is large (i.e., porin), ΔP is independent of the reflection coefficient (σ) of the channel. For small ω , such as nystatin, however, ΔP depends on σ . The model allows establishment of optimum conditions for fusing vesicles to planar membranes. Supported by NIH grant GM 27367.

W-Pos66 THERMAL PERMEABILITY PROPERTIES OF ARCHAEBACTERIAL LIPIDS. E. L. Chang and C. Montague. Bio/Molecular Engineering Branch, Code 6190, Naval Research Laboratory, Washington, D.C. 20375-5000; Geo-Centers, Newton Upper Falls, MA 02164.

The biomembranes of whole thermoacidophilic archaeobacteria are known to stay intact and non-leaky even at very high temperatures (boiling point of water). Permeability properties of archaeobacterial membranes are crucial to these organisms which often thrive in environments where there is an extreme in the concentration gradient of such ions as protons (thermoacidophiles) or sodium (halophiles). Is the unusual thermal stability (and possibly low permeability) of archaeobacterial membranes solely a property of the polar lipids? We explore this question by comparing the thermal permeability of several lipids, both conventional and archaeobacterial. Lipid vesicles are formed with self-quenching concentrations of carboxyfluorescein encapsulated. The exogenous fluorescence levels are monitored as a function of temperature. Lipids examined include: egg phosphatidylcholine (PC), dimyristoyl PC, diphytanoyl PC, and the polar fraction of tetraether lipids from *S. acidocaldarius*.

W-Pos67 THE P_{β}' PHASE IN LIPID BILAYERS: MOLECULAR INTERACTIONS IN THEORETICAL MODELS
H. L. Scott and P. A. Pearce, Physics Department, Oklahoma State Univ. Stillwater, OK 74078 and Mathematics Department, Melbourne University, Parkville, Vic 3053

The existence of the P_{β}' phase in certain lipid bilayers is proof that molecular interactions between lipids are capable of producing unusual large scale structures at or near biological conditions. The problem of identifying the specific interactions responsible for the structures is very difficult. Theoretically this involves devising models which are then analyzed as accurately as possible using Statistical Mechanics to determine if the experimentally observed phases and structures are present. To date only one such effort has been applied to the ripples in the P_{β}' phase. This is the model of Pearce and Scott (J. Chem. Phys. 77 951, 1982) in which it was shown that competing near and next-neighbor interactions can produce a ripple phase in a two dimensional model for a bilayer. In the present paper we present results of a new modeling effort aimed at further clarifying the interrelationships between intermolecular interactions and modulated structures (ripples). First the results of detailed numerical calculations of intermolecular interaction strengths will be given. This work involves calculations of potential energies of interaction between pairs and triplets of lipid molecules having different head group orientations, chain tile angles, and relative vertical alignments. The results of the calculations are then used to formulate a new theoretical model for the P_{β}' phase. The new model is less complex than the earlier model and it includes interactions which are more likely to be responsible for the ripple phase. Preliminary results of a study of the predicted phase properties of the model will be given.

W-Pos68 PARTITIONING OF EXCHANGEABLE FLUORESCENT PHOSPHO- AND SPHINGOLIPIDS BETWEEN LIPID VESICLES OF DIFFERENT COMPOSITIONS. Michael Gardam, Joseph Itovitch and John R. Silvius, Department of Biochemistry, McGill University, Montréal, Québec, Canada H3G 1Y6.

We have prepared a variety of phospho- and sphingolipid probes in which one acyl chain is 8 or 11 carbons long and is substituted at the methyl terminus with either a bimane or a (dimethylaminocoumarin-3-yl)carboxamido- (DMCA)- group. The distribution of these probes between two populations of vesicles can readily be monitored by including in one set of vesicles a nonexchangeable energy-transfer acceptor, as described previously by Nichols and Pagano (*Biochemistry* 21 [1982], 1720). These probes partition strongly into lipid vesicles but can redistribute between vesicles through the aqueous phase with half-times from seconds to several minutes. By contrast, the probes show negligible rates of flip-flop from the inner to the outer surfaces of lipid vesicles. By measuring the equilibrium distribution of a given probe between two different populations of unilamellar lipid vesicles, we can calculate a partition coefficient that reflects any differences in the free energy of the probe in the two different lipid environments. To date, we have examined the partitioning of several phospholipid probes (PC, PE, PS, PG and PA) between PC/PG vesicles and PE/PS vesicles, and of several anionic lipid probes between vesicles with different surface charges. While electrostatic effects on probe partitioning are clearly observed in the latter system, as expected, our results with the former system do not show a preferential interaction of 'strong hydrogen-bonding' species (PE, PS and PA) with like species in preference to 'weak hydrogen-bonding' species such as PC. We are now extending these studies to include sphingolipid probes and cholesterol-containing systems. (Supported by the MRC of Canada and les fonds FCAR du Québec.)

W-Pos69 THE EFFECTS OF TEMPERATURE AND HYDRATION ON THE CONFORMATION OF ALIGNED EGG YOLK PC STUDIED BY SOLID-STATE CARBON-13 NMR. V.L.B. Braach-Maksvytis, B.A. Cornell and R.P. Rand*. CSIRO P.O. Box 52, North Ryde N.S.W. 2113, Australia; *Biological Sciences, Brock University, St. Catharines, Ontario, Canada.

Egg yolk phosphatidylcholine was aligned on stacked glass cover slips and sealed in 10mm NMR tubes. The state of hydration of the lipid was controlled by equilibration with an atmosphere containing 33% relative humidity (5 H₂O per lipid molecule), 92% relative humidity (11 H₂O per lipid molecule), or by adding 50% by weight of bulk water to the dry lipid (maximally hydrated at 30 H₂O per lipid molecule).

Natural abundance solid-state cross-polarisation carbon-13 NMR spectra were obtained at various orientations of the bilayers relative to the magnetic field. The reduced chemical shift anisotropies for most of the different types of carbons in the lipid were estimated from spectra obtained at 20°C and 60°C for each hydration level.

The reduced chemical shift anisotropies of particular carbons depended on both temperature and hydration. The detailed form of this dependence was peculiar to each site in the molecule and was interpreted in terms of the local molecular conformation and order. We conclude that both temperature and degree of hydration each differently affects polar conformation.

W-Pos70 INVESTIGATION AND POLYMERIZATION OF LIPID ANALOGS ORGANIZED IN MONOLAYER ASSEMBLIES
Cynthia Palmer, Department of Chemistry and Graduate Biophysics Program, Syracuse University, Syracuse, New York 13244.

Conventional monolayer techniques such as pressure-area isotherms, ellipsometry at the air-water interface, and surface-potential measurements have been used to characterize monolayer films. FTIR-LD and photoacoustic spectroscopy have been used as probes to assess the structural organization of the polymerized and unpolymerized lipid analogs. The transmission FTIR-LD technique reveals steric arrangement of the styrene and amide groups in Langmuir-Blodgett (LB) monolayer and multilayer films, as well as modifications due to photopolymerization. The polymerization kinetics have been investigated, exploiting the area contraction of the monolayer film at constant pressure during irradiation with 254 nm UV light. The temperature-dependent kinetics suggest a possible mechanism for photopolymerization.